To the Graduate Council:

I am submitting herewith a dissertation written by Tivadar Farcas entitled "The Study of Column Packing Homogeneity and Flow Profiles in Packed Chromatographic Columns." I have examined the final copy of this dissertation for form and content and recommend that it be accepted in partial fulfillment of the requirements for the degree of Doctor of Philosophy, with a major in Chemistry.

Georges A. Guiochon, Major Professor

We have read this dissertation
and recommend its acceptance:

Accepted for the Council:

Associate Vice Chancellor and
Dean of The Graduate School

THE STUDY OF COLUMN PACKING HOMOGENEITY AND FLOW PROFILES IN PACKED CHROMATOGRAPHIC COLUMNS

A Dissertation

Presented for the

Doctor of Philosophy

Degree

The University of Tennessee, Knoxville

Tivadar FARCAS

May, 1997

ABSTRACT

This work continues a long history of efforts to study the flow of fluids through packed beds-- more specifically, through beds made of uniform packing particles, and generated under high pressure, -- and to probe the sources of band broadening in liquid chromatography, referred to more commonly as axial dispersion.

Any investigation of the radial distribution of local chromatographic characteristics should consider on-column, local, multichannel detection. The results presented in this work were obtained with an experimental set-up which can accommodate at least 10 optical fiber assemblies functioning as on-column, local microdetection probes when implanted into the exit frit of an HPLC column.

High performance liquid chromatographic columns are not radially homogeneous. A rather homogeneous core is surrounded by a thick layer of heterogeneous packing situated along the column wall. The thickness of this layer is variable. The flow distribution in these columns is cylindrical, nearly flat in the column center, within approximately half the column radius from the center and falls behind rather rapidly towards the wall. Because the concentration profile of an analyte along the wall passes later and is wider than in the column center, the signal of a bulk detector is bound to exhibit an increased width, and some degree of tailing. The extent to which the peak tails is proportional to the degree of deformation of the mobile phase flow profile.

The local column efficiency is at most locations higher than the overall

efficiency determined with an on-line conventional detector. It varies across the column cross-section as follows: it is higher in the central core region, while in the external region it decreases with decreasing distance to the column wall. As a consequence, analytical columns are operated under experimental conditions where a significant fraction of their potential performance is wasted. A small concentration sensor placed at the column axis would see narrower, better resolved and more concentrated bands.

The consequence of this heterogeneous behavior of the column is that the conventional elution profile is a complex convolution of the convection and dispersion phenomena taking place in a chromatographic column. Obviously, two space coordinates, the column length and its radius and not only the former, are needed in a realistic model of chromatography [Guiochon, 1995].

TABLE OF CONTENTS

LIST OF FIGURES

LIST OF TABLES

LIST OF SYMBOLS

A	column cross-sectional area
D_m	diffusion coefficient
d	column diameter
d_p	particle diameter
F	flow rate
G	intensity of the inertial field
h_0	geometrical constant
$HETP$	height equivalent to the theoretical plate
h	reduced HETP
$i.d.$	inner diameter
k'	retention factor
k_0	bed permeability
L	column length
MW	molecular weight
N	number of theoretical plates
r_c	column radius
Re	Reynolds number
T	absolute temperature
t_R	retention time
u	mobile phase linear velocity
u_c	mobile phase linear velocity at column axis
V	solute molar volume
$w½$	peak width at half height

Greek symbols:

$\alpha(\delta)$	pore size distribution
ΔP	pressure drop
δ	pore diameter
ϵ_e	external porosity
ϵ_i	internal porosity
ϵ_T	total porosity
Φ_f	fluorescence quantum yield
η	mobile phase viscosity
ρ	density
v	reduced velocity

CHAPTER I

INTRODUCTION

1.1 Chromatographic Column Packing Homogeneity

For the most part the chromatography literature treats columns as unidimensional. There are very few exceptions that consider it otherwise [Knox *et al.*, 1969, 1976; Eon, 1978; Baur *et al.*, 1988; Yun *et al.*, 1994], and most of these papers are nearly twenty years old. Unidimensionality assumes in this case that the radial dispersion is fast enough on the scale of the column radius such that radial fluctuations in local packing density would not cause any major problems in the separation process. The analyte bands are assumed to exhibit a constant concentration over the entire column cross-section. Similarly, when a preparative column is overloaded, the degree of overload, or loading factor, is assumed to be constant in the radial direction. There is little experimental evidence to support these assumptions, except for the feeling, not entirely unjustified, that should it be otherwise, column performance would be drastically decreased compared to what is routinely accomplished. Axial dispersion -- the primary phenomenon affecting column performance, -- has been studied extensively. It is due to a combination of molecular and eddy diffusion. Molecular diffusion is caused by concentration gradients that exist necessarily when a component zone of finite length migrates

along the column. It follows Fick's law. However, since diffusion cannot proceed along a straight line in a packed bed, the apparent axial diffusion coefficient is lower than the molecular diffusivity. Eddy diffusion results from the inequalities of the local values of the linear velocity in the different channels available for the stream to flow through. Giddings [1965] has shown that eddy diffusion depends on the mobile phase velocity. A molecule that is in a fast stream takes a step forward with respect to the zone. This step can end either because the velocity of the given streampath decreases, or because the molecule jumps by diffusion form one streampath to another. Thus, diffusion relaxes the radial concentration gradient that tends to build up because of the inequalities in the local flow velocity.

Axial dispersion along with band broadening caused by slow mass transfer inside the pores of a packing material are the factors considered to limit column efficiency. Nevertheless, column behavior could not be modeled satisfactorily in many cases. For example, often nonpolar, unretained analytes elute with unexpected tailing, and in general, peaks tail more than predicted by most available models. Something seems to be missing from the inventory of factors causing band dispersion inside a column, factors that are final for column performance.

If columns were radially heterogeneous to a large extent, the flow pattern of the mobile phase would be affected accordingly. Solvent volume elements migrating along pathways running through low packing density regions of the column would move at a higher local linear velocity than the bulk. The analyte molecules carried along by these volume elements would arrive first to the column

exit. Quite the opposite would be true for analyte molecules carried along by mobile phase volume elements that move in regions of high packing density (Figure 1.1.1). Large radial concentration gradients along the diameter of the column could not be relaxed by molecular diffusion since the values for the diffusion coefficient (D_m) in liquids are usually low ($1x10^{-6}$-$5x10^{-5}$ cm^2/s). The estimated time required for the molecules of a species having a large value for its D_m to diffuse across the diameter of a typical analytical HPLC column is 2100 s. Most chromatographic analysis are much faster. The resulting peak shape distortion (consisting of an increase in peak width and tailing) would most definitely affect the performance of the column.

1.2 Flow through Porous Media

A packed chromatographic column is a maze of channels through which flows the mobile phase. Along the way, it carries all the analyte molecules that happen to be dissolved into it at any moment. There are countless pathways along which a molecule of either the solvent or the analyte may migrate from one end of the column to the other (Figure 1.2.1). At any given time, the local velocity of molecules following different pathways, or moving at different locations along the same pathway, may be very different in magnitude and/or in direction. The flow pattern (*i.e.*, the detailed relative distribution of the mobile phase velocity in magnitude and direction) is essentially the sum of all the local velocity biases or

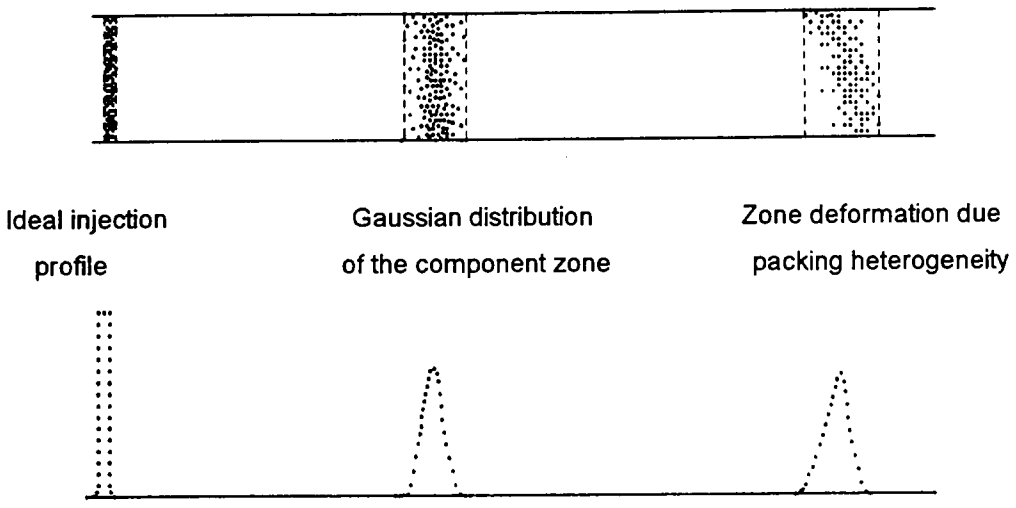

Figure 1.1.1 Spreading of the component zone of an unretained analyte, due to dispersion, as seen at three different times during elution.

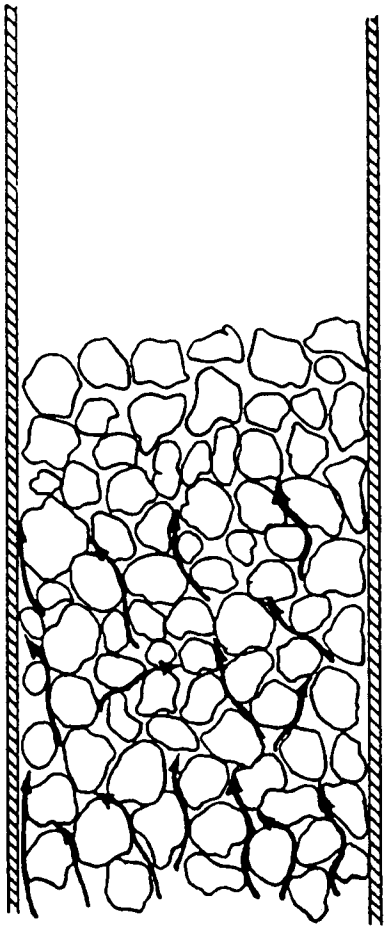

Figure 1.2.1 Flow through a packed bed depicting the countless pathways by which molecules in the mobile phase may travel from one end of the column to the other. Source: Karger, B., L. Snyder and Cs. Horváth, "*An Introduction to Separation Science*", Wiley, New York, NY (1973), 91.

differentials which are so important to the analyte zone spreading [Giddings, 1965; Peters *et al.*, 1974].

An impressive amount of work has been done in the field of fluid dynamics in porous media. This field in compasses a wide range of solid porous structures combined with fluids both different in nature and moving in different flow regimes. The properties of the migrating liquids to be considered are viscosity, diffusivity, and capacity to wet the solid surface of the porous medium they are flowing through. This variability in porous structures and fluids in motion makes the spectrum of practical situations to be investigated very large, since particular systems can be very different from each other.

Soil mechanics is one of the major fields that involve fluids in motion through porous media [Taylor, 1958; Lambe, 1979]. The characteristics of soils as porous media are usually difficult to consider in a unified approach because of the large variability in their mechanical properties, and their widespread structural heterogeneity. More homogeneous porous media of interest are granular packing materials widely used in the chemical industry in distillation and adsorption columns, or in heterogeneous catalysis reactors. Most often, the particles of these packing materials have a specific shape and their size distribution is relatively small. Due to these properties, the resulting beds are relatively homogeneous. The flow through such media has been thoroughly investigated by a wide range of methods.

Several investigators [Morales *et al.*, 1951; Schwartz, 1953; Vortmeyer and Schuster, 1983] have measured the velocity distribution within packed beds, while

many others were more concerned with heat and mass transfer coefficient measurements [Lerou and Froment, 1977; Callaghan *et al.*, 1992; Gladden, 1994; Rigby *et al.*, 1996] . Morales *et al.*, [1951] investigated the flow of air through a 2" i.d. bed of 1/8-3/8" cylindrical pellets using a hot wire placed above the bed. They found that at bed depths above 2 inches the velocity decreased both near the tube wall and near the center, giving a maximum value at a point between the center of the tube and the wall. Price [1968] placed a honeycomb structure on top of a porous bed in order to suppress by this measure the onset of radial flow components within the fluid having left the bed. He found higher flow velocities closer to the wall. Vortmeyer and Schuster [1983] performed measurements with a Laser-Doppler Anemometer placed also on top of the packed bed and showed that an important distortion of the flow profiles was encountered when measurements were performed within a free cross-section plane. They found that the flow profiles depended strongly on the distance between the exit plane of the bed and the actual plane where the measurements were taken.

Measurements performed inside the packing raised a number of problems. The local fluid velocity inside randomly packed beds varies in magnitude and direction, because of the tortuous nature of the flow path and the variations in the shape of the flow passage. Hence, many measurements of the local velocity are required to come to some average of the velocity in a cross-section of a packed bed [Lerou and Froment, 1977]. A further complication arises when the velocity sensing probe is more or less intrusive. For this reason, Cairns and Prausnitz [1959] used

probes with an adapted geometry. They too found that the velocity was higher in the wall region of the bed.

A higher velocity in the wall region is explained by an uneven radial distribution of the void fraction in packed beds. Benenati and Brosilow [1962] found that the radial distribution of the void fraction within a packed bed of uniform spheres shows a decrease from unity at the wall to about 38% in the interior of large beds. They showed that the perturbations in the voidage introduced by the presence of a retaining wall extended from wall on a distance of about 10 particle radii. Venneti *et al.* [1986], analyzed voidage profiles in randomly packed beds of uniformly sized spheres, by considering the first layer of spheres -- the one touching the wall -- highly organized, while the subsequent layers building up on the surface of the first one, in a less ordered fashion. They also concluded that the decrease in voidage from wall inwards is oscillatory, but is damped out at about 4 sphere diameters away from the wall.

Vortmeyer and Michael [1985] state that while the changes in porosity near the wall are well known, there is no general consensus on the precise flow profiles inside the packed bed. Nevertheless, they show that improvements in the theoretical prediction of reactor performance are obtained by assuming a non-uniform flow distribution within the packed bed. Such improvements were underscored by the results of Patzay and Takács [1994].

In recent years chemists and chemical engineers have shown an increasing interest in non-invasive measurement techniques such as Nuclear Magnetic

Resonance (NMR) for the study of fluid motion through porous media. Callaghan *et al.*, [1991; 1992] have investigated the diffusion of water in a bed of loosely packed polystyrene spheres (with a diameter of 13-19 μm) by Pulsed Field Gardient Spin-Echo NMR. Northrup *et al.* [1992], seeded the flowing liquid with 10 μm fluorescent particles in a bed made of 3 mm beads. Gladden [1994] and Rigby *et al.,* [1996], used different NMR techniques to investigate beds of 1-10 mm loosely packed pellets used in heterogeneous catalysis, for pore structure, and transport phenomena. The primary purpose of most of the recent studies was the measurement of axial dispersion coefficients and porosity distribution in randomly packed columns with an aspect ratio (the ratio of the bed diameter to particle diameter) of 1-30.

Knox and Parcher [1969] showed that a sharp increase in the value of the reduced HETP was observed for beds having aspect ratios smaller than 8. Vortmeyer and Michael [1985] consider that the flow profiles depend on the aspect ratio of the bed and that the similarity between small- and large-scale packed columns is questionable. The small aspect ratio of the packed beds used in the chemical industry, and the fact that the beds investigated by these authors were generated such that their structure be loose and random [Benenati and Brosilow, 1962; Venneti *et al.*, 1986; Callaghan *et al.*, 1991, 1992; Gladden, 1994] makes their results worth of reinvestigation for the case of chromatographic media. Most of these authors state that special care was taken to insure that the particles fill the

column loosely, in a random structure, and that no further compacting of the bed was sought. In addition, the flow of the mobile phase through chromatographic packings is in a range of Reynolds numbers many orders of magnitude smaller than the flow of fluids in columns used in the chemical industry (see chapter 1.3).

In the case of a chromatographic bed, the aspect ratio of the packing is orders of magnitude larger (250-5000). At the same time, the structure of the bed is very compact, and not random. It is determined by the uneven distribution of high stress applied to the packing material during column packing, as discussed later, in chapter 1.4.2.

The flow of fluids through such beds is governed by the laws of hydrodynamics through porous media, but altered by the particular features of the chromatographic media. In general, the average linear velocity, *u,* of a viscous fluid percolating through a packed bed under a pressure drop ΔP is given by Dracy's law:

$$u = \frac{k_0 d_p^2 \Delta P}{\eta L} \qquad (1.2.1)$$

where η is the viscosity of the fluid, d_p is the particle size of the packing material, L is the length and k_0 the permeability of the bed. As a consequence, the total volume throughput of fluid, F, of viscosity η, flowing through a packed bed of cross-sectional area A, total porosity ϵ_T, and length L, under a pressure drop Δp is given by the expression [Bristow and Knox, 1977]:

$$F = uA\epsilon_T = \frac{k_0 d_p^2 \Delta p}{L\eta}\pi r_c^2 \epsilon_T \qquad (1.2.2)$$

The local velocity of the mobile phase -- according to widely accepted views among chromatographers,-- follows the Poiseuille law in the narrow channels between adjacent particles of packing material. In Poiseuille flow the radial distribution of the mobile phase flow velocity in straight channels has a parabolic shape, and velocities are nearly constant along these channels, at a constant distance away form channel wall. At the same time, at channel walls the fluid velocity is considered to be zero. The Poiseuille model is a good approximation for the flow of fluids in open circular tubes. It gives an analytical solution for an idealized situation. This model has to be modified as soon as the flow space has a different cross-section, by adding correction terms. Booji *et al.*, [1995] showed that simple laser-Doppler velocimetry measurements in pipes having a rectangular cross-section prove that the Poiseuille profile does not hold anymore in this case.

The same considerations suggest that what may be true for the flow of a fluid in laminar regime through straight circular capillaries having a well defined diameter may not hold for chromatographic media. In the case of a porous bed the last condition is definitely not met, since the interparticle channels are not straight capillaries, their diameter is changing with position.

1.3 The Structure of the Chromatographic Bed

The size and relative location of the pores, channels, and cavities of a chromatographic bed determine the rate of the fluid flow and the nature of the various dispersion and mass transfer phenomena. All these interrelationships have an important role in the effectiveness of any separation. It would be most desirable to be able to define a geometrical quantity that would characterize the pore system in any porous medium. Unfortunately, the pore system of a porous body forms a very complicated surface, one that is difficult to describe geometrically.

Intuitively, one would like to talk about the 'size' of pores, a convenient measure of the 'size' being the 'diameter'. However, the term diameter makes sense geometrically only if the pores are of spherical shape, unless some further specifications are made. If we consider the flow of fluids through interparticle space, the pores must be visualized instead as rather tube-shaped voids. One would then call the diameter of such a tube the 'pore diameter'. Unfortunately, this visualization of the term diameter is again geometrically quite meaningless unless the tubes are cylindrical. In general they will not be so, and (which makes matters worse) they will not even possess a pattern for their cross-section since the walls will be irregularly diverging and converging [Scheidegger, 1974].

With randomly arranged channels, a small element of fluid in laminar flow will zig-zag erratically as it strives to avoid the solid particles in its path. While moving along such a channel, the volume elements of the fluid would do so at a constantly

changing local velocity, depending upon the local size of the 'pore diameter' they are crossing at a given moment. These elements of fluid would also constantly change their relative positions, when filling a larger void, or immediately next, while squeezing into the narrow space situated between two adjacent packing particles. Thus, in reality, the fluid is not moving in a capillary as in Poiseuille flow, since the interconnecting voids generate a tortuous streampath which does not have continuous walls. It's the local 'diameter' which determines the local flow rate (*i.e.,* local linear velocity), and which changes constantly and erratically. The moving fluid can fill this nondescript space only by rearranging its elements constantly. The resulting constant mixing inside the interparticle channels is resembling to some extent to that encountered in turbulent flow, with the capital difference that it does not involve the whole volume of fluid, but it is limited to the volume of fluid moving in a particular interparticle channel, and it's not the energy state of the fluid elements responsible for this mixing, but the chaotic change in flow space characteristics (such as volume and direction of flow) throughout the bed.

In granular materials like those found in packed chromatographic columns, turbulence starts more readily as a result of the irregularity of the flow pattern. However, turbulence does not occupy suddenly all regions of flow space. Instead, turbulent conditions may be envisioned as beginning in a few of the larger void spaces between particles and gradually spreading throughout the remaining void regions as the velocity increases. This growth occurs mainly in the range of values for the Reynolds number of Re = 1-100 [Bear, 1972]. Some authors put the lower

limit for the Reynolds number for which the flow in porous media becomes turbulent to 0.1 [Scheidegger, 1957; Lambe and Whitman, 1969]. This number -- expressing the ratio of inertial to viscous forces -- is used as a criterion to distinguish between laminar and turbulent flow through conduits. By analogy, a Reynolds number is defined also for flow through porous media:

$$Re = \frac{d\rho\bar{u}}{\eta} \qquad (1.3.1)$$

where *d* is some length dimension of the porous matrix. Although, by analogy to the Reynolds number for pipes, *d* should be a length dimension representing the elementary channels of the porous medium, it is customary to employ some representative dimension of the grains, like the mean particle diameter, d_p, for *d* [Bear, 1972].

In HPLC the typical value for *Re* (calculated using for *d* the mean value of the particle size, d_p) is 0.001-0.005, which corresponds to 'creeping flow'. When one or more of the mobile phase components are liquids of high viscosity, and the chromatographic column is operated at low linear velocities, the Reynolds number can be as low as 10^{-6}. Consequently, any significant turbulence involving the bulk of the fluid flowing through the packing of high performance liquid chromatographic columns is out of question.

Now if we think of the flow regime inside the interparticle channels as laminar flow -- which is "nonturbulent flow of a viscous fluid in layers near a boundary",--

than the movement of the mobile phase through the pores of a chromatographic bed can hardly be considered as such. The flow in chromatographic columns is definitely nonturbulent (as indicated by the low values for the Reynolds number), since the volume elements of the liquid do not possess the kinetic energy required to overcome the viscous forces governing the flow. It is the "flow... in layers" that does not fit in the picture. The structure of the chromatographic packing, being very different from the flow space of an open capillary, is responsible for inducing a constant mixing of the fluid elements inside the interparticle channels, which is not compatible with a flow in layers.

All interconnecting tube-shaped voids add together into a total volume available for the fluid to flow through, defining its residence time inside the chromatographic packing at a given value of the flow rate. The ratio of total void to total column volume is called *porosity.* If the calculation of porosity is based upon interconnected pore space- which is accessible for the mobile phase- instead of total pore space (which includes the unaccessible intraparticle pore volume too), the resulting quantity is termed the *effective* porosity. The effective porosity has two components: one corresponding to the sum of the volumes of all accessible intraparticle pores (*i.e.*, the internal porosity, ε_i), and a second one corresponding to the sum of the volume of all voids existing between particles, called inter-particle, interstitial or external pore volume (*i.e.*, external porosity, ε_e). The difference between the total porosity and the effective porosity gives the above mentioned

unaccessible intraparticle pore volume, ε_c, which is the sum of the volumes of pores formed during the synthesis of silica that have been closed at some stage of particle growth.

The measurement of the porosity of a granular material can be achieved by a great variety of methods. Among them, the *gas expansion method* (or pycnometry) gives the volume of solid material (including the volume of unaccessible pores) of a sample. From this volume the apparent density and the porosity of the material can be calculated. The basic principle of the gas expansion method is the direct measurement of the volume of air or gas contained in the pore space. This can be achieved by enclosing the specimen of known bulk volume and a certain amount of gas in a container of known volume under pressure, and then connecting this container with an other one of known volume and which has been evacuated. The new pressure of the system is read off and permits one to calculate immediately from the ideal gas law the volume of gas that was originally in the porous medium [Scheidegger, 1974].

The gas expansion method is not suited for the measurement of the effective porosity of chromatographic columns. This parameter can be derived from the retention volume -- resulting from chromatographic data -- of an unretained analyte which is not excluded from most of the interconnected pore volume. Uracil in methanol mobile phase or benzene in methylene chloride as mobile phase can be used in the case of columns packed with octadecilsylane-modified silica (ODS columns).

Besides the total effective porosity, the average local velocity must also depend upon the frequency of pores of a specific diameter encountered along the stream path. The pore size distribution is defined as the fraction $\alpha(\delta)$ of the total pore space that has a 'pore diameter' between δ and $\delta+d\delta$. The method most frequently used for its determination is that of injection of mercury into the pore system. In this manner, a capillary pressure curve is obtained which, in turn, can be interpreted in terms of pore size distribution [Scheidegger, 1974].

1.4 Chromatographic Column Packing Techniques.

The procedures used for the packing of columns for high performance liquid chromatography are dry packing, slurry packing and packing under stress (axial, radial or annular). Dry and conventional slurry packing is used for most analytical and some preparative columns [Poole and Poole, 1993]. Dynamic mechanical compression, either in the axial [Roussel-Uclaf, 1976; Godbille *et al.,* 1976; Colin *et al.,* 1990; Wu *et al.*, 1994; Sarker *et al.*, 1995, 1996], the radial [Little *et al.,* 1976; McDonald *et al.,* 1980, 1981; Rausch *et al.,* 1980; Sarker *et al.,* 1994, 1996] or annular direction, is used for packing wide bore columns meant to be used for preparative applications (radial compression has also been used for analytical columns [Little *et al.,* 1976; McDonald *et al.,* 1980; Rausch *et al.,* 1980]). All these packing techniques involve the application of a certain level of mechanical stress

to the particles, either individually (in the slurry) or as a group (in the growing bed). The magnitude of this mechanical stress is widely different depending on the axial and radial position inside the column. The local values of the packing density, the external porosity and the permeability are a function of the history of the local stress applied during packing and during the life of the column [Guiochon *et al.*, 1995]. This could provide for a general mechanism explaining all the factors considered above.

Experience suggests that column beds are sometimes unstable. Cavities of various sizes develop at the column inlet, resulting in a dramatic loss of efficiency due to intense, local convection of the liquid phase in these cavities. This is attributed to the packing being too lose at the beginning of column operation. In most cases, these troubles seem to be associated with the application of insufficiently intense vibrations to the bed when a dry packing technique is used [Sie and van den Hoed, 1969; Prusiewicz *et al.*, 1982; Klaviter *et al.*, 1982] or with an insufficiently high packing pressure (hence packing fluid flow rate) in slurry packing methods [Poole and Poole, 1993]. In both cases, the bed consolidates progressively, its overall packing density increases, its external porosity and its permeability decrease. The packing density of a column bed depends on the packing conditions and may vary significantly when those are not maintained constant. There are no reasons, however, for these conditions to be uniform throughout the bed in the absence of an appropriate averaging mechanism [Guiochon *et al.*, 1995].

1.4.1 Slurry Packed Columns

In the first procedure columns are packed by forcing a more or less dilute slurry (ca 5-30% packing material suspended in a solvent such as methanol, isopropanol, etc., which wets and disperses well the material [Bristow, 1978; Unger, 1979; Poole and Poole, 1993]) into the column, and which has its exit end closed with a frit. A pushing solvent is pumped at high flow rate, under a head pressure of up to 800 atm into the slurry container and then through the column pointing either upward or downward [Kamiński *et al.*, 1982]. Bed consolidation is achieved by running the pushing solvent for 15-30 minutes through the packing.

The interaction between the particles and the high velocity fluid stream has two origins. First, the particles in the slurry are carried rapidly by the fluid stream and impinge vigorously onto the rising surface of the bed. They get imbedded in it and find a metastable position. Second, the viscous shear of the fast moving stream of solvent pushes the particles forward and consolidates the bed. The extent of this consolidation is illustrated by the finding that the external porosity of the packed bed decreases linearly from 0.434 to 0.399 (a 10% decrease), with increasing pressure of the packing solvent, for columns packed with Zorbax 10 μm particles, under head pressures ranging from 72 to 770 atm. In the same time, the column permeability is decreased by 45%, a value that is in agreement with the Blake and Kozeny correlation which provides a relationship between column permeability, k, average particle diameter, d_p, the external porosity of the column,

ε_e, and the internal porosity of the column, ε_i:

$$k = \frac{d_p^2 \epsilon_e^3}{h_0(\epsilon_i+\epsilon_e)(1-\epsilon_e)^2} \qquad (1.4.1.1)$$

where h_0 is a geometrical constant depending upon the shape of the packing material particles [Bird *et al.*, 1960].

An estimate of the consolidation stress can be obtained by comparing the flow rates obtained under a given head pressure and the one achieved under inertial flow [Giddings, 1991]. The former is given by the Hagen-Poiseuille law, while the latter is the flow rate at which the mobile phase would percolate through the column under its own weight in a huge gravity field (or in a centrifuge). If these two flow rates are equal, the pressure gradient is equal to the inertia or gravity potential [Giddings, 1991]. Hence, $\Delta P = \rho G L$, where ΔP is the head pressure, ρ the packing solvent density, G the intensity of the inertial field, and L the column length. The result is independent of either the nature of the solvent, i.e., its viscosity, or the particle size of the packing. For isopropanol ($\rho = 0.785$ g/cm^3) and a 10 cm long column packed under ΔP = 770 atm (i.e., 10000 psi), G is an enormous 100 000 g. Thus, it is not surprising that beds consolidate to a considerable extent under such high levels of stress. One fact neglected in this calculation is that the bed and the fluid filling the interparticle voids are compressible and that the exact column length is most probably a function of the mechanical stress applied. When the flow is stopped at the end of the packing operation, the

column length may rebound slightly. It will probably contract again as soon as the flow is resumed, and the extent of the contraction at any moment will be determined by the magnitude of the flow at that time.

Finally, the reproducibility of the external porosity of the bed (*i.e.*, of its packing density), and at the same time of the other properties of columns packed by slurry methods, is only fair [Stanley *et al.*, 1996; Guan-Sajonz *et al.*, 1996]. It is typically about 1 and 2% for 4.6 and 10 mm i.d. columns, respectively [Stanley *et al.*, 1996]. Accordingly, the reproducibility of the retention factors measured on a series of columns packed and operated under the same conditions is only fair, again. Surprisingly, however, this reproducibility is not much different from the day-to-day reproducibility of the retention factors on any individual column [Stanley *et al.*, 1996]. There seem to be several parameters which are not controlled well enough during the packing and operation of HPLC columns.

1.4.2 Axial Compression Columns

These columns are similar to huge syringes which have their barrels filled with packing material. Their piston is moved by a hydraulic jack which can apply a mechanical stress adjustable up to *ca* 100 kg/cm^2 [Godbille *et al.*, 1976; Colin *et al.*, 1990; Sarker *et al.*, 1995]. The column barrel is filled with a slurry (ca 30% of packing material homogeneously suspended in the packing fluid) and closed with a frit held by a bolted flange. When the piston is moved in order to compress the

slurry, the excess liquid is expelled at the end opposed to the piston and a consolidated bed builds up progressively. The force of the jack moving the piston causes a stress applied against one end of the packed bed. However, stress does not convey homogeneously in solids, whether divided or not, as it does in liquids and no mechanism guarantees that the local stress be constant throughout the bed volume. It has been shown by Train [1956; 1957; 1960] that the distribution of stress in a powder mass during its compression inside a cylindrical die is far from uniform in the entire volume of the resulting tablet. Under a compression stress equivalent to 45 kg/cm^2 applied to the piston located at the top of a 5.3 x 14.5 cm die, the local stress at the end of the bed opposite to the piston was approximately 15 kg/cm^2 (Figure 1.4.2.1). At the same time, this stress was 20 kg/cm^2 in the geometrical center of the bed, and against the piston wall, at its center. The stress increased with increasing distance from piston center toward the corner formed by the piston and the die wall. Three annular regions of increasing radii experienced a stress of 30, 40 and 50 kg/cm^2, respectively, with the highest stress measured in the very corner, in compassing the annular region situated between the limits $0.7xr_c$-$1.0xr_c$ [Train, 1957]

Sarker and Guiochon [1996], and Stanley and Guiochon [1996] have recently studied the consolidation of several conventional packing materials such as Hyperprep, Impaq, Kromasil, and Zorbax in chromatographic columns. The amount of dry packing material used for each column was measured before slurrying it. The volume of solvent expelled and the position of the piston were recorded while the

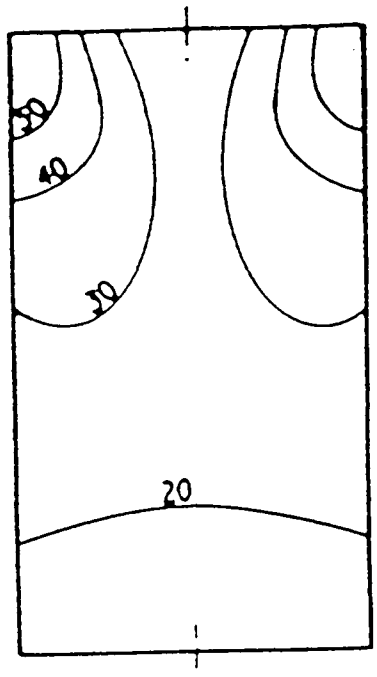

Figure 1.4.2.1 Plot of the distribution of stress (in kg/cm^2) in a powder mass during its compression inside a cylindrical die (under an applied pressure of 45 kg/cm^2). Source: D. Train, "Transmission of forces through a powder mass during the process of pelleting", in *Transactions. Institution of Chemical Engineers*, **35**(1957), 263.

axial stress applied to the bed was increased progressively from a 0 to nearly 100 kg/cm^2, by steps of a few to about 10 kg/cm^2. This allowed for the determination of the packing density as a function of the axial stress applied. The results obtained depended much on the nature of the specific packing material studied and on whether it was a first compression process or a recompression of a bed previously consolidated under the same or a higher stress. Recompression of silica based materials was elastic, reversible, and gave values of the Young modulus which were of the order of 200 (Kromasil) to 460 (Zorbax) MN/m^2 [Stanley *et al.*, 1996]. These values correspond to those of fine sands.

For the first cycle of consolidation, the behavior of the bed depended on whether the particles of the packing material were irregular or spherical. A column of initial length of 25 cm, packed with irregular particles, shrunk by nearly 25% when the axial compression stress was raised from 1 to 80 kg/cm^2 [Fernandez *et al.*, 1995; Sarker *et al.*, 1996]; the corresponding Young modulus was an order of magnitude smaller than during further recompression. Under the same conditions, a column packed with spherical particles shrunk only by less than 10% [Stanley *et al.*, 1996]. The Young modulus in this case was only 20 to 50% lower than during the subsequent recompression of the bed. Furthermore, the kinetics of shrinkage caused by step increases of the applied axial stress was different for irregular and spherical particles. It took several hours for a column packed with irregular particles to reach a constant length upon an increase of the compression stress. This consolidation took place by chaotic steps of random height occurring at random

intervals in time [Fernandez *et al.,* 1995]. For columns packed with either roughly spherical particles or rugous spherical particles the time needed for bed consolidation was about one hour; during this time, the column length decreased both continuously and through a few random steps. Consolidation took less than a minute for smooth spherical particles and the process was monotonous [Sarker *et al.,* 1996]. Finally, little breakage of the spherical type of particles was observed, while abundant fragmentation and chipping of irregular particles took place under axial compression stresses of 80 kg/cm^2 or less [Fernandez *et al.,* 1995; Sarker *et al.,* 1996]. Aggregation of irregular particles into lumps stable under conventional ultra sonication has also been reported [Sarker *et al.,* 1996].

The packing density increases with increasing compression stress, while the external porosity and the permeability of the column decrease, in agreement with the Blake-Kozeny correlation [Bird *et al.*, 1960]. Particle breakage do not seem to contribute much to this effect [Guiochon *et al.*, 1995; Sarker *et al.,* 1996]. On the other hand, the nature of the slurry solvent is important for the packing density. The beds obtained with C_{18} silica particles are more compact when prepared with a slurry in n-heptane than with slurries in acetone, acetonitrile, 2-propanol, or methanol. However, using methanol, isopropanol, or acetone as packing solvent produced better columns (i.e., presumably more homogeneous ones) than using acetonitrile or heptane, although these solvents wet the packing material well. No obvious correlation was found between the overall packing density and the efficiency of the column. The column efficiency, which was measured on the bulk

eluent, not locally, is only moderately affected by the compression stress. It increases with increasing stress at low values of this stress and decreases at high values of the stress. Values of the reduced HETP close to 2 have been obtained with Kromasil [Sarker *et al.*, 1995]. For other packing materials, these values are usually close to 3, or even larger [Sarker *et al.*, 1995; 1996].

1.4.3. Radial Compression Columns

These columns use a plastic cartridge closed at both ends by frits and have a stream distributor at inlet. The cartridge is filled with the packing material and is placed inside a steel cylinder. The designs of the plastic cartridge and of the steel cylinder allow a leakproof seal at both ends. A hydraulic fluid is introduced under pressure to fill the space between the plastic cartridge and the steel cylinder and in this manner compress the bed radially [Little *et al.,* 1976; McDonald *et al.,* 1980; Rausch *et al.,* 1980]. Implementations of this method of bed compression are available for both analytical and preparative columns. Columns prepared with this procedure exhibit good performance [Eon, 1978; Sarker *et al.,* 1994, 1995, 1996; Carta *et al.,* 1995]. Measurement of the porosity and the permeability of these columns have demonstrated the strong influence of the intensity of the radial compression stress on these properties [Sarker *et al.*, 1994; 1996]. The external porosity of the bed decreases with increasing compression stress while the head pressure required to achieve a certain flow rate increases accordingly. This result

shows that the permeability follows the Blake - Kozeny correlation [Bird *et al.,* 1960]. Nevertheless, the effects observed here are smaller than in axial compression columns due to the fact that the design of the instrument allows only a much lower compression stress (100 psi versus 1500 psi in axial compression).

Although the geometry of the stress distribution in a radially compressed bed is more complex than in an axially compressed bed, a model has been proposed to relate the compression stress with the mobile phase flow rate, and the head pressure [Carta *et al.,* 1994]. This model is in agreement with experimental measurements obtained by Sarker *et al.* [1994; 1996]. It shows that the radial compression stress applied should correspond to a hydraulic pressure in the compression chamber in excess of half the head pressure. Insufficient compression levels result in dramatic failure in column performance, which is a result of cracks being formed in the bed. This model could be used, along with the independent data on the Young modulus acquired with axial compression columns, to relate the intensity of the radial compression stress to the distribution of the packing density throughout the column bed.

CHAPTER II

FLOW PROFILES IN CHROMATOGRAPHIC COLUMNS

2.1 Introduction

Most authors of basic references on fluid dynamics in porous media and more particularly in chromatography consider a thorough treatment of micro scale flow patterns in packed beds (see Figure 2.1.1 and the capillaric models of packed beds [Collins, 1961; Scheidegger, 1974; Vortmeyer and Schuster, 1983; Giddings, 1991]), but give only rather evasive descriptions of the overall flow profile over the column cross-section.

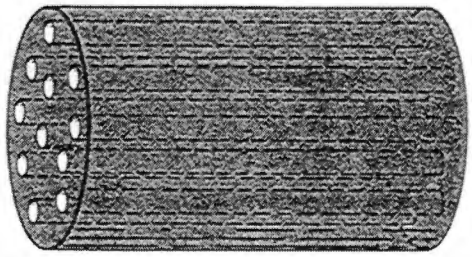

Figure 2.1.1 Capillaric model of a packed column. The flow space is assumed to consist of a bundle of parallel capillaries. Source: Giddings, J.C., "Unified Separation Science", Wiley, New York, 1991, 64.

One can read that "there is no general consensus on the precise flow profiles inside the packed bed" [Vortmeyer and Schuster, 1983], that "the complicated flow pattern in packed beds is not amenable to rigorous theoretical treatment", and that "the most uniform flow profile can be obtained when beds are packed *carefully* with spherical particles of equal size". Furthermore, such "a most uniform profile" would fall short of a surprise since "in well-packed columns the diversity of channel diameters and velocities in the individual channels is small" [Karger et al., 1973]. Complementarily, "poorly packed columns, in which the range of pore sizes is large, tend to have highly variable flow rates (that is, an erratic velocity profile) within the medium" [Giddings, 1991]. What usually remains in memory of this elusive description is that overall, the flow in packed beds is plug-flow. This means that simplistically, the distribution of the "average" local velocity (averaged out over $(10xd_p)^2$ area of column cross-section) supposedly has an overall flat profile across any diametral cross-section of the column. Such opinions are quite often heard in classrooms and in public discussions at meetings but could not be clearly documented in the scientific literature. As a matter of fact, one of the most popular textbooks on chromatography [Poole and Poole, 1993] does not have much to say on this issue. The most poignant approach is that of Karger, Snyder and Horvath [1973], who state bluntly that "the exact flow profile depends on the packing structure and *is not known*, but in practice this type of flow is often considered plug flow".

Today this (idyllic) picture has to be amended at least by mentioning the 'wall

effect'. The 'wall effect' is the consequence of packing heterogeneity resulted during slurry packing when a differential degree of sedimentation is induced by the proximity of the column wall [Farkas *et al.*, 1996]. The extent to which this effect distorts the mobile phase flow profile is arguable, especially in the case of large diameter columns, in which most of the packing material is filling a volume that is not situated close to the wall and consequently should not experience this wall effect during packing. Apart form this wall effect, there is now incontrovertible evidence that the core region of chromatographic beds does not experience an even flow. There is a significant dispersion in the value of the local velocity along the many tortuous stream paths which run more or less parallel to the column axis.

2.2 History of Research on Flow Profiles in Chromatographic Beds

In the early development stage of high performance liquid chromatography, Knox and Parcher [1969], and Knox et al. [1976] showed that packed columns are not radially homogeneous. Using a dual-(micro)electrode polarographic detector, Knox *et al.* [1976] were the first to demonstrate this phenomenon, by recording the elution of a band of p-nitrophenol at various radial locations, at the exit of a 11.7 mm i.d. column packed with 64 μm solid glass beads. These authors reported marked differences between the local values (which are averages of contributions taking place all along the column) of the residence time and of the apparent efficiency along a column diameter. Knox concluded that there is a region of the packing that

has different properties than the core. This region seems to be extending to *ca* 30 particle diameters from the wall, and is less homogeneous than the column core region of the packing. If the column is sufficiently wide in relation to its diameter and to the particle size, the molecules of a sample injected in the center of the column would not have time to reach the wall region before they elute. Thus, the zone would move in a highly homogeneous packing in the center of the column, and the column performance would be as good as if the wall region were not existent and the packing were entirely homogeneous. By contrast, if a significant proportion of the molecules in a zone can reach the wall region and experience the dispersive effect of this different and less homogeneous part of the packing, the apparent column efficiency drops markedly [Knox *et al.*, 1976]. Knox *et al.* recommended the use of columns having a diameter in excess of four standard deviations of the radial dispersion of a centrally injected band. For all practical purposes, these columns would be equivalent to "infinite diameter columns" [Knox *et al.,* 1969].

The technological developments of liquid chromatography have made this approach practically impossible to operate analytical instruments with central injection. Conventional 1/4" o.d. columns are somewhat long and narrow, making marginal the achievement of the infinite column diameter condition. A 250x4.6 mm column packed with 10 μm particles has to be operated at a reduced velocity, ν, in excess of 5 (ν should exceed 2 with d_p=5 μm, 20 with d_p=20 μm) to satisfy the infinite diameter column condition [Knox *et al.,* 1976]. Since these columns are

usually operated at reduced velocities around 8 in most analytical applications, the condition would be satisfied provided the injection was made at the very center of the column inlet and the diameter of the injected pulse was very small. In reality, since syringe injection has been universally replaced by valve injection, it is impossible to perform an axial injection. The sample band is carried into the column by the mobile phase stream which flushes the content of a sample loop and spreads the injected sample over the entire column inlet cross-section. The use of valve injection is not compatible with the operation of any column under the "infinite diameter column" mode.

Later, Eon [1978] studied radial dispersion in chromatographic columns and confirmed most of these results. Eon [1978] also showed that the variance of the values of the efficiency measured at constant radius, in eight different positions equidistant to the column center, increases with increasing value of the radius, suggesting increasing packing disorder from the center to the wall of the column. Furthermore, he showed that radial dispersion proceeds at a slower pace than axial dispersion. This is in agreement with the results of Knox *et al.* [1976] and with the general results derived from thin layer chromatography [Geiss, 1987]. However, his careful measurements demonstrated that, as a larger and larger fraction of the sample penetrates into the wall region, the column HETP appears to increase with increasing column length instead of remaining constant, which is a basic tenet of the theory of linear chromatography. This fact may explain various inconsistencies found in the literature regarding the plate height equations and, in Eon's opinion,

casts some serious doubts regarding the validity of the conclusions of many publications made in this area [1978]. Finally, Eon [1978] showed that radial compression improves markedly column performance, presumably because it reduces the difference in packing density between the wall region and the column core.

Both Knox *et al.* [1976], and Eon [1978] studied dry-packed columns, and found that the average mobile phase velocity and the column HETP were higher at the wall of the column than in its center. There is now incontrovertible evidence that slurry-packed chromatographic columns are not radially homogeneous either [Baur *et al.*, 1989; Farkas *et al.*, 1994, 1996; Bayer *et al.,* 1989; Tallarek *et al.*, 1995; Fernandez *et al.*, 1995]. While the results obtained by Knox *et al.* [1976], and Eon [1978] with dry-packed columns are mostly similar to the ones published later [Baur *et al.,* 1988, 1989; Farkas *et al.,* 1994] on slurry-packed columns, some important differences arise. With slurry-packed columns, the hold-up time and the HETP are both higher close to the column wall than in its center. The difference between the flow velocity distribution in dry- and slurry-packed columns is probably related to differences in the bed structure induced by these packing procedures, as discussed in Chapter 1.4.

More recently, NMR imaging of solute bands during their migration along chromatographic columns has shown considerable differences between the 3-D-profiles recorded experimentally for these bands and the flat profiles usually assumed in theoretical discussions [Fernandez *et al.*, 1995; Tallarek *et al.*, 1995;

Bayer *et al.,* 1995]. In some cases, the differences are due to flow perturbations caused by the viscosity difference between the pure mobile phase and the solution of the feed components [Femandez *et al.,* 1995]. Even when these differences are negligible, however, the bands were found to look somewhat like canvass walls in a stormy wind [Bayer *et al.,* 1995]. The profiles exhibited many local irregularities superimposed on a general trend which is not planar. The local thickness of the bands corresponded to values of the reduced column HETP on the order of 1.2 to 1.5, while the average value given by a bulk detector was on the order of 3 [Tallarek *et al.,* 1995].

Recent experimental results show that in efficient analytical size columns the radial distribution of the local velocity and the local column efficiency across the outlet cross-section of the column exhibit a cylindrical symmetry and that the length of the projection of the velocity distribution onto the column axis is relatively small for such columns (*i.e.*, that there are small differences in the average velocity of molecules moving along different stream paths). Furthermore, the more efficient a particular column, the higher the degree of radial symmetry which is exhibited by its flow pattern [Bayer *et al.,* 1995; Farkas *et al.,* 1996].

CHAPTER III

THE INVESTIGATION OF FLOW PROFILES IN CHROMATOGRAPHIC COLUMNS

3.1 Introduction

The flow profile is the image of the redistribution of the mobile phase volume elements during their travel through the column packing. It is impossible to monitor the movement of these elements with a detection system commonly used in chromatography. In fact these detectors are designed so that their response to the mobile phase be as small as possible. In the same time, these detectors monitor promptly the passage of analyte molecules carried along by any mobile phase volume element. If these molecules travel along the column all the time with the liquid element they entered the column with, they can function as markers of the mobile phase propagation through the column. The three dimensional redistribution of the concentration maximum within the band of an unretained analyte exiting the column should reflect the flow profile inside the chromatographic column.

In all previous work single channel detection has been considered for mapping out the three dimensional shape of an analyte band. This means that during one run, one series of data points was collected at one point of the column exit, and compared later to data points collected in other points during subsequent runs. In this manner any variations in experimental conditions between runs could

influence the differences resulted from data comparison. For this reason, we decided to map out the flow profile inside the column by performing local, multiple-channel detection, with a number of parallel detection channels increasing with increasing column diameter. This approach can compensate for inevitable experimental variations in the peak height, area, shape and retention time which are usually encountered even when experimental conditions are maintained constant with special care.

How intrusive such a measurement system can be for the targeted flow profile? Fluid dynamics [van Dyke, 1982] shows that the local perturbations of the flow pattern caused by the presence of the probes or concentration sensors take place well downstream the tip of the probes while the concentrations are measured at the probe tip (microelectrodes in an electrochemical detector, Farkas *et al.*, 1994) or in a volume element situated right in front of, and moving toward the probe tip (spectrofluorescence detection using optical fibers, Farkas *et al.*, 1996). Figure 3.1.1 shows that the axysimmetric flow past a Rankine ogive at a Reynolds number of 6000 based on the diameter, remains attached and laminar. Such a high value for the Reynolds number corresponds to a linear velocity of about 2400 cm/s for a standard 0.46 cm i.d. tube used for making chromatographic columns, and this value of the linear velocity is many orders of magnitude larger than the one chromatographic columns are operated at. In our case, the probe tips resemble more nearly the revolution body in Figure 3.1.2. In this case, still at a Reynolds number of 6000 based on the diameter, the flow is disturbed again only well behind

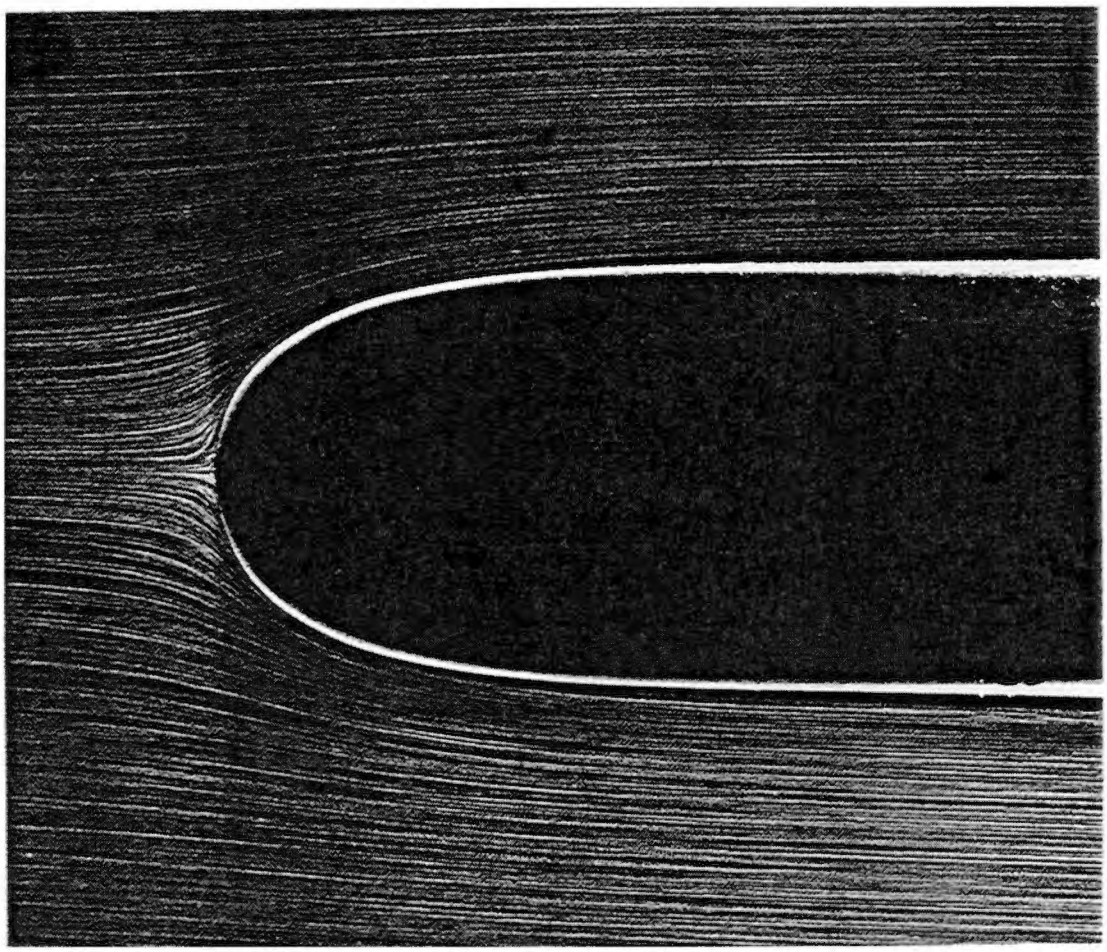

Figure 3.1.1 Axisymmetric flow past a Rankine ogive. At a Reynolds number of 6000 based on diameter, the flow remains attached and laminar. Streamlines are made visible by tiny air bubbles in water, illuminated by a sheet of light in the mid-plane. *ONERA photograph, Werle,* 1962. Source: M. van Dyke, "An Album of Fluid Motion", The Parabolic Press, Stanford, CA (1982).

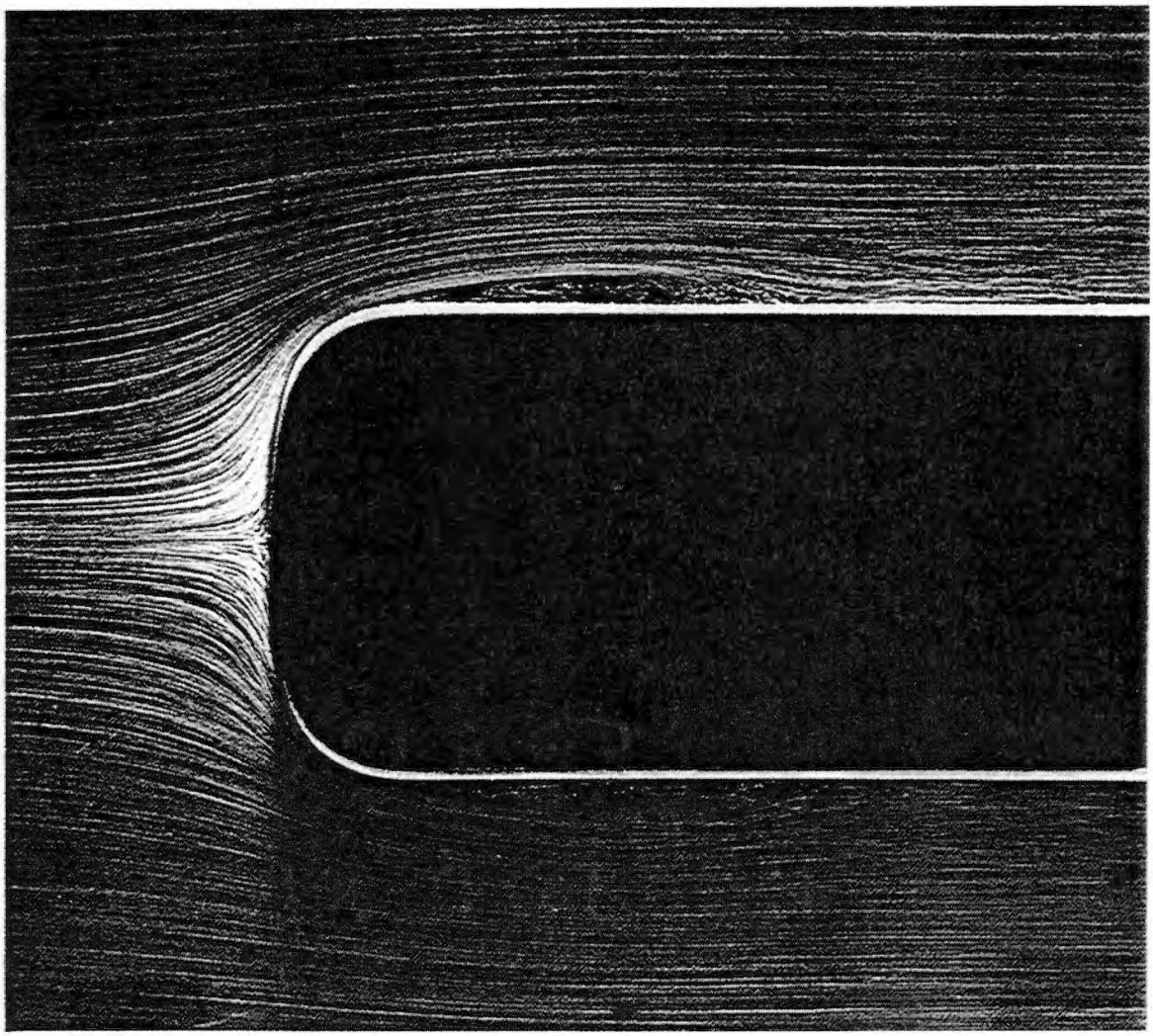

Figure 3.1.2 Boundary layer separation on a body of revolution. This shape is sufficiently blunter than a Rankine ogive of Figure 3.4.1 that, at the same Reynolds number of 6000 based on diameter and zero incidence, the laminar boundary layer separates. It then quickly becomes turbulent and reattaches to the surface, enclosing a short thin region of recirculating flow. Visualization is by air bubbles in water. *ONERA photograph, Werle,* 1962. Source: M. van Dyke, "An Album of Fluid Motion", The Parabolic Press, Stanford, CA (1982).

the blunt tip of the body. Considering that in a chromatographic column the regime is creeping flow (Reynolds number around 0.001, *i.e.,* much lower than 6000), we can assume that the presence of the probe tips in the stream does not distort at all the flow pattern and the results of the measurements.

3.2 Experimental Set-up Using Local Amperometric Detection

3.2.1 Detection Device

Conventional detectors measure the cross-section average composition of the bulk eluent at column outlet assuming band broadening is not caused by the detector. The distribution in axial direction of the analyte molecules in this bulk eluent leaving the column and heading for the UV-VIS detector in axial direction is classical. The determination of the radial distribution requires local, on-column determination of the analyte concentration at different points of the cross-sectional area, allowing for mapping of the analyte distribution over this area before all molecules reunite in the effluent, heading for the post-column bulk detector. Any post-column dispersion due to convection is eliminated in this manner.

Like Baur and Wightman [1989], we used electrochemical detection in the amperometric mode, with gold electrodes placed close behind the column outlet frit. The gold microelectrodes were prepared by inserting a 50 μm nominal diameter gold wire into a 25-30 mm long section of a 150 μm i.d. fused silica capillary tubing

(Polymicro Technologies, Inc., Phoenix, AZ). The space between the gold wire and the inner wall of the tube was filled with an epoxy resin (Epon (R) Resin 828-Shell Chemical Company, Houston, TX). The tips of the electrodes were polished with diamond paste (sizes 1 then 1/4). The other end of the gold wire was connected to a copper conductor by means of a silver epoxy connection (Epo-tek H20E-Epoxy Technology Inc., Billerica, MA), insulated with the same epoxy resin. Cyclic voltammograms were run with a BAS 100 Electrochemical Analyzer (Bioanalytical Systems, West Lafayette, IN) in order to assess for the actual surface area of the electrodes.

To avoid obvious electrical problems, the electrodes were inserted in holes drilled into a non-metallic frit (Upchurch Scientific, Oak Harbor, WA) made out of ultra-high molecular weight polyethylene placed at the outlet end of the chromatographic column. Four electrode tips were placed at different radial positions, facing a second, identical frit placed against the column packing and holding it when the external frit was rotated to permit the acquisition of other sets of data (Figure 3.2.1.1). One electrode was placed near the center of the frit, two other electrodes were placed at almost equal distance from the axis, at about r/2, in perpendicular directions, while a fourth electrode was placed close to the column wall (Figure 3.2.1.2). In order to acquire more data points over the column cross-section area, each experiment was made four times, and the holding frit was rotated by steps of 90° around the column axis between successive experiments. Thus, 16 data points were collected in each case. The electrode positions are shown in

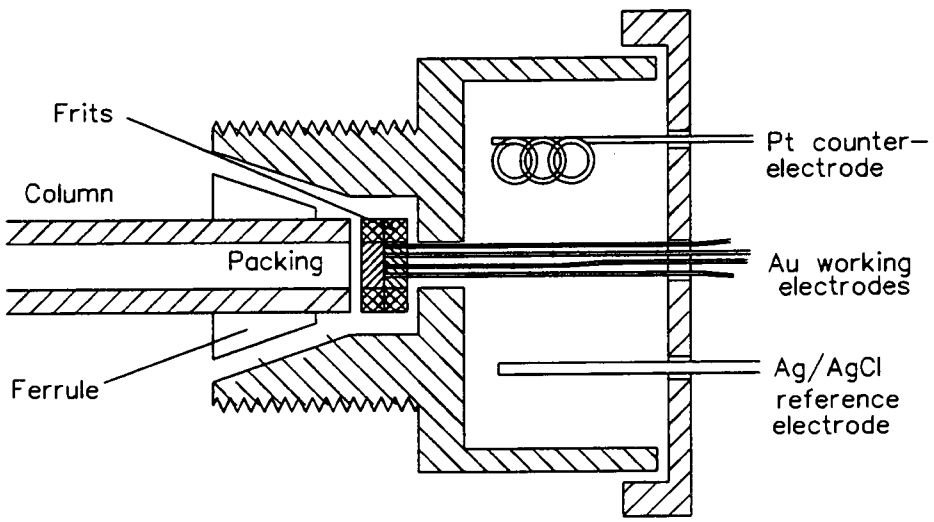

Figure 3.2.1.1 Modified column exit fitting used in the electrochemical detection system.

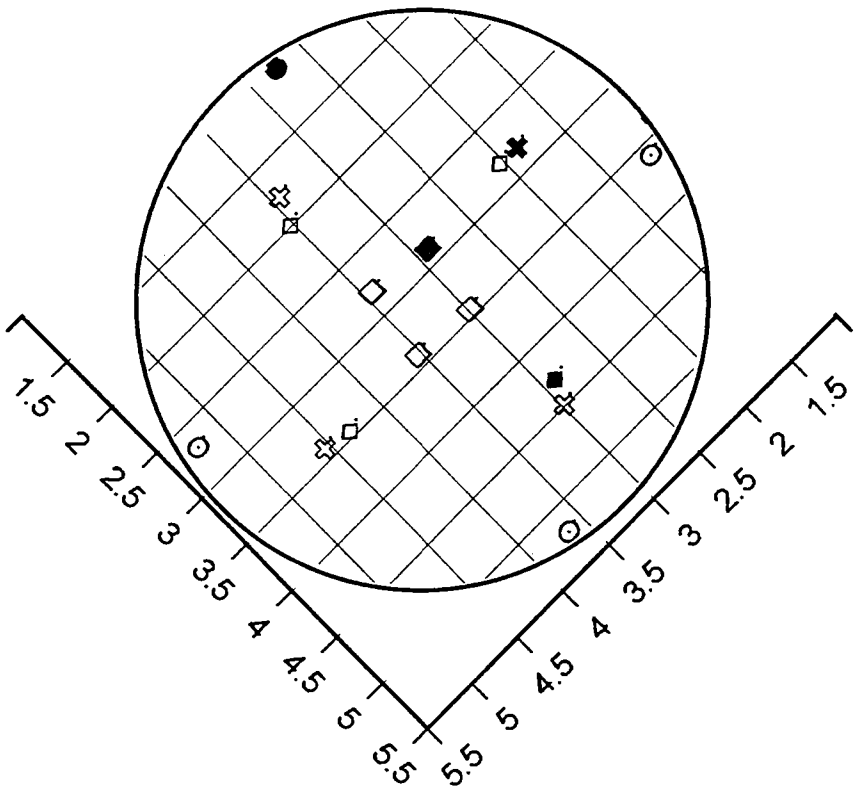

Figure 3.2.1.2 Positions over the column cross-section where the microelectrode tips were located initially, and after rotating the holding frit with steps of 90^0 around column axis. The locations marked with solid symbols are those where the analyte concentration was monitored during the same run, for a given position of the holding frit.

Figure 3.2.1.2, with the four solid symbols corresponding to the points where data was collected at one position of the frit.

When the polished electrode surface was investigated under microscope, all four electrode tips protruding slightly from the frit could be simultaneously brought into focus. Thus, the four electrode tips were approximately in the same plane perpendicular to the column axis. The outlet fitting of the column was modified in order to allow for a three electrode set-up, for the amperometric detection of electroactive analytes. A platinum counterelectrode, and a Ag/AgCl reference electrode were placed behind the outlet frit into the cup-shaped fitting (Figure 3.2.1.1). The output of each working electrode was amplified by means of a Voltammograph Model CV-37 (Bioanalytical Systems Inc., West Lafayette, IN). Systematic electrode fouling was experienced. The electrode tips were cleaned before each experimental run by sweeping the applied potential from -1 to +1V (electrolytic cleansing).

3.2.2 Liquid Chromatography Equipment

The chromatographic system consisted of a Waters (Milford, MA) HPLC Pump Model 510, a Spectraflow Model 575 Absorbance Detector (Applied Biosystems, Ramsey, NJ) as the bulk detector, when needed, and a Rheodyne (Cotati CA) HPLC injection valve Model 7010. The data of either the UV detector or the four electrochemical detectors were acquired using a Waters System

Interface Module with two A/D convertor boards permitting the simultaneous monitoring of four detectors. A Waters Maxima 820 version 3.3 software was used to collect the data at a rate of 10 data points per second. The data files were uploaded to one of the computers of the University of Tennessee Computer Center for further calculations.

3.2.3 Injection Profile

3.2.3.1 Investigation of the Injection Profile in Analytical Size Columns

The shape of the injection profile has a critical importance in this work. Significant spacial deviations of the profile of the injected plug of sample from the shape of a rectangular band propagating under plug-flow conditions would affect the elution profile as much as the lack of radial homogeneity in the column packing that we tried to investigate. It is important to determine the possible contribution of the injection profile to our results. The ideal injection profile for any chromatographic system would be a "rectangular band" having a constant concentration throughout its entire volume. The representation of this band in concentration-time coordinates corresponds to a pulse function of constant height determined by the concentration of the injected sample, and a width determined by the injection volume and the mobile phase flow rate. In the present study, this band should be narrow compared to the retention volume of the solute. However, any experimental injection profile differs somewhat from this ideal model, as discussed later.

The problem of the influence of the design and operating conditions of the injection device on the band profile has been lucidly discussed by Kirkland *et al.*, [1977]. Only the considerable improvements made during the last twenty years to the chromatographic equipment have affected the conclusions of his work. Modern columns are closed with a low porosity frit which is tightly compressed in the column inlet. This provides a relatively flat profile for the front of the injection band when it reaches the column inlet. Because of the parabolic profile of the flow velocity across the connecting tubing, the rear of the injection profile has also a parabolic shape. The use of a narrow, coiled capillary tube as sample loop enhances the radial diffusion inside this tube and contributes to alleviate the curved rear of the injection profile. It is not possible to rule out entirely at this stage a possible contribution of the injection band profile to the radial distribution of the solute concentration. However, this seems doubtful given the principle, design and mode of operation of the sampling valve.

Measurements of the electrode responses to the injection of samples in a column of length L = 0, resulted by removing the column with its packing and by placing the assembly of electrodes described earlier directly against the inlet frit and distributor disk inside the modified inlet fitting were expected to elucidate some of the questions related to the shape of the injection profile. The experimental data showed an almost flat injection band, although its axial profile was far from rectangular. Figures 3.2.3.1.1 and 3.2.3.1.2 show typical peaks recorded at column inlet under the same conditions as those used for the chromatograms discussed

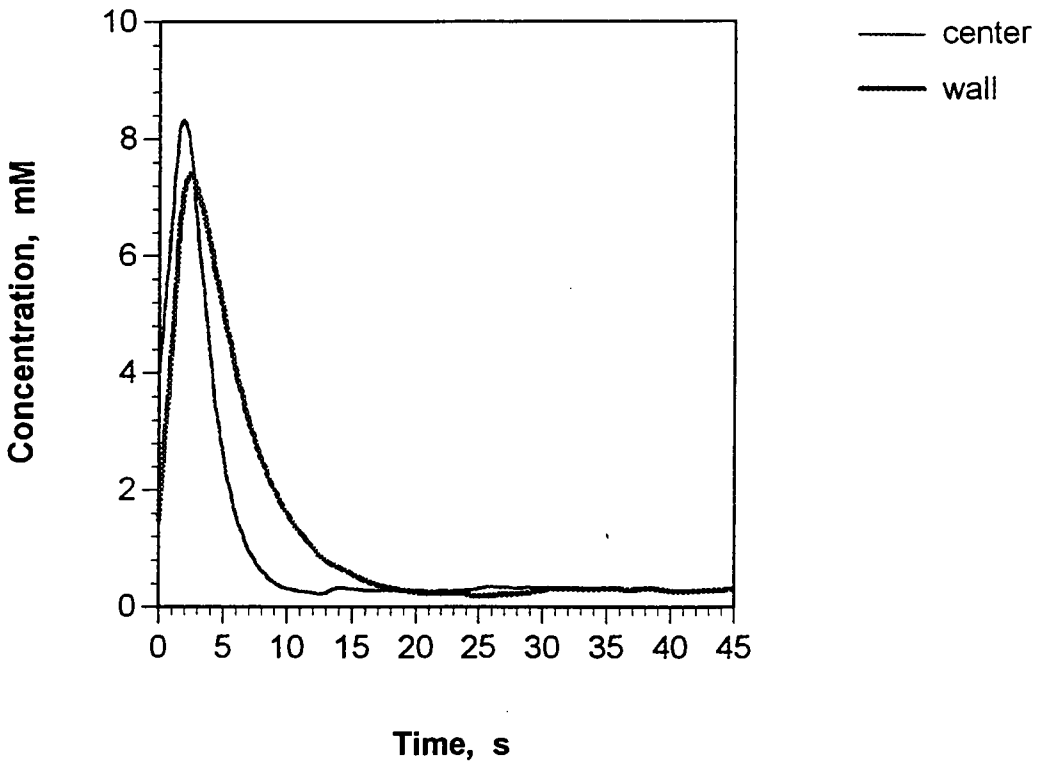

Figure 3.2.3.1.1 Injection profiles recorded with the electrode assembly placed right behind the inlet frit and distributor disk (column removed). Operating conditions: flow rate, 1 ml/min 0.1 M KCl in methanol-water 20:80; injection volume, 20 µl of 0.01 M p-benzoquinone solution in 0.1 M KCl in methanol-water 20:80.

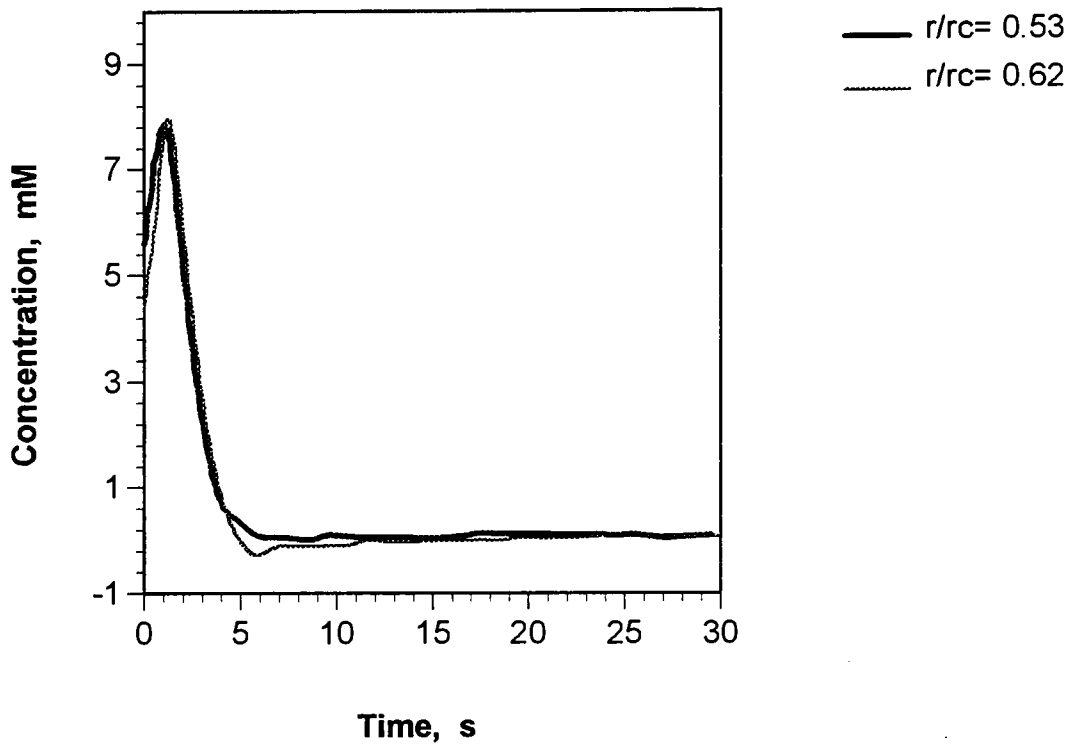

Figure 3.2.3.1.2 Injection profiles recorded with the electrode assembly placed right behind the inlet frit and distributor disk (column removed). These profiles were recorded with two electrodes placed close to each other at about half way between column axis and column wall. Same operating conditions as in Figure 3.2.3.1.1.

later in this report that were obtained with 10-24 cm long columns. The sample concentration rises and decays slightly more slowly along the column wall than in its center. However, there is little difference between the maxima of the two profiles and the delay between the maxima of the profiles recorded at the column center (first arrived) and along the column wall is on the order of 0.5 s only. This value is to be compared with values on the order of 12 s observed at the column exit between the residence times of the corresponding profiles at the column center and along its wall.

It is obvious that the shape of the bands generated by common injection devices is different from the ideal injection band described earlier. The experimentally detected peaks differ from a pulse function firstly by lacking a concentration plateau, at least in the case of analytical size injection volumes, and secondly, by exhibiting diffuse sides. The lack of a concentration plateau at column inlet right after injection suggests that the front and rear borders of an injection plug are rapidly eroded during and right after injection. This erosion starts during the transfer of the injection volume inside the loop of the sampling valve, and continues while the sample passes through the tubing connecting this valve with the column inlet, and through the inlet fitting itself, also. This fast decay is caused mainly by convection and also by molecular diffusion along the concentration gradients. Nevertheless, the peaks recorded at different radial locations at column outlet do not differ significantly, and this means that in this respect - of radial uniformity - the experimental injection profile emulates the ideal one. This demonstrates that the

results reported below are due essentially to phenomena taking place inside the column. The contribution of the equipment and, more specifically, of the injection device to these results is essentially negligible.

3.2.3.2 Investigation of the Injection Profile in Axial Compression Columns

In the case of preparative columns, the large size of the cross-section area allows a simpler and clearer determination of the distribution of the concentration density of the feed sample at column inlet. A sample of the silica used in the other experiments reported here was impregnated with a small amount of sodium hydroxide (in a methanol solution). The column was packed in the conventional way, using a methanol slurry of this modified silica. The thickness of the packing layer was approximately 7 mm. The column was operated with pure methanol at 25 ml/min. After one minute, an injection of 0.5 ml of a 1 mM solution of acetic acid in methanol was performed and the methanol flow was stopped after another minute. The packing bed was extruded from the column, cut with a cork cutter, and partitioned into four circular sectors and twelve regions (Figure 3.2.3.2.1) which were collected in separate vials. These twelve fractions were titrated for the amount of sodium hydroxide remaining per gram of the packing material. Each vial was dried to constant weight (which caused the silica to agglomerate tightly) , treated with a solution of 0.01 N hydrochloric acid solution (in excess) and the unreacted

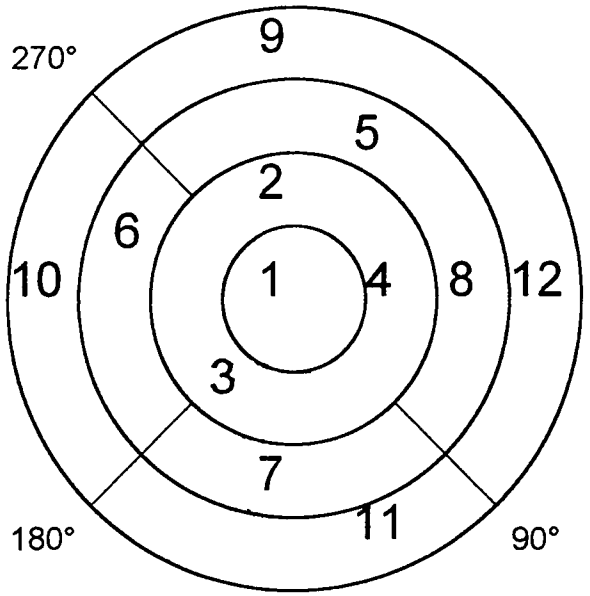

Figure 3.2.3.2.1 Fractionation of the layer of NaOH-modified silica for the determination of the concentration distribution at injection.

acid was back-titrated with a solution of sodium hydroxide in the presence of phenolphthalein.

Sodium hydroxyde reacts with silica and forms sodium silicate. The amount used here was much less than needed to transform the silica quantitatively. Sodium silicate formed by ion exchange at the silica-methanol interface, and could not dissolve into methanol. Although the solubility of sodium hydroxide in methanol is far from negligible (0.21 g/ml), no significant extraction by methanol takes place during the experiment, as confirmed by a blank experiment. Again, ion exchange takes place upon reaction with acetic acid. Back titration is required, however, because sodium hydroxide is released too slowly from the agglomerated dry silica obtained after drying and weighing. Sodium acetate is readily soluble in methanol and it does not affect the titration of a strong base in the presence of phenolphthalein. The results of the titration are shown in Table 3.2.3.2. They demonstrate that after injection of the acid sample, the sodium hydroxyde content of the treated silica remained even over the entire cross-section area of the column (relative standard deviation for the 12 fractions, 1.34%). This proves an even radial distribution of the concentration of the injected sample at the inlet of the preparative column, *i.e.*, a flat injection profile.

Table 3.2.3.2 Results of the investigation of the injection uniformity over column cross-section for the LC-50 column.

Sector number	Sample weight	mmol of NaOH/g sample
1	0.1843	0.667
2	0.4271	0.681
3	0.3579	0.660
4	0.4305	0.660
5	0.6832	0.661
6	0.8866	0.658
7	0.8945	0.671
8	0.8452	0.686
9	1.2055	0.656
10	1.0659	0.670
11	0.9616	0.670
12	0.8925	0.664
	Average NaOH load	0.667(σ_{n-1}=1.34%)

3.2.4 Chromatographic Columns

Most of the columns investigated here (having dimensions of 4.6x150-240 mm) were packed in our laboratory with commercially available packing materials. 40 µm glass beads (EM Separations, Gibbstown, NJ), 10 and 16 µm porous silica and C_{18}-modified silica (PQ Corporation, now BTR Separation, Wilmington, DE) were used. A Kromasil (Eka Nobel, Bohus, Sweden) KR10-16-C_{18} column packed by the manufacturer was also studied. All columns were tested in a conventional HPLC chromatographic system consisting of a Waters (Milford, MA) pump, a Rheodyne (Cotati, CA) injection valve, and a Spectraflow Model 575 UV-VIS absorbance detector (Applied Biosystems, Ramsey, NJ).

3.2.5 Chromatographic Mobile Phase

A 0.1M KCl aqueous electrolyte solution was used as the mobile phase, except for the reverse-phase columns packed with C_{18} silica. Since this material is poorly wet by water [Kőrösi *et al.*, 1980], 20% methanol had to be added to the mobile phase. This concentration was chosen because it was the highest at which the amperometric detector still worked satisfactorily. It was insufficient, however, to achieve good efficiencies with reversed phase columns. Figure 3.2.5.1 shows a conventional plot of the reduced height equivalent to a theoretical plate for benzoquinone (see next section) on this column as a function of the reduced

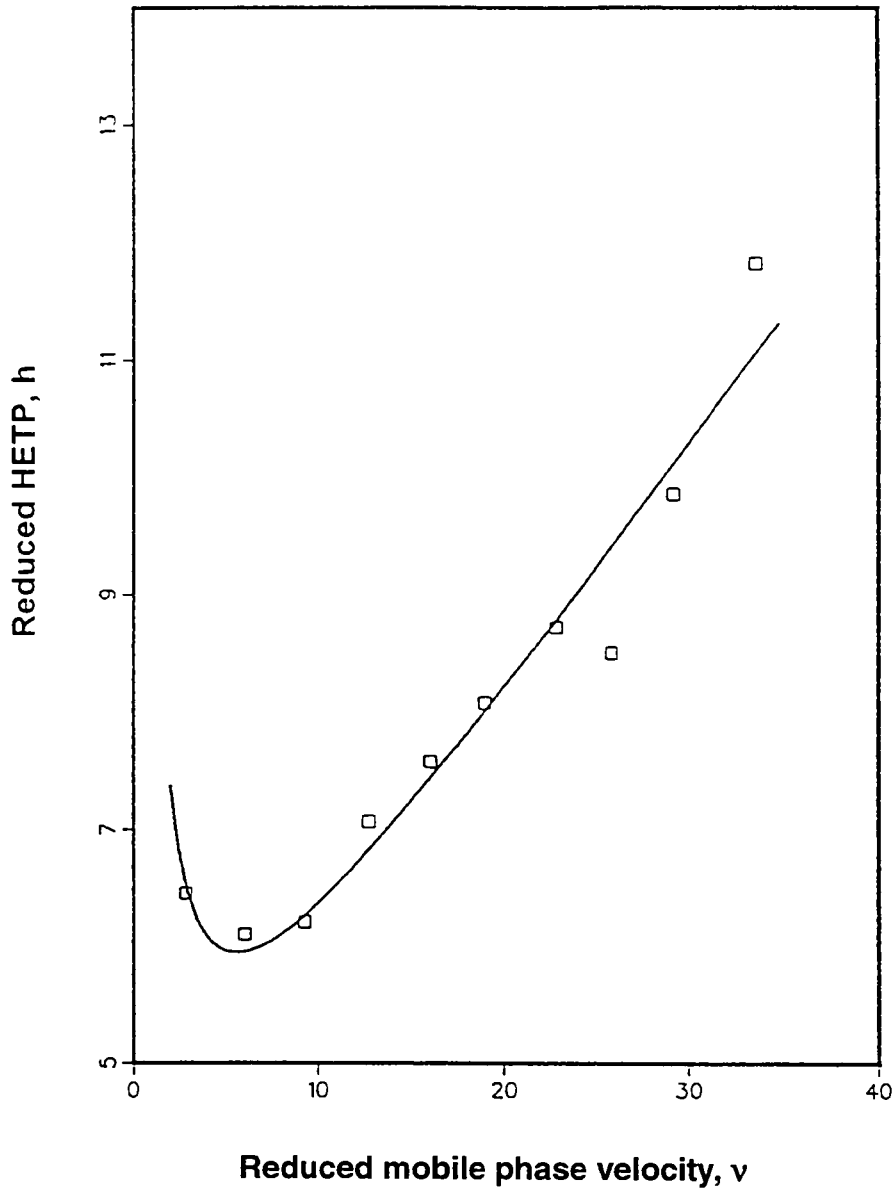

Figure 3.2.5.1 Van Deemter plot for the 4.6x150 mm Kromasil KRO100-16-C_{18} column packed with C_{18}-modified 16 μm particle size spherical silica; injected sample: 20 μl of 0.54 g/l p-benzoquinone (k'=0.3) solution in methanol-water 20:80.

velocity. The data plotted in Figure 3.2.5.1 were obtained with a UV-VIS detector, by calculating the column efficiency from the concentration profiles recorded when performing detection on the bulk stream of mobile phase. A 40% lower value for the minimum plate height was found for the same column and test analyte when a 40:60 water/methanol KCl solution was used as the mobile phase. The decrease in column efficiency with decreasing methanol:water ratio is related to the change in the value of the diffusion coefficient of the analyte in the mobile phase. The small value of the minimum reduced plate height suggests that this commercial column is well packed.

The use of a saline, water-rich solution as eluent for a silica column guarantees low or negligible retention factors for most analytes. Anyway, retention would not be a problem in this work, as we study the hydrodynamic properties of the packed bed. Their effects on band profiles is expected to be independent of the possible retention, and to contribute to the total band width following the rule of variance additivity [Sternberg, 1966].

3.2.6 Samples

As explained above, the molecules of a nonretained analyte will redistribute while migrating through the column packing in the same way as mobile phase molecules do. Thus, such an analyte can act as a marker for the movement of mobile phase volume elements inside the column. The samples were chosen to

optimize the behavior of the amperometric detector, since sensitive detection is not an issue here. Several electrochemically active compounds such as potassium ferricyanide, hydroquinone, and benzoquinone could easily be detected electrochemically under conditions satisfactory for our purpose. However, the corrosive electrolyte mobile phase required dissolves enough Fe^{2+} from the stainless steel column wall to form Prussian Blue with the ferricyanide analyte and to cause rapid fouling and clogging of the column and exit frit. This ruled out the use of the ferricyanide/ferrocyanide redox couple.

Dilute solutions of benzoquinone in the electrolyte solution used as the mobile phase proved to be much more stable than the readily oxidizable hydroquinone solutions. Because of the poor solubility of benzoquinone in the electrolyte solution used as mobile phase, low concentration (1×10^{-3} to 1×10^{-4} M) solutions were used. The applied potential difference between the working electrode and the reference electrode for optimum benzoquinone detection was -0.45V. 20 µl samples were injected during each experiment.

3.2.7 Calibration

Calibration proved to be the most difficult task of this work. In order to calculate the local concentration of analyte from the value of the current drawn during the experiment, the response factor for each microelectrode had to be determined. Cyclic voltammograms were run as mentioned previously, and from

the value of the resulting limiting current, the actual area of the electrode could be calculated. This parameter could be used for calibration only with due skeptism because of two reasons.

First, the gold surface of the electrode proved to be highly sensitive to electrochemical fouling that could not be entirely removed by rinsing or ultrasonication. This fouling reduced the active area of the electrode, hence diminished the response factor. Thus, a frequent, systematic electrochemical cleaning was necessary. However, each cycle of electrolytic polishing removes also a thin metal layer from the fresh gold surface, and later also small pieces of epoxy insulation around the electrode tip. As a consequence, the active area of the electrode increases in time. These two phenomena have opposite effects. Overall, we found that the limiting current increased significantly during the first week of using the electrode, and then decreased gradually to very small values because of irreversible surface deactivation. The cyclic voltammograms recorded before using the electrode, and after a few weeks of usage are shown in Figure 3.2.7.1, demonstrating the effects of an initial increase of the active electrode area, followed by electrochemical fouling of the electrode tip.

The electrode response factor could not be determined by elution experiments because, although the initial concentration of the injected sample was known, the local, actual concentration at the electrode tip was unknown since the analyte concentration could be radially redistributed during its passage through the column packing. Recalculating the actual electrode area after every short series of

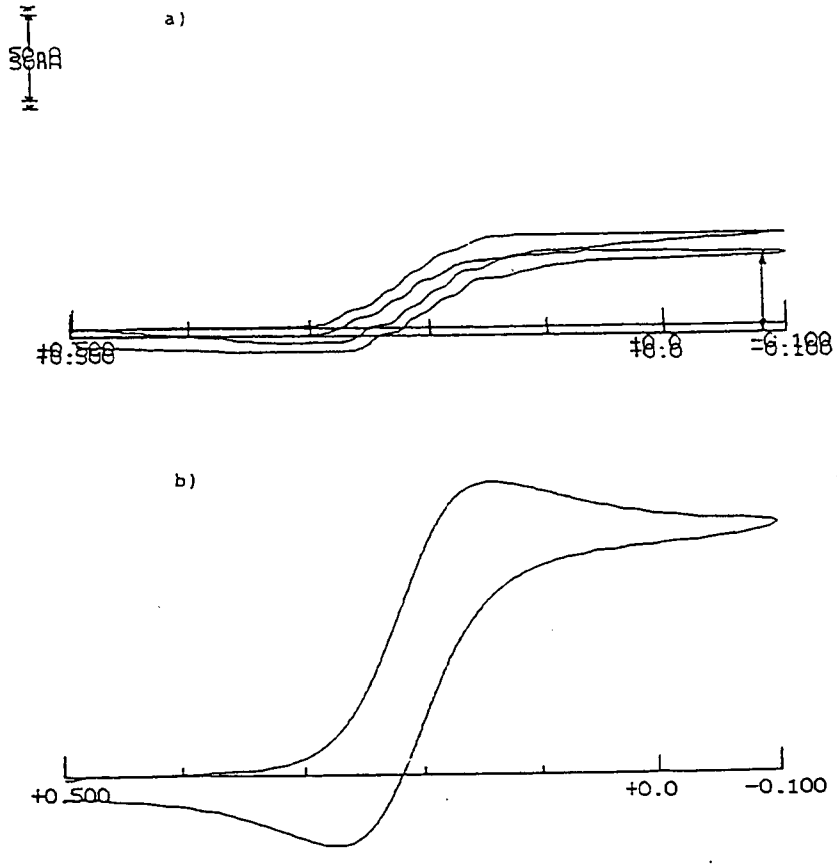

Figure 3.2.7.1 Cyclic voltammograms run (a) with the electrodes in their initial clean state, and (b) after one week of experiments. Solution, 0.05 M benzoquinone in 0.1 M KCl; scan rate: 20 mV/s.

experiments by running cyclic voltammograms under steady-state conditions was not practical because of the poor mechanical resistance of the electrodes.

Frontal analysis provides the only practical solution. In this case, the four electrodes are measuring the concentration of the same solution when the plateau at the injection concentration has been reached. This permits for the calibration of each electrode relative to the others at the beginning and end of each such experiment. However, the method is quite time consuming, and the extent to which it can be used is limited by electrode tip fouling, hence only a small number of calibration points can be acquired. Consequently, it was carried out only in connection with the measurements made for the determination of the radial distribution of the analyte concentration. Other experiments were performed without relating the signals of the individual electrodes to the solute concentration.

3.2.8 Procedures and Reproducibility

Each experiment consisted in the injection of a small, known amount of benzoquinone as a dilute solution, and the recording of the four electrode signals upon its elution. The experiment was repeated a number of times, after rotating the electrode holder by an angle of 90° between successive determinations.

The reproducibility of the experiment was reassessed periodically by performing series of injections without intermediate rotations, with successive rotations of 360° angles, and with successive rotations of 90° angles. The first

series of such experiments gives the reproducibility of the injection and detection systems. The results of one such experiment are reported in Figure 3.2.8.1. The profiles obtained are identical. The slight shift between the successive peaks is due to fluctuations in the delay between the manual actuation of the injection valve and of the data acquisition device. Table 3.2.8 shows the reproducibility of the differences between the retention times measured with two different electrodes (6 different pairs). Since the two electrodes placed $r_c/2$ away from the column center are at 90° angle, the difference between the residence time of their peak-maximum is small and less reproducible than for the other five pairs.

Table 3.2.8 Reproducibility of Retention Time Differences

Electrode Pair	Δt_R (sec)	σ (sec)	σ/t_R (%)
center-wall	7.23	0.53	7.2
center-midway1	2.10	0.10	2.8
center-midway2	3.90	0.25	6.5
midway1-midway2	1.15	0.36	32
midway1-wall	10.5	0.48	4.6
midway2-wall	7.80	0.40	5.0

Note: The injections were done without moving the electrodes between successive injections. Average and standard deviation of 8 experimental results. The reduced radial position of the electrodes (r/r_c) was: 0.18 (central); 0.53 (midway1); 0.62 (midway2); 0.94 (wall). (see Figure 3.2.1.2).

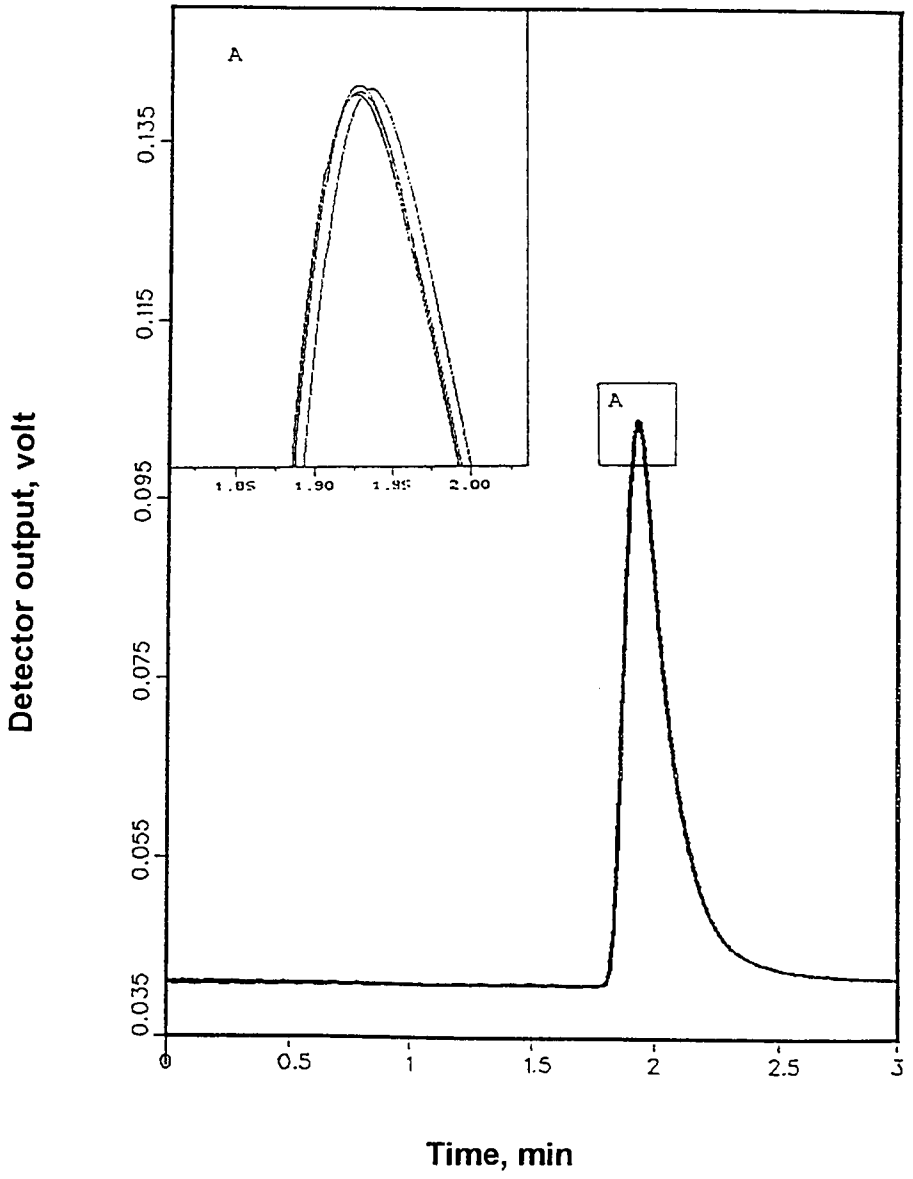

Figure 3.2.8.1 Reproducibility of measurements. Four successive chromatograms obtained with the central electrode, without moving the electrode assembly between successive measurements, overlaid.

The second series of experiments resulted in peaks that when overlaid, depict the contribution of the additional error made in repositioning the electrodes. Typical results are given in Figure 3.2.8.2 which shows essentially the same degree of repeatability. The results of the third series of experiments are illustrated in Figure 3.2.8.3, as plots of the difference between the retention times measured from the signal of the central electrode and from each of the three other electrodes. The repeatability of the signal of the central electrode is the same as in Figure 3.2.8.2, and its fluctuations are due to errors in the timing of the initial data point. This error does not affect the differences shown in Figure 3.2.8.3. The reproducibility of this difference under the conditions of Figure 3.2.8.1 is 0.3 s. The fluctuations seen in Figure 3.2.8.3, especially at the wall, demonstrate that the velocity distribution is not exactly cylindrical. Obviously, the fluctuations of the retention time observed across the column cross-section exceeds greatly the errors of measurements.

3.2.9 Remarks on the Experimental Set-up Using the Electrochemical Detection System

We wanted to extend this work to a systematic investigation of the behavior of large diameter columns used in preparative chromatography. The results of NMR imaging studies [Tallarek *et al.*, 1995; Bayer *et al.*, 1995] suggest that a rather large number of local measurements would be necessary for that purpose. Because of the considerable cost of the electronic devices required to operate electrochemical

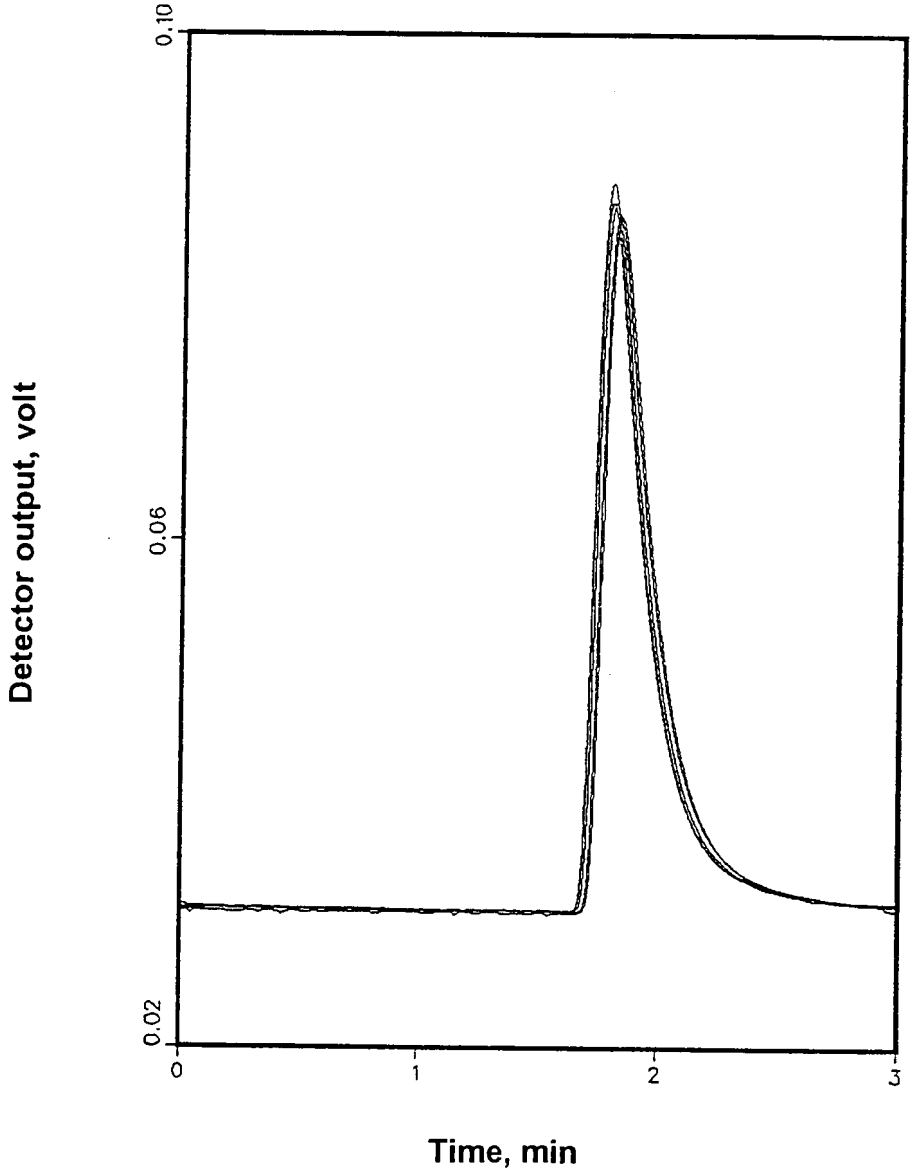

Figure 3.2.8.2 Reproducibility of measurements. Four successive chromatograms obtained with the central electrode, when rotating the electrode assembly with one full turn between successive measurements, overlaid.

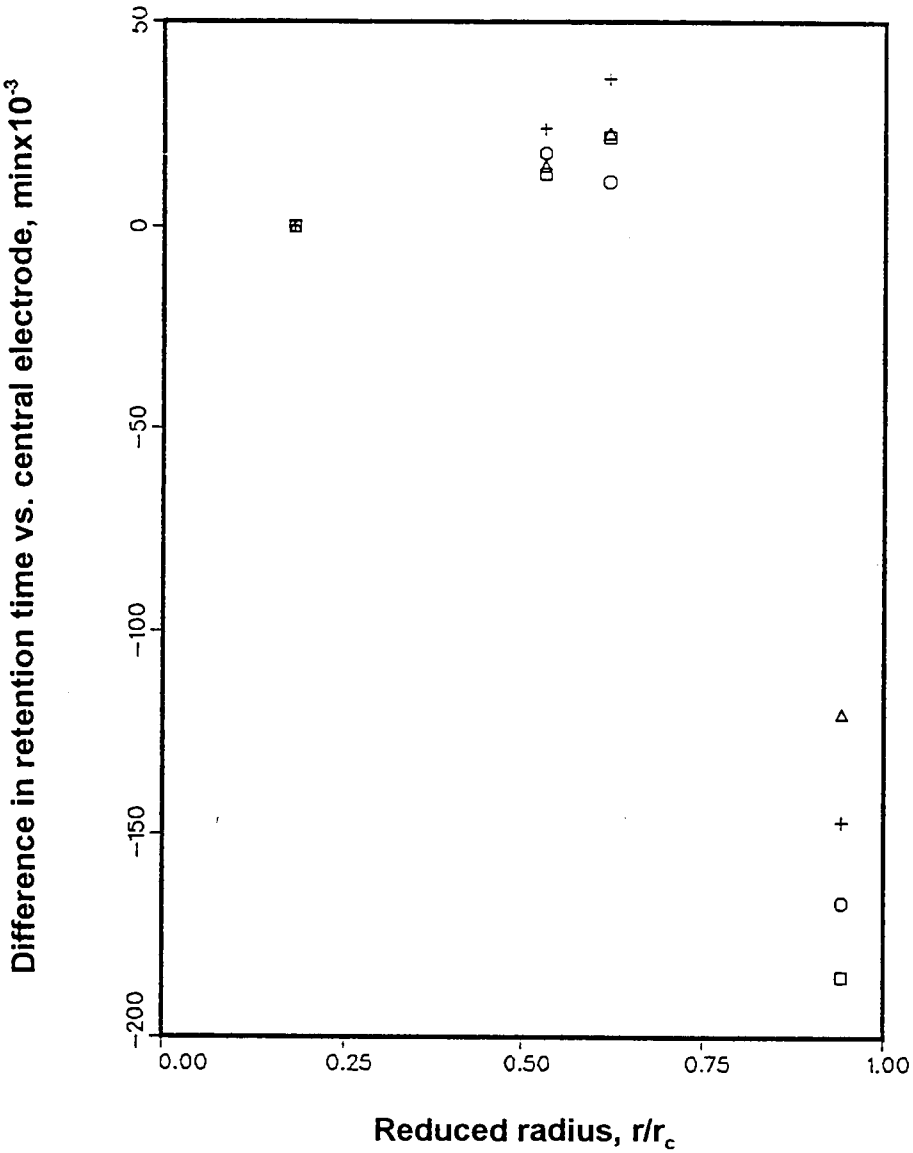

Figure 3.2.8.3 Reproducibility of measurements. Differences in the value of the retention time for peaks recorded by the central electrode and any of the other electrodes placed at four different positions on a circle of radius r/r_c.

detectors, it was impossible to use simultaneously more than the two double units of our original work [Farkas *et al.*, 1994]. Furthermore, a new instrumental set-up was necessary in order to overcome serious difficulties related to the electrochemical detection system used previously [Farkas *et al.,* 1994]. The gold microelectrodes proved to lack both mechanical and chemical stability. They broke easily, their response in time showed a fast decay, while electrochemical cleansing could not regenerate the electrode surface but for very few cycles only, by contrast with what previous authors have reported [Baur *et al.,* 1988, 1989; Krijči *et al.,* 1981; Knecht *et al.,* 1984; St. Caire *et al.,* 1985]. Replacing a microelectrode required a new calibration step. This way the continuity in data collection within a given set of experiments could not be insured.

3.3 Experimental Set-up Using Laser Induced Fluorescence Local Detection

3.3.1 Detection System

The local, on-column electrochemical detection system was replaced with local on-column laser induced fluorescence detection of an eluting laser dye analyte. The beam of an Argon ion laser is directed with optical fibers to locations of choice at the column outlet. The fluorescence signal induced by exciting the analyte molecules is collected by other optical fibers and carried to the appropriate elements of a photodiode-array. An electrical signal proportional to the amount of

light received by each photodiode was acquired and stored in a computer. The only requirement for choosing an analyte was that its retention factor be small on columns packed with conventional packing materials. The choice of a laser dye is beneficial on grounds of its high detection sensitivity. The use of optical fibers allows the easy selection of the locations where detection will be carried out. Each of the components of the system needs now to be described in detail.

3.3.2 Optical Fiber Assemblies

The new experimental design consists of a number of optical fiber assemblies inserted perpendicularly into the column exit frit (see insert in Figure 3.3.2.1.). Such extrinsic optical sensors are widely used for fiber optic remote, *in-situ* measurements. These sensors utilize the fiber as a means of transmitting light between the measurement instrumentation and an external transducer that is located within the sample, proximal to the opposite end of the fiber [Sepaniak *et al.*, 1988]. Direct sensors measure the inherent spectroscopic signals of the analyte of interest such as its absorbance or fluorescence [Coleman *et al.*, 1984; Sepaniak *et al.*, 1985].

In our case, each assembly contains two fibers, one of which carries the excitation light beam from the source to the investigated spot, while the other fiber collects part of the light signal emitted by fluorescence and transmits it to the

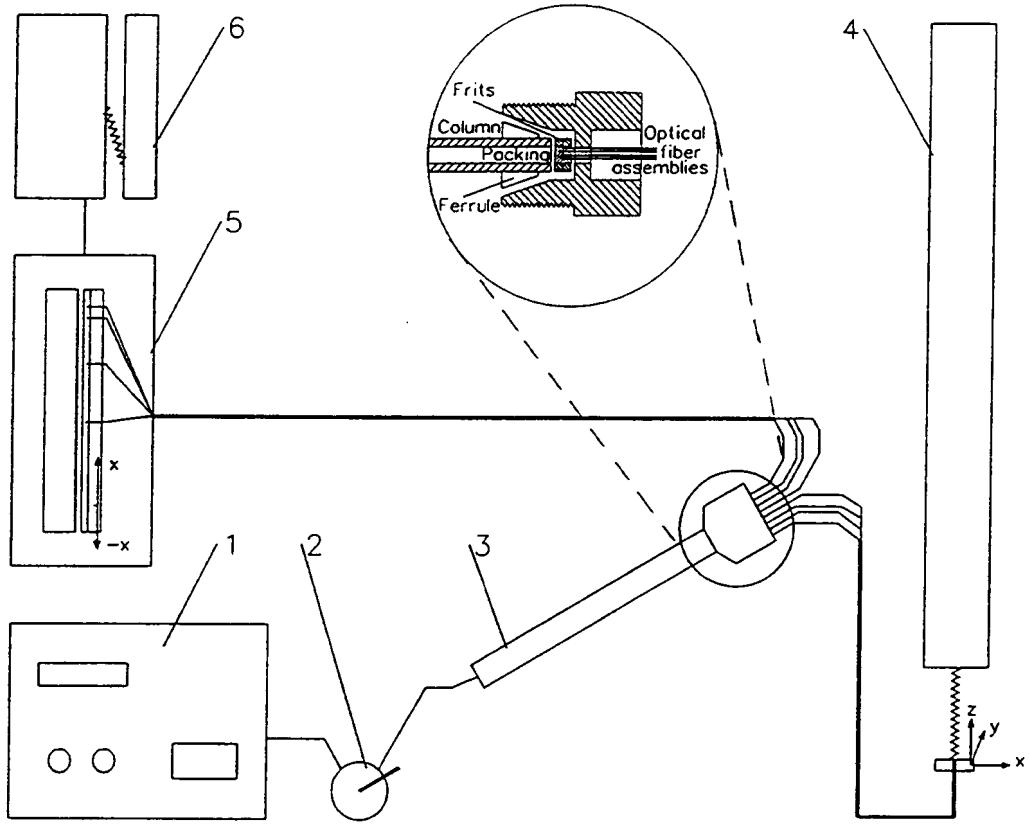

Figure 3.3.2.1 Instrumental set-up for local on-column fluorescence detection using optical fibers. (1) HPLC pump; (2) injection valve; (3) chromatographic column; (4) argon ion laser; (5) photodiode array detector; (6) microcomputer. The insert shows the cup shaped fitting with the optical fiber assemblies implanted into the exit frit.

detector. These assemblies allow for the on-column local fluorometric detection of the analyte molecules using an external photodiode-array as light detector.

The design of the optical fiber assemblies is illustrated in Figure 3.3.2.2 The quartz fibers (General Fiber Optics, Cedar Grove, NJ) have a core diameter of 105 μm and are 90 cm long. The thickness of the cladding layer -- which is not removed-- is 10 μm. The jacket at one end of each fiber was removed on a distance of 6 to 7 mm. The uncovered quartz tips were inserted in a 5 mm long, 0.25 mm nominal i.d. stainless-steel needle-gauge tubing (Hamilton, Reno, NV). This metallic sheath protects the uncovered silica cores which are very brittle and makes the handling of the fiber assemblies easy. Epoxy resin (Epon Resin 828; Shell, Houston, TX) was used to seal the fibers inside the metallic tubing. The epoxy filling prevents assembly fouling by analyte deposition inside the tubing and ensures the mechanical rigidity of the joint. This assembly design was meant to keep the two optical fiber tips as close as possible, such that their acceptance cones overlap to the largest extent. Such a geometry should ensure the best efficiency in collecting the fluorescent light emitted as a result of the passage of the analyte molecules by the fiber tips. The assembly tips are then inserted in a Delrin holder and wheel-polished with diamond paste and alumina. This step ensures the removal of excess epoxy from the assembly tips and generates fiber tips which are reasonably flat, thus causing less light dispersion. Excessive light dispersion would decrease the signal to noise ratio since the individual diodes integrate the light

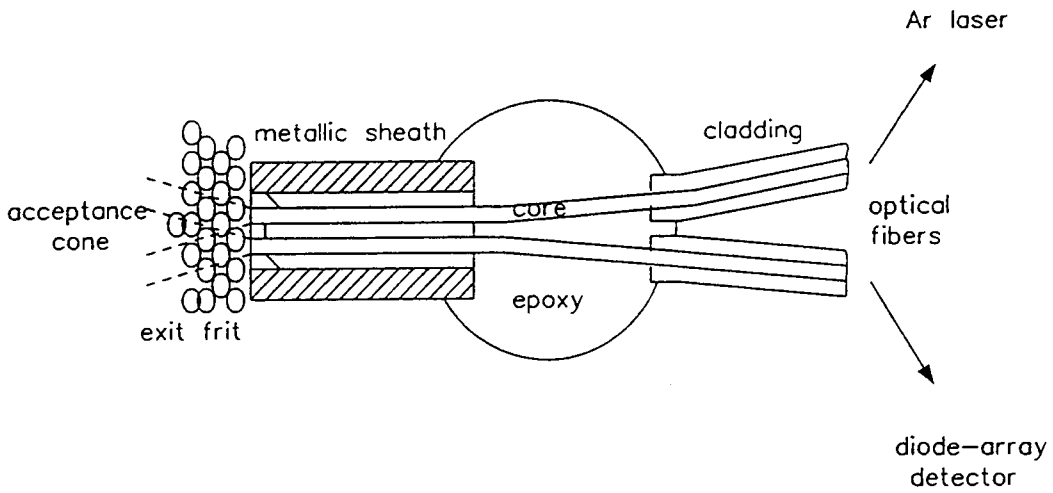

Figure 3.3.2.2 Schematic of an optical fiber assembly facing the exit frit.

shone onto them and effective scattered light rejection is hindered because of spatial constraints.

The initial locations of the assembly tips over the column cross-section are shown in Figure 3.3.2.3. By rotating the holding frit within the modified exit fitting (see insert in Figure 3.3.2.1) by one or several steps of 45° around the column axis, further locations could be investigated and data could be collected with the same assemblies along different diameters of the column cross-section. This system allows for a rather detailed mapping of the band profile at the column exit.

Frontal analysis experiments were run for each set-up of optical fiber assemblies. The advantage of frontal analysis over elution for these studies is that, even if the packing is heterogeneous, the composition of the whole effluent becomes eventually homogeneous, given enough run time. The ratio of the steady-state signal heights measured at different locations over the column cross-section versus the one obtained at the column center was used as a correction factor for the differences in fiber-assembly responses. Indeed, there are several reasons for which the heights of the concentration plateaus recorded during one run at different locations be different.

Firstly, the intensity of the excitation beams carried by the fibers to the different locations monitored are different because the fibers tips at the laser end of the assemblies cannot be placed at similar locations within the cross-section of the laser beam. This beam is narrow and exhibits a Gaussian intensity distribution around its axis. The farther an optical fiber tip is placed from the beam axis, the

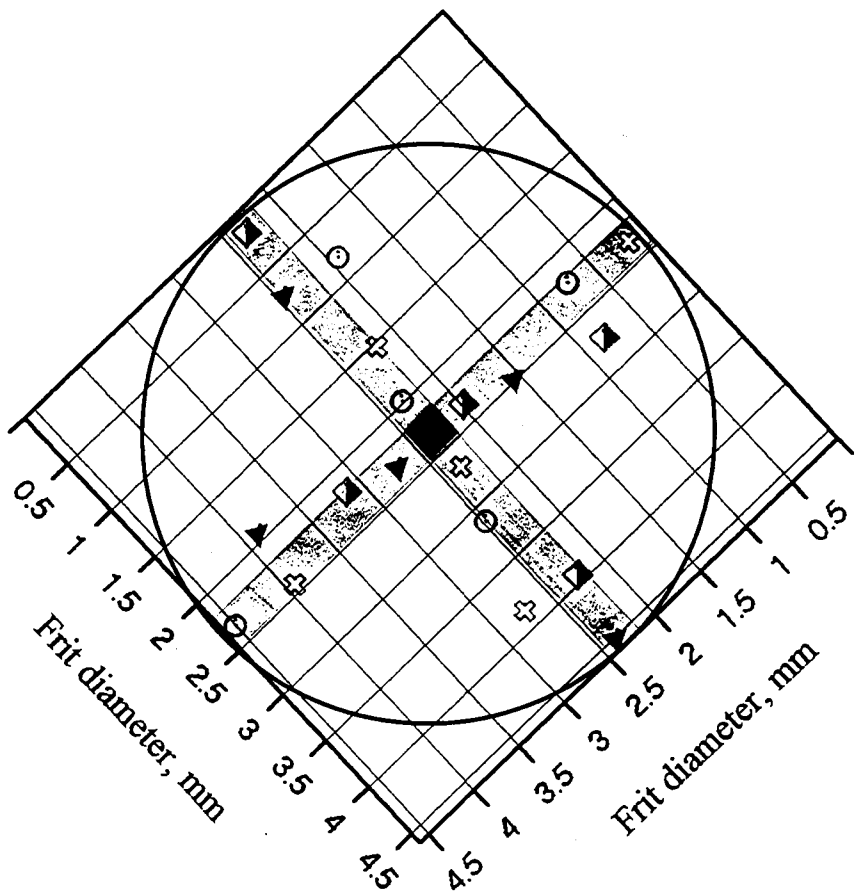

Figure 3.3.2.3 Positions of the optical fiber assembly tips over the column cross-section. The locations marked with a given symbol are those where the analyte concentration was monitored during a given run, for a given position of the assembly holding frit.

less light it collects. The optimal situation is when all tips are placed on the same circle around the beam axis, which proved difficult to accomplish with precision. Secondly, the fiber tips cannot be made perfectly flat so that little light would be reflected from their surface. We chose to cleave the quartz cores by scratching the fiber ends with a sapphire cutter and pulling the two pieces apart. The fiber tips obtained were reasonably flat but still different. Another important factor that determines the assembly response is its geometry. As stated before, the more the acceptance cones of the two fibers within an assembly overlap, the higher the fluorescence collection yield. The degree of overlap of these cones depends much on the lateral distance between the walls of the two fibers and the axial distance between their tips. Besides these factors, the positioning of the emission fiber tips at their PDA end is difficult to accomplish in such a manner that each fiber be centered onto its target diode simultaneously. This positioning is attempted by adjusting the horizontal position of the fiber holder that replaces the diffraction grating unit of the PDA in front of the photodiode array, and which is meant to hold the emission fiber tips perpendicular and very close to the surface of the array. Finally, the different elements of the diode array did not show the same sensitivity to light (because of uneven aging).

3.3.3 Optical System.

The excitation source was an Ar ion laser Model INNOVA 100-15 (Palo Alto, CA, USA) operated at 488 nm. The resulting fluorescence was detected and measured with an LDC (Riviera Beach, Fl) Analytical SpectroMonitor 5000 photodiode array detector (PDA) by scanning its elements one by one, much like individual detectors. The analog output of the PDA was recorded by running a program written on an IBM ValuePoint PC [Staller, 1994]. Such an approach offers the potential of recording data on 35 parallel channels, while using actually a single detector unit. Actually, we used the photodiode array detector not according to its initial intent, but rather in a simplex mode, such that each photodiode integrated the light shone onto it by the emission optical fiber. In this manner we could perform multiple channel detection while using one detection unit, and thus reducing the cost of required instrumentation. In practice, however, we found that only every second--or even better every third --diode element of the array could be used selectively because of optical cross-talk between neighbor array elements. This optical cross-talk was caused partly by dispersion that took place at fiber tips that could not be cleaved evenly, and also probably because the collected light was somewhat dispersed in the plastic filter layer that separated the fiber tips from the diode-array. Since at the miniature scale of the detector elements there was no room for a monochromator or line filter to be placed in front of each diode, we placed a transparent color filter (Edmund Scientific, Barrington, NJ) between the fiber tips

and the diode array. This filter (#809 STRAW) reduced considerably the high background signal caused by scattered excitation light.

3.3.4 Liquid Chromatography System

The chromatographic system consisted of a Beckman (Fullerton, CA) HPLC Pump Model 110B, a Rheodyne (Cotati, CA) injection valve Model 7010, the LDC photodiode array detector (see previous section), and a Spectraflow (Applied Biosystems, Ramsey, NJ) UV-VIS absorbance detector Model 575 as a bulk detector when needed. The data of the UV-VIS detector were acquired by using a Waters system interface module (Waters Maxima 820 version 3.3 software, Milford, MA) operated at a rate of 10 data points per second. The data files were uploaded to one of the computers of the University of Tennessee Computer Center for further calculations.

3.3.5 Samples

Due to their high molar absorptivity and large fluorescence quantum yields, laser dyes are excellent candidate chemicals for our measurements, although elution problems can be foreseen because of their large molecular weight and polarizability. An nonretained or a weakly retained compound was needed since the primary effects of the phenomenon studied here (*i.e.*, the degree of homogeneity

of the packing density) were hydrodynamic in nature. Mobile phase optimization could overcome the problems related to an excessively large retention factor. After several tentative runs made with different laser dyes, while looking for optimum capacity factor and peak shape, three potential analytes were selected for a more detailed investigation:

- Fluorescein (3',6'-Dihydroxyspiro[isobenzofuran-1(3H),9'-[9H]xanthen]-]-one), MW= 332.30;

- Disodium Fluorescein (disodium salt of the previous compound), MW= 412.31;

- Pyrromethene 556 (Disodium-1,2,5,6,8-pentamethylpyrromethene-2,6-disulfonate-difluoroborate), MW= 484.21;

all products of Exciton (Dayton, OH). The first dye proved to be susceptible to pH changes and showed poor peak shape reproducibility. The use of a buffered mobile phase did not help in solving this problem.

Pyrromethene (PM) showed consistently good peak shapes, and a fairly high detector response due to its high molar absorptivity-- ϵ_{492}= 7.2x10^4 liter mol^{-1} cm^{-1}-- and its good fluorescence quantum yield (Φ_f= 0.73 in water). PM was soluble enough in the mobile phase used. In order to be consistent with our previous work [Farkas *et al.,* 1994], we used a 40% methanol-60% water mixture as mobile phase in reverse-phase columns. The electrolyte used in the prior work (KCl, required by the electrochemical detection method) was replaced by borax (at a concentration of 5x10^{-3} M) needed as a buffer that ensured good peak shape reproducibility. The

concentration range of the PM samples was $1x10^{-3}$ to $7.5x10^{-4}$ M (0.5-0.35 g/L) in the mobile phase solvent. For each run the injection volume was 20 µl (0.7 mg PM per injection).

3.3.6 Chromatographic Columns Investigated

Six standard 4.6 mm i.d. and three larger (7.8, 9.4 and 10 mm i.d., respectively) HPLC columns were investigated. While most of these columns were packed in our laboratory, we also investigated three commercial columns. Different commercially available packing materials were used for packing these columns: KROMASIL (EKA Nobel, Surte, Sweden), a spherical, C_8 and C_{18} bonded silica, 16 µm average particle size; ZORBAX (BTR Separations, Wilmington, DE), a spherical, C_8 and C_{18} bonded silica, 5 µm and 10 µm average particle size, respectively; and Alltech Econosil C_{18} (Deerfield, IL) 10 µm average particle size. Column lengths varied between 100 and 300 mm. All columns were tested in a conventional HPLC chromatographic instrument consisting of a Waters (Milford, MA) pump, a Rheodyne (Cotati, CA) injection valve, and a UV-VIS absorbance detector (Applied Biosystems, Ramsey, NJ). The analytes used for column testing are either nonretained on C_{18} modified silica (uracil and PM) or show a relatively small value for k' (uracil on some of the columns, phenol and toluene) in the buffered methanol-water mixture described above as the mobile phase. Figures

3.3.6.1 and 3.3.6.2 and 3.3.6.3. show van Deemter plots for three of the columns discussed later in detail.

3.3.7. Investigation of the local injection profiles resulted with the injection system used for half-inch diameter columns.

Any differences in the shape of the locally recorded elution bands obtained at different radial positions over the exit column cross-section should be compared to the initial differences induced by a possible uneven injection. Chapter 3.2.3.1 presents the results of the investigation of the injected band when a Rheodyne injection valve with a 20 µl loop and connected to a standard inlet fitting is used. The injection profiles recorded by attaching the microelectrode assembly right next to the distributor disk inside the ¼" i.d. fitting showed only small differences versus the radial position of detection (Figures 3.2.3.1.1 and 3.2.3.1.2).

Similar experiments were made to investigate the radial uniformity of the injected band in the case of larger (½" o.d.) columns, by removing the chromatographic column and placing this time the optical fiber assembly-holder frit right inside the inlet fitting. A PEEK alloyed with Teflon (PAT; Alltech, Deerfield, IL) frit had to be placed between the metal wall of the fitting nut and the optical fiber tips, in order to reduce the back scattering -- on the shiny metal surface -- of the excitation beam coming from the laser. Figure 3.3.7.1 shows profiles recorded at five different radial locations of the ½" injection system. The largest difference -of

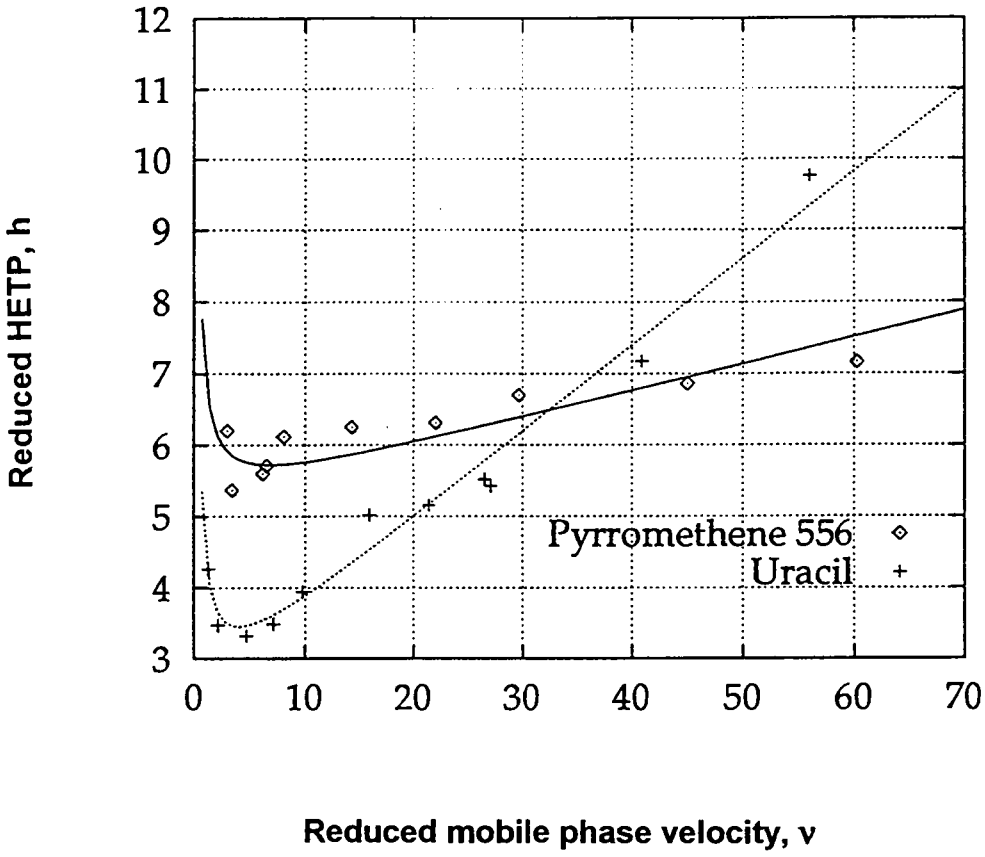

Figure 3.3.6.1 Van Deemter plot for a 4.6x100 mm column packed with Zorbax PRO10/150 C_{18}-modified spherical silica; particle size 10 μm.

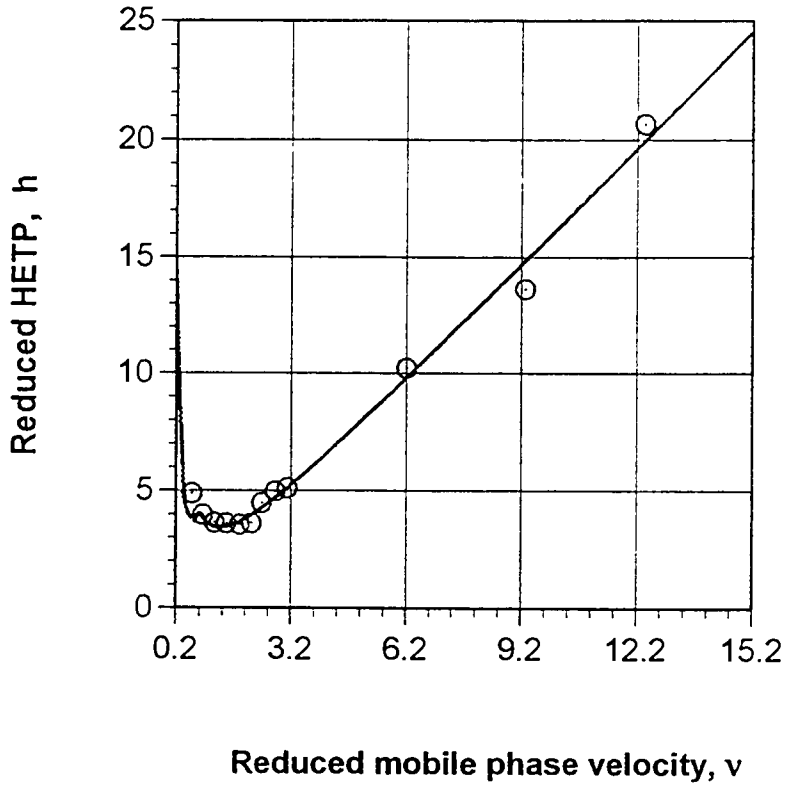

Figure 3.3.6.2 Van Deemter plot for a 10x250 mm Alltech column packed with 10 μm particle size Econosil C_{18}-modified spherical silica; injection volume, 20 μl of 0.01 M p-benzoquinone solution in 0.1 M KCl in methanol-water 20:80.

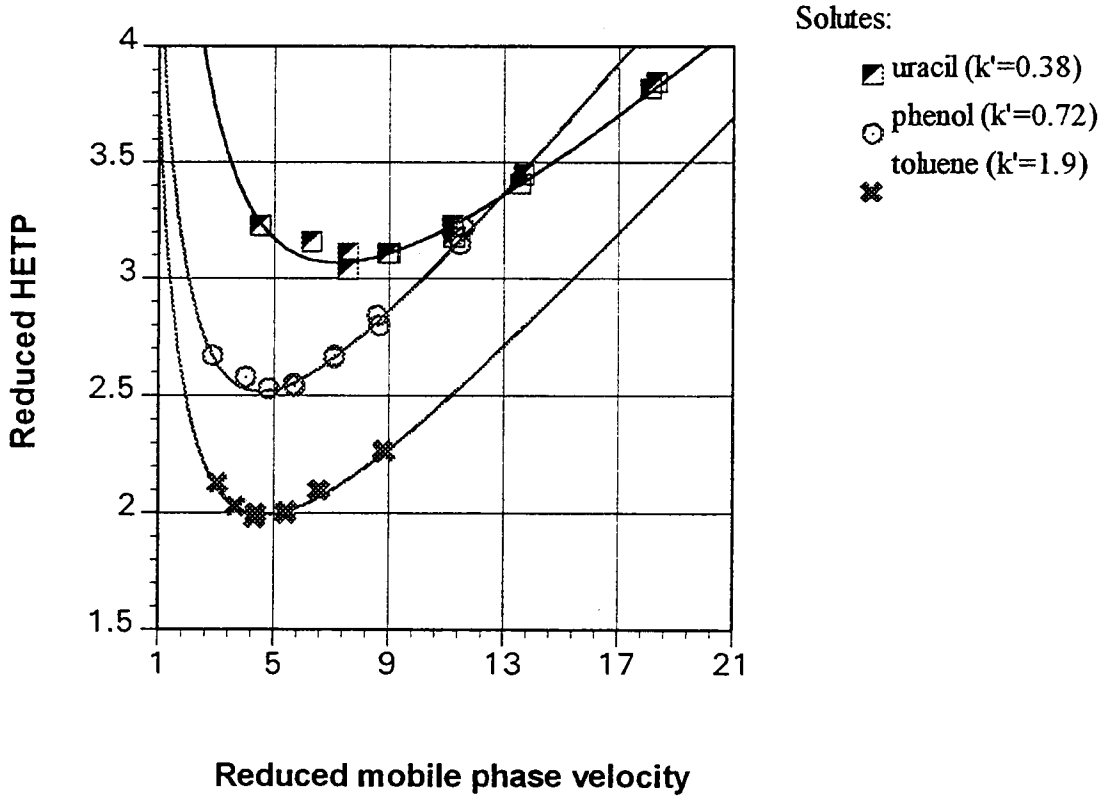

Figure 3.3.6.3 Van Deemter plot for a 9.4x250 mm Zorbax XDB-C8 column packed with 5 µm particle size C_8-modified spherical silica; injection volume: 20 µl of 5, 200, and 850 mg/ml uracil, phenol and toluene respectively, in methanol-water 80:20.

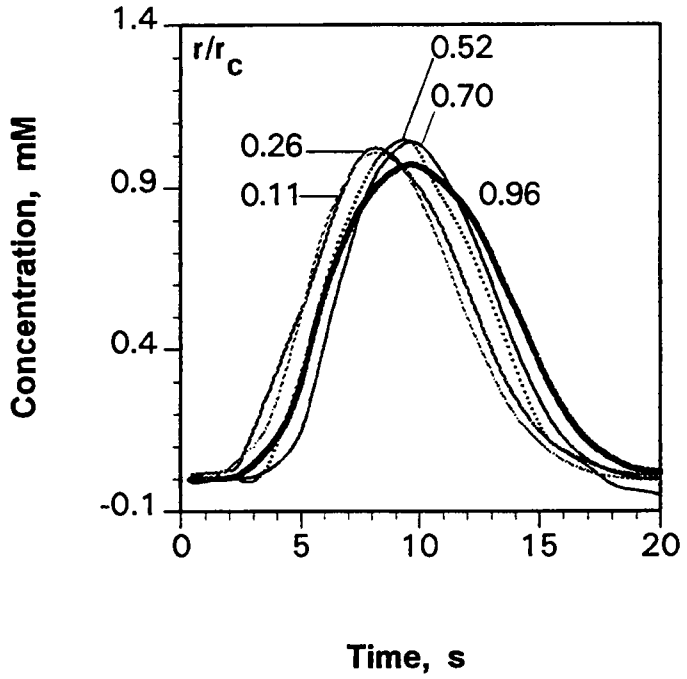

Figure 3.3.7.1 Injection profiles recorded with the optical fiber assembly-holder frit placed right behind the inlet frit inside a ½" fitting (column removed). Operating conditions: flow rate, 2 ml/min methanol-water 80:20; injection volume, 20 µl of 0.15 mM Disodium Fluorescein solution in methanol-water 80:20.

1.5 s - in the residence times of the peak maxima was recorded between the reduced radial locations 0.11 (center) and 0.96 (wall). Except for the residence time of their maxima, the profiles presented in Figure 3.3.7.1 are very similar. The profiles recorded at locations of reduced radii equal to 0.11, 0.26, 0.52 and 0.7 respectively, differ in their area, height and width by less than 2.1%, 1.46% and 1.8%, respectively. The profile recorded at a reduced radius of 0.96 is slightly wider and lower in height because of somewhat higher dispersion inside the inlet frit. The differences recorded in the injection profiles shown in Figure 3.3.7.1 are small compared to the differences recorded at column outlet, as presented later in chapters 4.1.2 and 4.2. This means that the injection band can be considered as radially homogeneous for the purpose of this study.

3.4 Experimental Set-up Used with the Axial Compression Column

This work consisted again, in recording simultaneously the elution profiles of a chromatographic band in a number of different locations in the exit cross-section of the column and in comparing the characteristics of these profiles. Both electrochemical and laser induced fluorescence detection methods gave the same results with analytical size columns, but the second one turned out to be more practical [Farkas *et al.*, 1996]. For this reason all large i.d. columns were investigated using the laser induced fluorescence detection system.

Local, on-column detection is easier to implement with preparative scale columns than with analytical size ones. Spatial constrains are less stringent in the former than in the latter case and bulkier, hence much sturdier, sensors may be used. The number of sensors which can be accommodated at column outlet is larger. At the same time, however, the ratio between the volume element of the column sampled by a specific microdetector and the overall volume to be investigated (the component zone) is much smaller in the case of preparative columns than in the case of the previously investigated analytical size columns [Farkas *et al.*, 1994, 1996]. This makes necessary the implementation of a large number of detection units. In practice, this number is limited only by the number of parallel channels on which detection can be performed simultaneously.

The diode array detector (DAD) used in the experiments reported here has 35 photosensitive diodes. Not all these diodes can be used as parallel detectors because of optical cross-talk caused by the light scattering that takes place in the small volume situated between the very end of an emission optical fiber and the surface of the diode the fiber is shining its light on. Because of this light scattering, part of the emitted light collected by a given fiber reached the diodes situated to the right and left of the primarily targeted diode. For this reason, in practice, only every second diode was targeted with fibers arranged accordingly. Furthermore, a proper arrangement of the sequence in which the different locations investigated within the column outlet cross-section were connected to the elements of the diode-array facilitated accounting for any possible optical cross-talk. Every photosensitive diode

integrated the light shone onto it without discriminating between the light brought by the fiber centered onto it and the scattered light coming from neighbor fibers. For this reason it was important either to check that the amount of scattered light was small at the level of a particular diode, or to insure a shift in time between the detection of the light coming from two different sources. The way to do this was to insure that two adjacent parallel channels are always connected to sensors giving signals exhibiting important or considerable difference in their retention time. In such a case, the effect of the optical cross-talk between the channels results in small parasite peaks seconding the actual peak recorded on the specific diode. This small peak precedes or follows the main peak, depending on the case. At the same time, its characteristics match those of the peak resulted on the channel where the scatter took place and hence can conveniently be checked for self-consistency. This eliminates peak-shape distortion caused by differences in optical response and/or electronic signal manipulation at specific diode level.

3.4.1 Detection System Used with the Axial Compression Column

The instrumental set-up (Figure 3.4.1.1) is similar to the one described in our work on analytical columns investigated by on-column, local, multichannel laser induced fluorescence detection [Farkas *et al.* 1996] . The beam of an Argon-ion laser is directed through a bundle of optical fibers (excitation fibers) to selected locations at the column outlet. Each excitation fiber is mated to an emission fiber

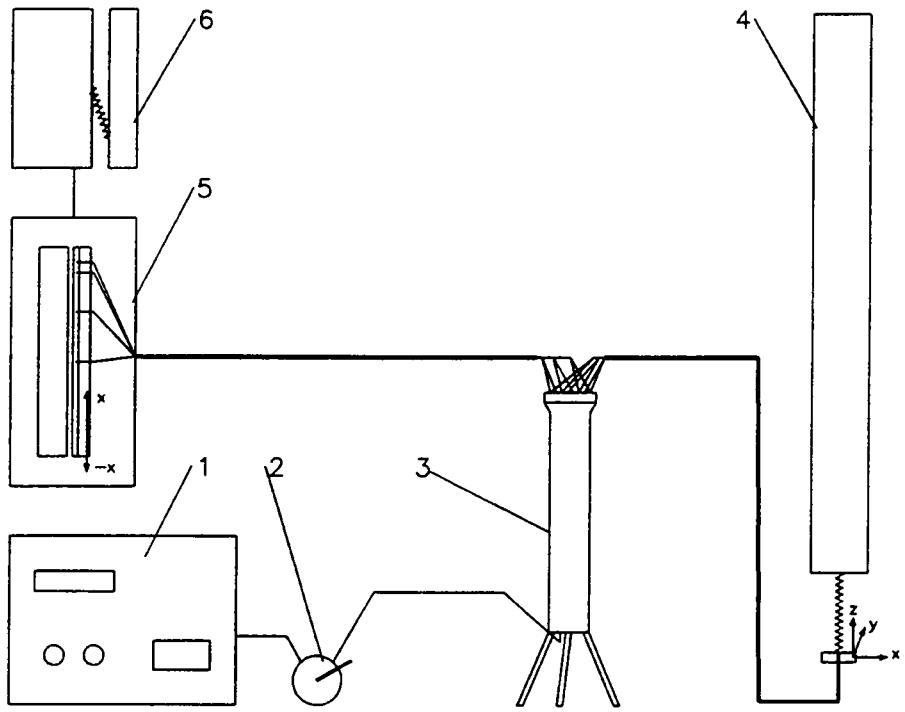

Figure 3.4.1.1 Instrumental set-up for local on-column fluorescence detection using optical fibers. (1) solvent delivery system; (2) injection valve; (3) axial compresssion chromatographic column; (4) argon ion laser; (5) photodiode array detector; (6) microcomputer.

which collects the emitted fluorescence of a laser dye (used as the analyte) in the immediate vicinity of the excitation fiber, and transmits it to a photodiode-array detector. The collected light is shone onto the appropriate pixel of the PAD and translated into an electrical signal which is acquired and stored by a microcomputer.

The Argon-ion laser (Model INNOVA 100-15, Palo Alto, CA) was operated at 488 nm. The estimated power at the sensing side of the optical fibers was 800 mW. When operated at a higher power (1.0 W) the jacket of the optical fibers at their end facing the laser beam became charred. The optical fiber assemblies were made in the same way as described previously [Farkas *et al.*, 1996], using quartz fibers (P/N: 16-0105-HAS-C22 of General Fiber Optics, Cedar Grove, NJ) having a core diameter of 105 μm.

Few adjustments had to be made in order to accommodate the large size column. The length of the optical fibers was increased from 0.9 m to about 1.5 m. The length of the metal sheath holding and protecting the uncovered fiber cores was increased to about 7 mm, to permit its easy penetration into the outlet frit of the preparative column used (see below). This frit is much thicker than the frits used with analytical size columns (5 mm versus 1.575 mm). The joint reinforcement of each optical fiber assembly was increased in volume in order to confer more mechanical resistance to the joint (shown in Figure 3.3.2.2). This was necessary because of the larger spacing between the different assemblies which prevented increasing their mechanical resistance by bonding them into a bundle, as was previously done [Farkas *et al.*, 1996]. Arranged in this manner, each fiber couple

probed a volume in front of the frit which was less than 0.5 mm in diameter, *i.e.*, less than 0.01% of the column cross-section area. Calibration of the fibers was carried out by running a series of frontal analysis experiments. After a solution of the analyte has percolated through the column for a certain time past the breakthrough passage, all probes were measuring the concentration of the same solution.

3.4.2 Liquid Chromatography System Used with the Axial Compression Column

The chromatographic system consisted of a DYNAMAX (RAININ Instruments Co., Woburn, MA) Solvent Delivery System Model SD-1 with a maximum flow rate of 800 ml/min; a 5 cm i.d. LC-50 Axial Compression Column skid (PROCHROM, Indianapolis, IN), and a LINEAR (Linear Instruments, Fremont, CA 94537) UVIS 204 absorbance detector. This detector was used only for testing the columns after packing them, in order to follow the progressive stabilization of their bed and make sure that the beds studied were those of typical, efficient columns [Sarker and Guiochon, 1995a, 1995b]. The column skid has been described previously [Sarker and Guiochon, 1995a]. It allows the packing of columns up to 30 cm long, axially compressed under a mechanical stress with a maximum value of 100 kg/cm^2 and can be operated under an inlet pressure up to 150 atm. Note that mechanical stress does not convey homogeneously in solids like pressure in liquids and that the

distribution of the mechanical stress in the packing is certainly heterogeneous [Train, 1956, 1957, 1960].

3.4.3 Axial Compression Columns Investigated

The chromatographic column was slurry packed using a suspension of 270 g of ZORBAX PRO-10/150 C_{18} bonded spherical silica (BTR Separations, Wilmington, DE) in 800 ml of 2-propanol. The average particle size is 10 μm and the average pore size 150 Å. Further detail regarding the physical properties of these particles are available elsewhere [Guan *et al.*, 1996]. The slurry was treated by ultra sonication for five minutes prior to being poured into the open column. Next, the outlet frit was put in place, the outlet flange bolted, and proper axial compression stress was applied without turning on the mobile phase flow. The liquid expelled from the column at its end opposite to the piston was collected and its volume measured [Sarker and Guiochon, 1995b]. The reading on the oil gauge during column packing was 110 bar which translates into an average stress of approximately 45 kg/cm^2 applied by the piston to the top of the packing. The phenomena observed during consolidation of the bed have been described and discussed previously [Guiochon and Sarker, 1995, Sarker *et al.*, 1996]. In the next step, methanol was run through the column for two hours at a flow rate of 50 ml/min to promote bed stabilization [Sarker and Guiochon, 1995a, 1995b]. Subsequently, the column was tested with methanol as the mobile phase, at a flow rate of 50

ml/min. Two different solutes were used as test samples: 0.4 g/L uracil and 0.35 g/L Disodium Fluorescein (disodium salt of 3',6'-Dihydroxyspiro[isobenzofuran-1(3H),9'-[9H]xanthen]-]-one) with the UV-VIS absorbance detector set at 254 nm and 488 nm respectively. The latter compound is the fluorescent species used for local detection.

Two columns packed following the same procedure were investigated. Both columns were approximately 150 mm long. The packing used for the first column was recovered and reused for packing the second column. The column was open, the packing cake pushed out of the cylinder by raising the piston, and the cake was suspended in the proper amount of solvent by ultrasonication. As shown later, in the section on column efficiency, recycling the packing did not affect negatively the performance of the second column. This result is in agreement with previous observations made on ZORBAX [Sarker and Guiochon, 1995a; Sarker *et al.*, 1996] but is not valid for many other packing materials [Sarker *et al.*, 1996]. These two columns exhibited the same properties as previously reported [Sarker *et al.*, 1995a, 1995b, 1996] and were considered as representative, hence useful for further study.

After testing a column, its top flange and frit were carefully removed and replaced with a modified flange which embraced a new frit holding eleven optical fiber assemblies (Figure 3.4.3.1). These assemblies were positioned in the outlet cross-section of the column in such a way that measurements of the elution profile were carried out at different, well-spaced values of the reduced column radius, along two perpendicular directions (Figure 3.4.3.1). New measurements were

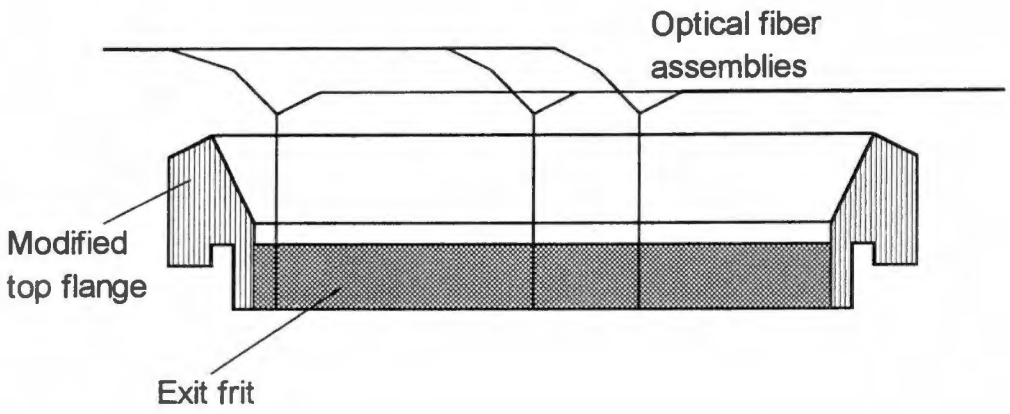

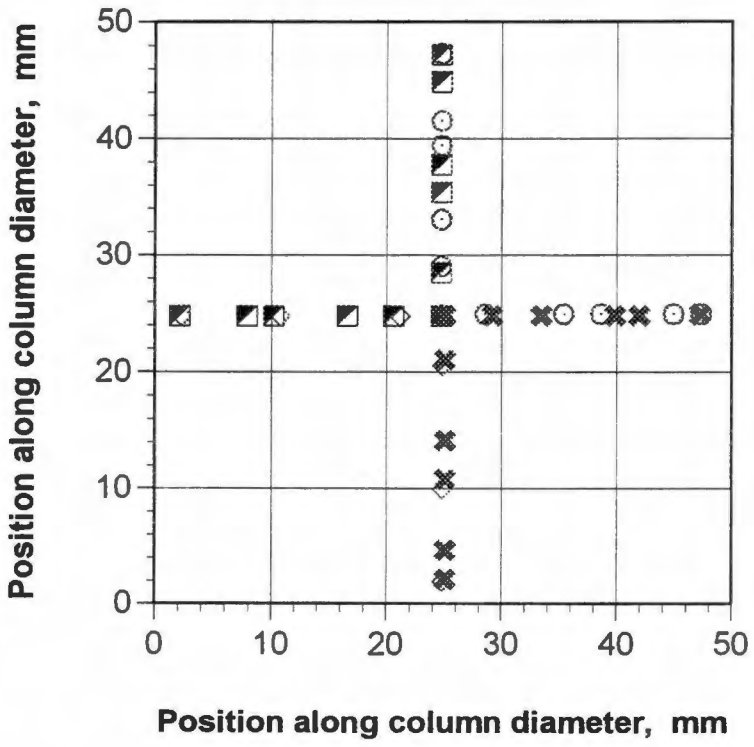

Figure 3.4.3.1 Modified top flange of an axial compression column with exit frit holding the optical fiber assemblies, and locations investigated over the column exit cross-section.

carried out after successive rotations of the holding frit by steps of 90^0 angle around the column axis. This allowed most fibers to relocate between points in which measurements had been carried out in the previous position of the top flange, and a few others in points which had not been targeted previously. This allowed for the confirmation of previous measurements by revisiting the same site with other fiber assemblies during different runs and by permitting checks for self-consistency of the results.

The sample selected for on-column detection was 1.15 10^{-3} M Disodium Fluorescein (a laser dye having a good quantum yield, purchased from Exciton, Dayton, OH) dissolved in 40% methanol+ 60% water [Farkas *et al.*, 1996]. The sample solvent had the same composition as the mobile phase. A six position VALCO injection valve operated by an electric actuator (VICI, VALCO Instrument Co., Inc.) and having a 0.5 ml sample loop was used for each run.

CHAPTER IV

RESULTS ON FLOW PROFILE MEASUREMENTS IN CHROMATOGRAPHIC COLUMNS

4.1 Radial Distribution of the Mobile Phase Velocity in Chromatographic Columns

4.1.1 Analytical Columns

It would be difficult and meaningless to measure the velocity in any given point of the column. This velocity is chaotic, not only in space (since the available flow space changes constantly), but also in time, because of the eddies which form constantly between particles. The velocity varies rapidly and considerably from the wall of a particle to the center of each interparticle channel. Some averaging is necessary. The cross-section averaged linear velocity, $u = L/t_0$, is widely used to characterize the convective transport along the column. To study the distribution of the local linear velocity we need to average the velocity over a distance which is short compared to the column diameter, but large compared to the particle size. The electrode diameter (50 μm) is barely larger than the coarser particles used in this work (40 μm), but the electrode is placed in a silica sleeve (150 μm), hence averaging on a space scale of the order of a few particle diameters, which seems to be sufficient. In the plots presented next we give the relative difference, $(u - \bar{u})/\bar{u}$

(in %), between this local average velocity and the cross-section averaged velocity, $\bar{u} = L/t_0$.

In a tube packed homogeneously, the radial profile of the velocity averaged over a few particle diameters should be essentially constant, from the axis to the wall. The effect of a lower packing density in the region situated next to the wall -- as a consequence of the particles being unable to penetrate into a smooth column wall and arrange into a tightly packed network,-- would be averaged out if the measured velocity were an average calculated over a few particle diameters, and the lower density region did not extend further than few particle diameters away from column wall. The classical Poiseuille parabolic velocity profile applies to empty tubes, to some extent to the interparticle channels (which have too small an aspect ratio for this law to apply strictly), but not to packed columns. Experimental results show important deviations from this idealized model of flow through packed columns.

Normalized frontal analysis breakthrough curves exhibit a residence time and a slope which depends on the location of the measurement. The curve having the steepest slope (*i.e.,* showing the highest efficiency) was also recorded to elute the first. Its location of detection is situated around $r_c/3$ away from the column axis. It is not eluted much earlier nor is it much steeper than the breakthrough curve recorded at the column axis (Figure 4.1.1.1). Still, the linear velocity at which the concentration maximum propagates in this region seems to be showing a slight edge over the very central region of the column. The slowest and less steep

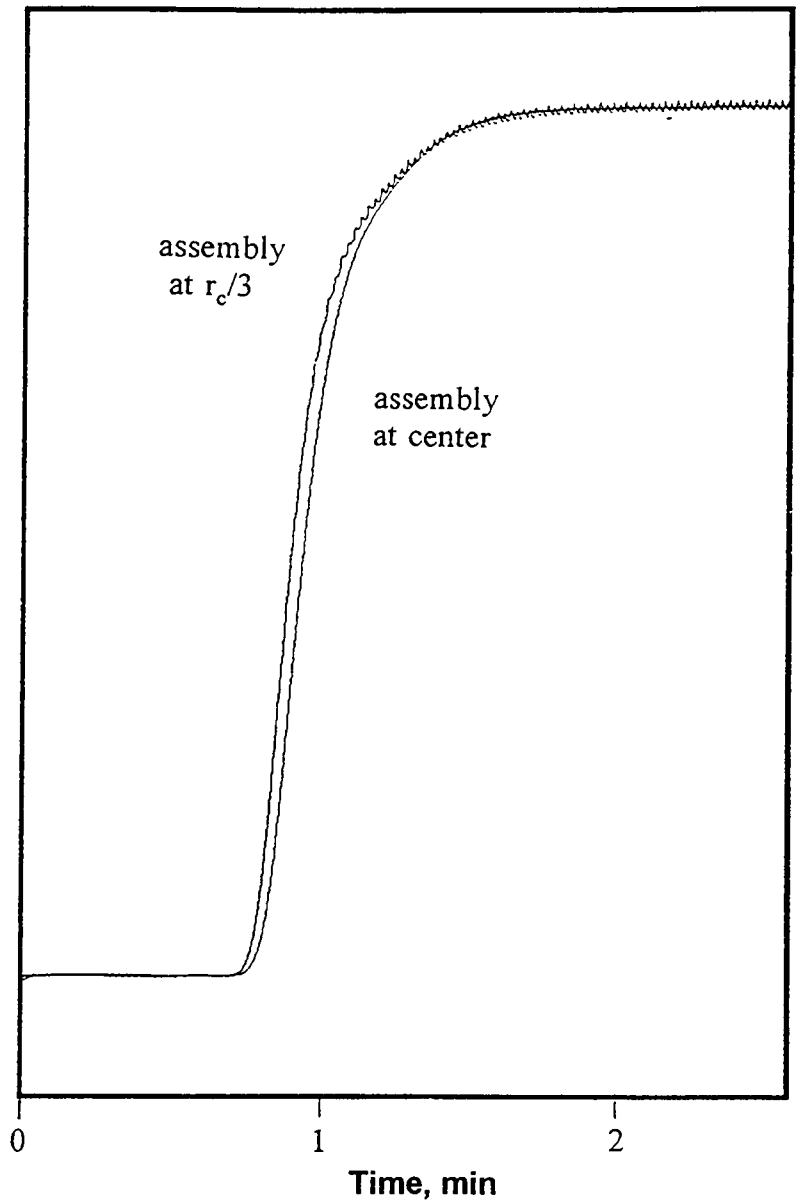

Figure 4.1.1.1 Normalized break-through curves recorded during the same run at column center and a point located at $r_c/3$ away from the column axis. 4.6x150 mm Kromasil KRO100-16-C_{18} column packed with 16 μm particles.

breakthrough curve was recorded close to the column wall (Figure 4.1.1.2). This observation seems to suggest that the packing permeability is the lowest close to the column wall, since the mobile phase flow velocity is slowest there, and the concentration plateau builds up in this region at the slowest pace. This finding is in agreement with the predictions of Vortmeyer and Michael [1985].

At the same time, the elution profiles measured at the same locations over the column exit cross-section show characteristics that are consistent with the remarks made on the break-through curves presented in Figures 4.1.1.1 and 4.1.1.2. As seen in Figure 4.1.1.3, the front of the peak recorded with the concentration sensor placed close to the column wall has a less steep slope than the one recorded at column axis. It is not only a higher degree of dispersion of the band encountered in the region close to the column wall, but also a shift in the residence time of the concentration maximum that makes the two bands different. The same figure compares these elution profiles with the injection profiles described earlier (Figure 3.2.3.1.1). It is obvious that the difference in retention time between the two peaks recorded at the end of the column is induced during the migration of the zone through the column and not by an uneven injection.

The difference in the values of the residence times of the concentration maximums recorded at different radial locations over the cross-section at the outlet of the column was used to calculate the relative difference between the value of the local linear velocity at a given location versus the velocity measured at column center. The plots in Figures 4.1.1.4-4.1.1.10 show the results obtained for the

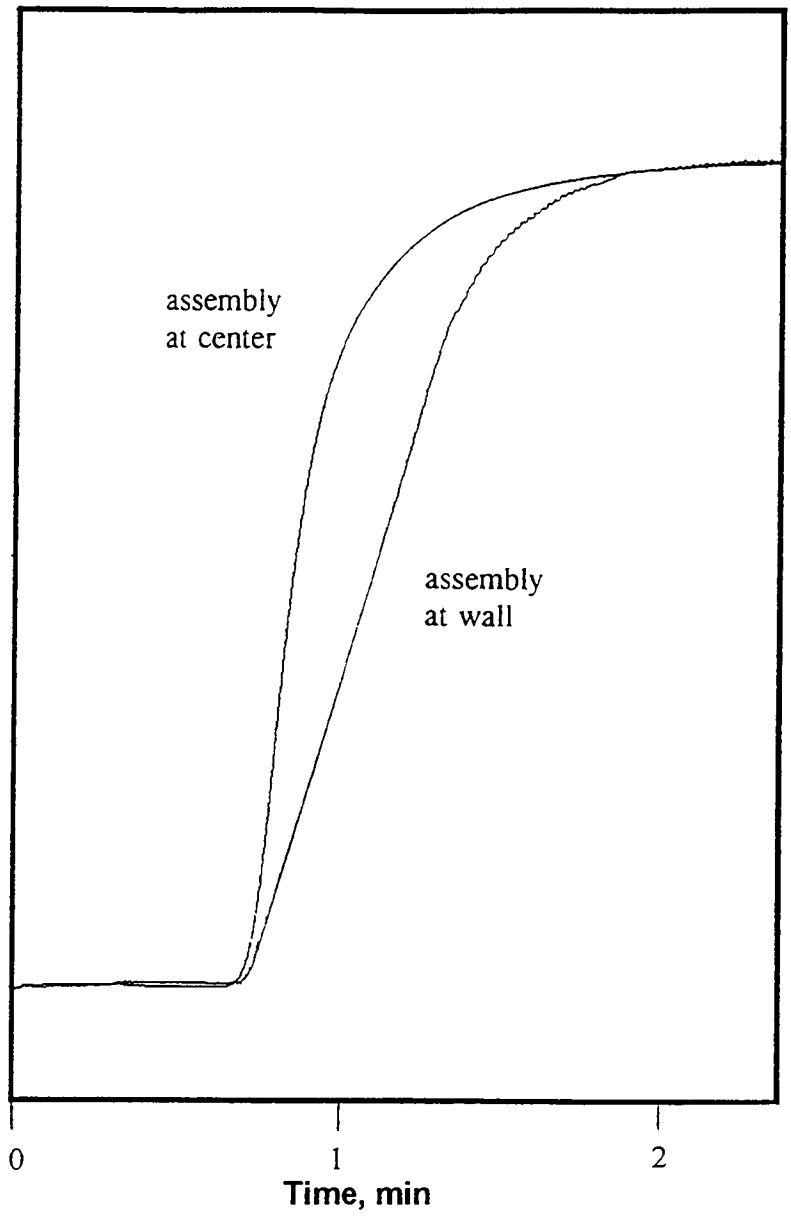

Figure 4.1.1.2 Normalized break-through curves recorded during the same run at column center and a point located close to the column wall. 4.6x150 mm Kromasil KRO100-16-C_{18} column packed with 16 µm particles.

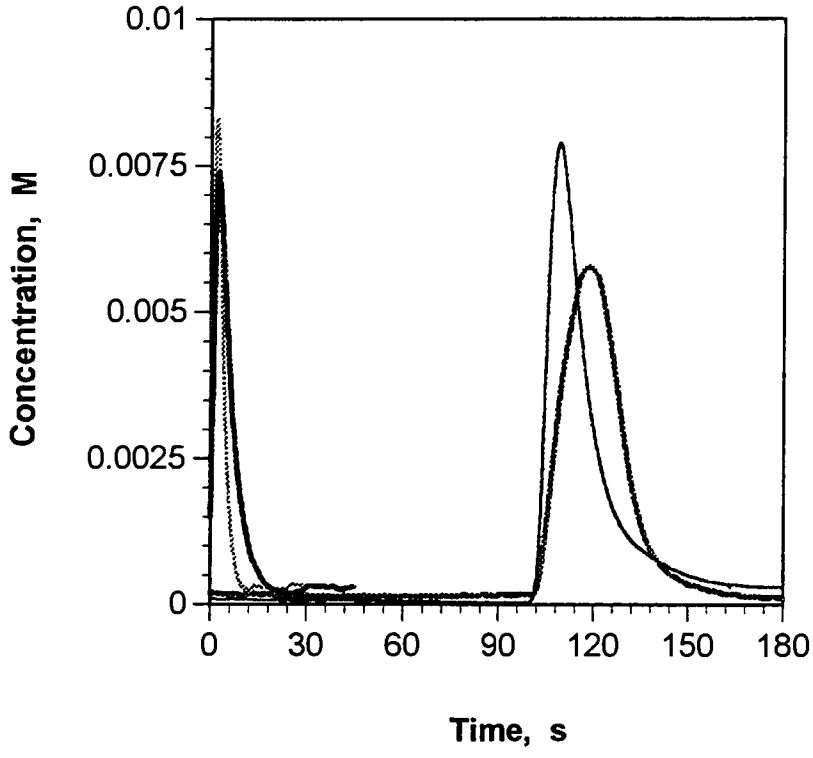

Figure 4.1.1.3 Comparison between chromatograms recorded with the central and the wall electrodes resulted on a 4.6x240 mm column packed with 40 μm glass beads and the injection profiles recorded at the same positions over the cross-section when the column has been removed (same profiles as in Figure 3.2.3.1.1); operating conditions: flow rate, 1 ml/min 0.1 M KCl in methanol-water 20:80; injection volume, 20 μl of 0.01 M p-benzoquinone solution in 0.1 M KCl in methanol-water 20:80.

distribution of the relative mobile phase linear velocity in the different columns studied. Figure 4.1.1.4 shows a three-dimensional plot of the velocity versus the position of the electrodes in the 40 μm glass bead column. It is obvious that the mobile phase velocity is systematically lower in the region close to the column wall than in the center of the column (with up to 8%). There seems to be a high velocity ridge about half-way from column axis to the wall, where the velocity is maximum. This ridge is more clearly visible in Figure 4.1.1.5, in which the data from Figure 4.1.1.4 has been projected onto the YZ plane, and shows a local velocity higher with about 2-3% than the one measured close to the column axis.

The phenomenon is unambiguous. The time differences observed are important, much larger than the experimental errors, as shown in Figure 4.1.1.6 and in the section on reproducibility (see Figures 3.2.8.1-3.2.8.3). For example, the delay between the elution of the fastest peak (electrodes half way from the center to the wall) and the slowest peak (eluting at column wall) is of the order of 14 s (12% of t_R), while the band width at half-height of these peaks does not exceed 10 s, and the standard deviation on the retention time of a peak is between 0.1 and 0.5 s, depending on the experimental conditions.

The glass bead column was unpacked, then repacked two more times. The new results are shown in Figure 4.1.1.7, as a plot of the local relative velocity difference versus the radial position of the electrode for all measurements made on these two columns. The significance of the four different symbols used in this plot--either open or solid -- is that the data plotted at a given value of the reduced radius

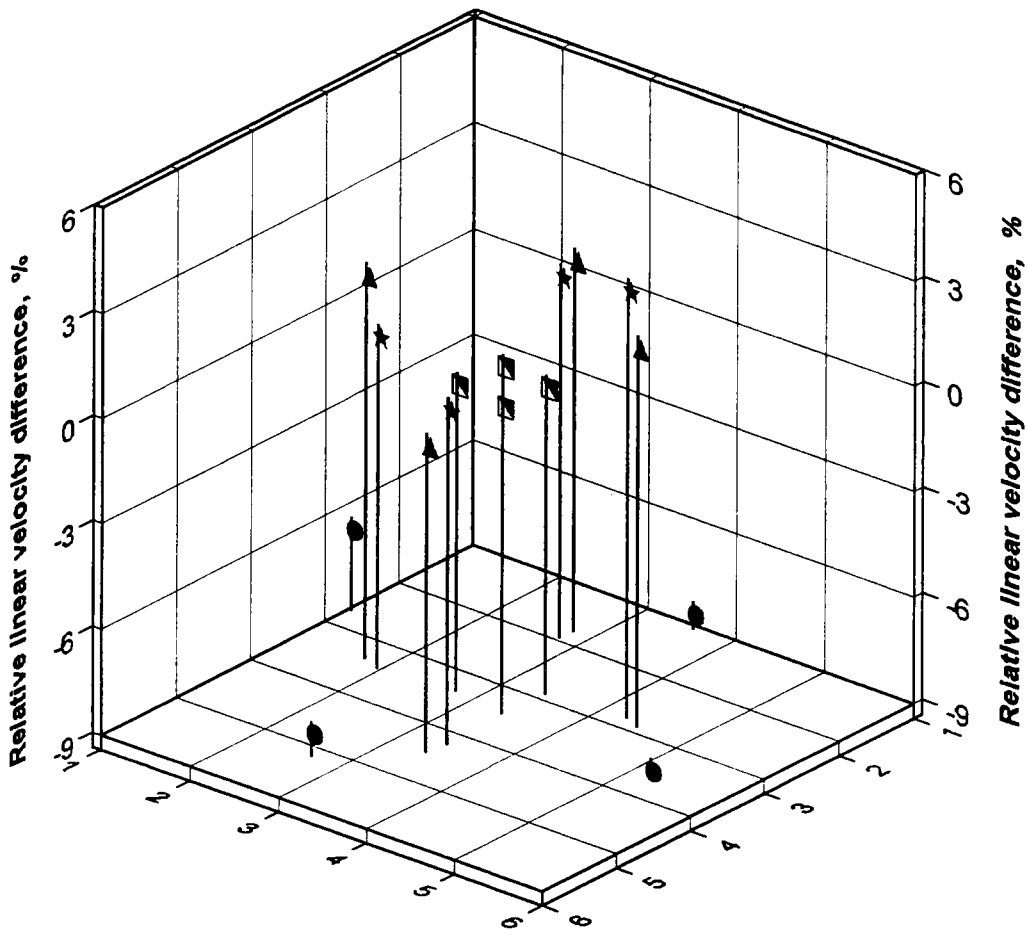

Figure 4.1.1.4 3-D view of the mobile phase linear velocity distribution for a 4.6x240 mm column packed with 40 μm particle size glass beads.

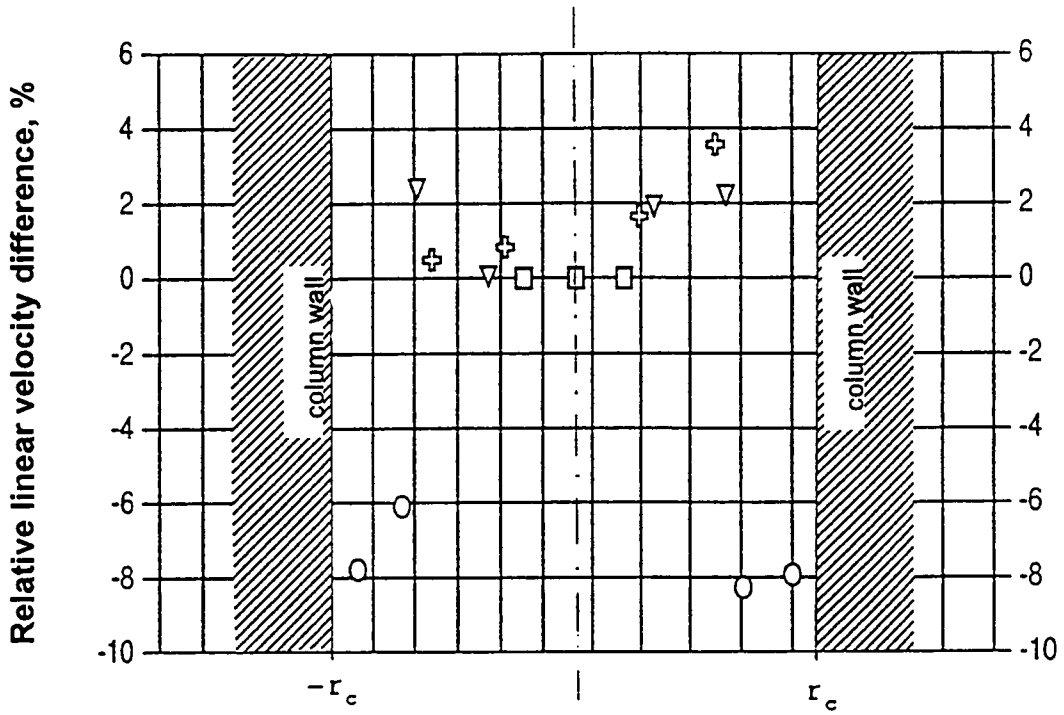

Figure 4.1.1.5 The distribution of the relative linear velocity difference of the mobile phase along the column diameter for a 4.6x240 mm column packed with 40 µm particle size glass beads. Projection of the 3-D plot in Figure 4.1.1.3 on the y, z plane.

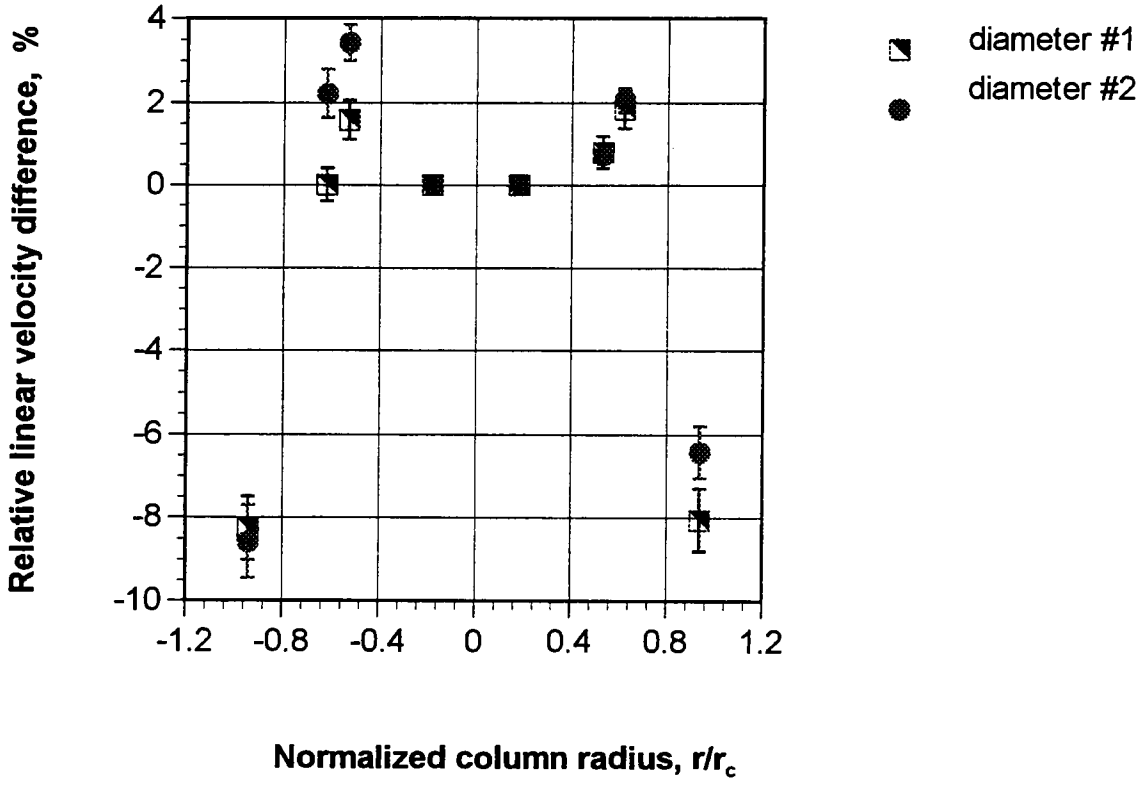

Figure 4.1.1.6 Distribution of the mobile phase velocity at the column outlet. 2D plots of the linear velocity versus the radial position of detection along two perpendicular diameters for a 4.6x240 mm column packed with 40 μm particle size glass beads, overlaid.

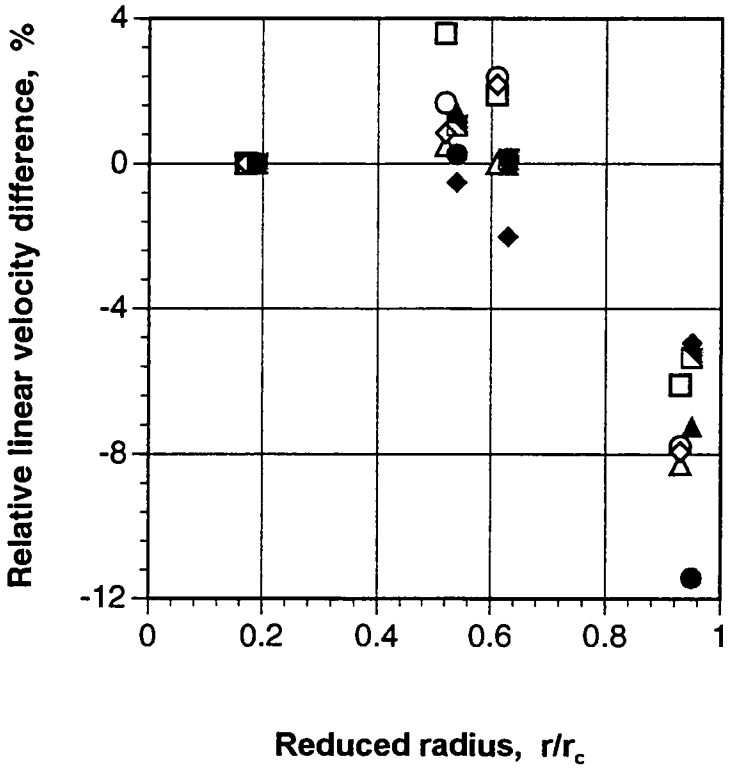

Figure 4.1.1.7 Plot of the relative linear velocity difference versus the location of detection along the column radius for two different 4.6x240 mm columns packed with 40 μm glass beads, overlaid.

r/r_c, was not recorded at the same location, but at four different locations along the same circle of radius r/r_c, but 90^0 apart. This plot shows that the velocity distribution is highly reproducible, except, maybe, at the column wall, where significant angular fluctuations exit (Figure 4.1.1.7). This result demonstrates that the packing method used provides column beds which are highly reproducible, even though they are not ideal. Finally, Figure 4.1.1.8 compares the results obtained with one of the 40 μm glass bead columns, and a column packed with 10 μm irregular silica particles, which was also packed by us. This last column shows smaller, but still significant differences in the values of the local linear velocity along the column radius, and less dispersion in the values measured at locations of equal reduced radii (*i.e.*, the flow profile obtained for this column shows a higher degree of radial symmetry). The flow profiles obtained for the two columns compared in Figure 4.1.1.8 are nearly identical in shape in spite of the fact that the retention factor of benzoquinone on the second column was different from 0 (k'=0.22). This shows that the phenomenon observed -- as expected from its hydrodynamic nature -- does not depend on the solute retention.

The uneven flow in the core region of a chromatographic column was not observed by Knox *et al.* [1976], who report "little [radial] variation of peak-maximum velocity" for an 11 mm i.d. dry-packed column, but still a 4% *higher* velocity at the wall than at the center. Eon [1978] obtained similar results with two 17 mm i.d. columns (also dry-packed), one made of steel, the other of Teflon (for radial compression). The velocity near the wall was 3 to 4 % *higher* than in the column

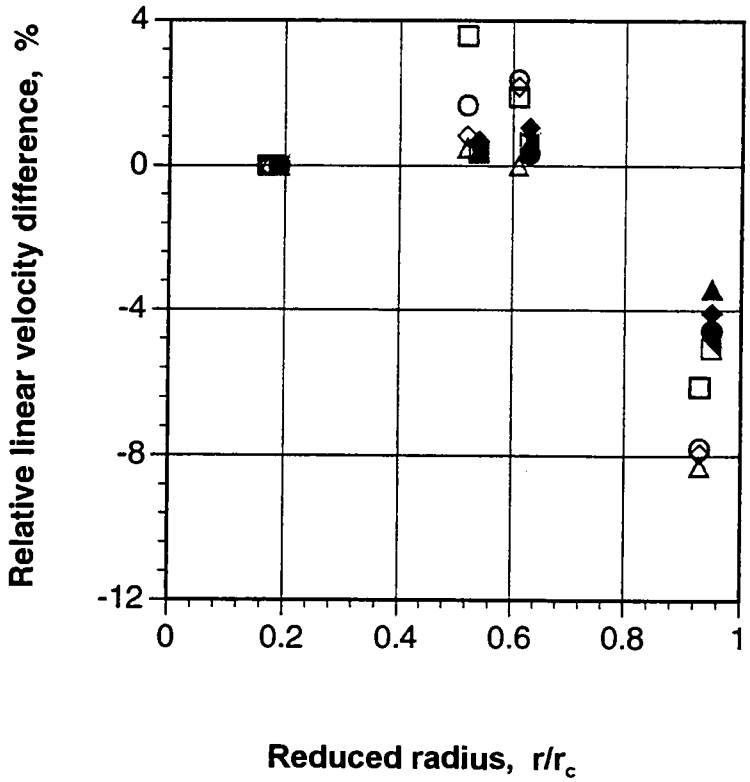

Figure 4.1.1.8 Plot of the relative linear velocity difference versus the location of detection along the column radius for two different columns: one packed with 40 μm glass beads (4.6x240mm) and one packed with 10 μm irregular porous silica (4.6x200 mm), overlaid.

center. In neither case was there any velocity ridge around the column core region. Results similar to ours were reported by Baur *et al.* [1988] who used a 3.2 mm i.d. slurry-packed column, and found that the retention time increases by a few percents close to the wall (2% at 0.2 mm from the wall, *i.e.*, at 65 particle diameters). In our columns, the thickness of the wall region seems to be *ca* 15% of the column diameter, or 30 particle diameters, a figure in excellent agreement with the values reported by Knox *et al.* [1976] and by Eon [1978] for the thickness of the wall region in their columns. Opposite to these authors' findings, however, and in agreement with Baur *et al.,* [1988], we observe that the velocity is lower at the wall, by up to 12 %, and not higher.

Furthermore, the columns investigated with the laser induced fluorescence detection method -- which has been described earlier in chapter 3.3, -- showed flow profiles that are very similar to those presented in Figures 4.1.1.4-4.1.1.8. Figure 4.1.1.9 shows the radial distribution of the local linear velocity measured on a 4.6x100 mm column packed with 10 μm particle size Zorbax PRO-10/150 C_{18}-modified spherical silica. The region of maximum velocity for this column is located at about 1/3 to ½ column radius off column axis. The velocity measured in the center of the column is somewhat lower than the one in this annular region (by less than 1%). The velocity close to the column wall is about 2% lower than that at the column center. It is obvious that this flow profile follows mostly the pattern found in our work using local amperometric detection [Farkas *et al.,* 1994], and in previous reports studying highly efficient columns [Baur *et al.*, 1988; 1989]. Overlaid plots of

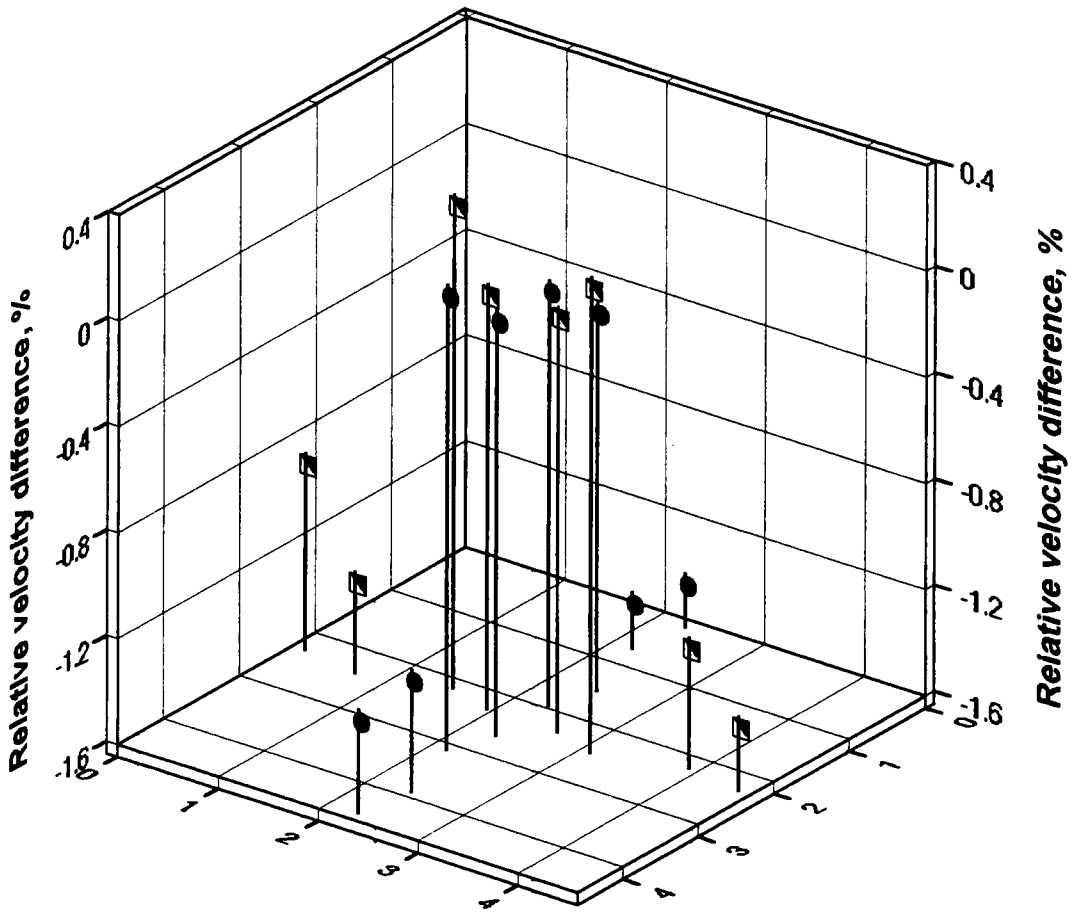

Figure 4.1.1.9 3-D view of the mobile phase velocity distribution for a 4.6x100 mm column packed with 10 µm particle size Zorbax PRO-10/150 C_{18}-modified spherical silica.

the flow profiles measured along two perpendicular diameters show a very good agreement between the two directions and a reasonable degree of radial symmetry for the velocity distribution in this column (Figure 4.1.1.10). A plot of the relative standard deviation (rsd) of the relative velocity difference calculated from eight data points collected at locations situated on the same circle of normalized radius r/r_c but 45^0 apart (Figure 4.1.1.11), shows that the velocity distribution in this column is cylindrical to a reasonable extent in the core region of the packing (rsd = 6% at r/r_c = 1/3) but that its radial fluctuations increase markedly close to the wall (rsd = 20% at $r/r_c = 0.95$). This observation can be explained by considering the corresponding fluctuations in local packing density and is in good agreement with the previous results of Eon [1978].

These findings were recurrent for the five different chromatographic columns studied with one of the two local detection systems described in chapter 3 (and also with the results presented later in chapter 4.1.2 on large diameter columns). This means that the same phenomenon -- the redistribution of the mobile phase volume elements during their passage through a chromatographic packing of an analytical size column -- has been investigated with two different experimental methods and the results obtained were consistent. Figure 4.1.1.12 shows the resulted flow profiles for five different analytical size columns, overlaid. The highest local linear velocities were recorded at locations situated in an annular region around the column axis, at about $r_c/3$-$r_c/2$ away form center. The linear velocity measured in the center of the column was about 2-3% lower than in this annular region. The

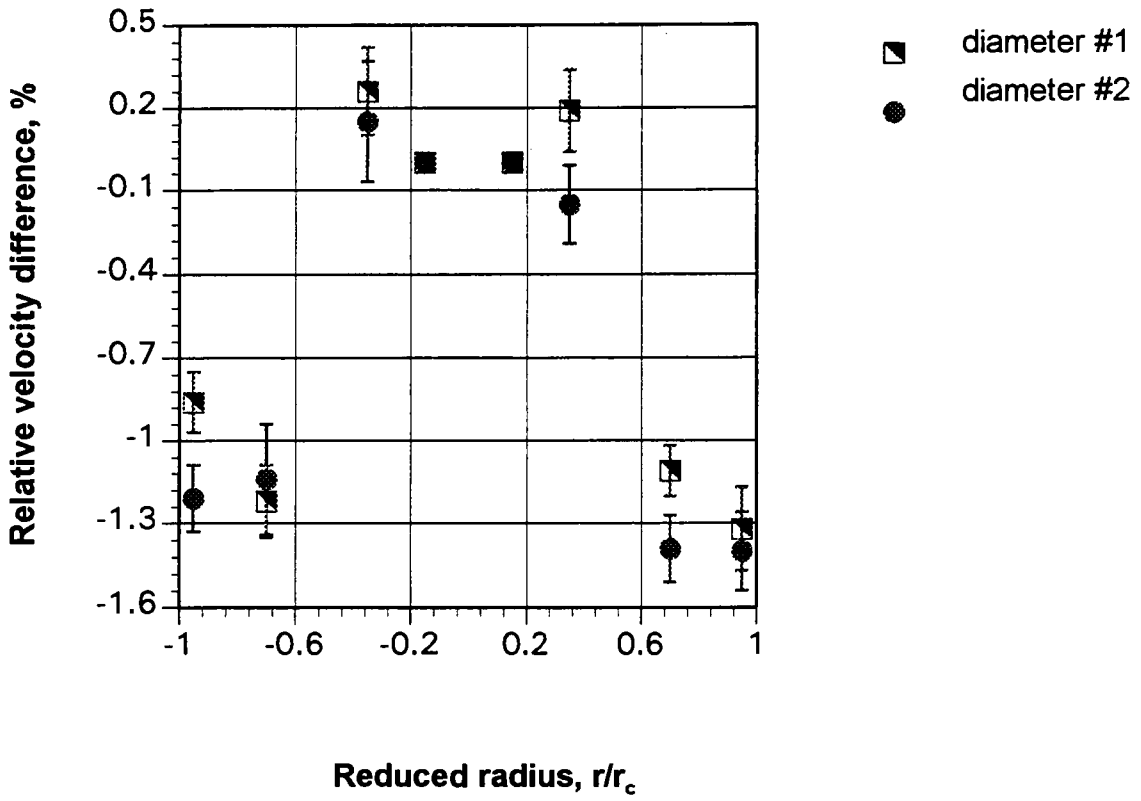

Figure 4.1.1.10 Distribution of the mobile phase velocity at the column outlet. 2D plots of the relative linear velocity difference versus the radial position of detection along the two perpendicular diameters considered in Figure 3.3.2.3, overlaid; 4.6x100 mm column packed with Zorbax PRO-10/150 C_{18}-modified spherical silica.

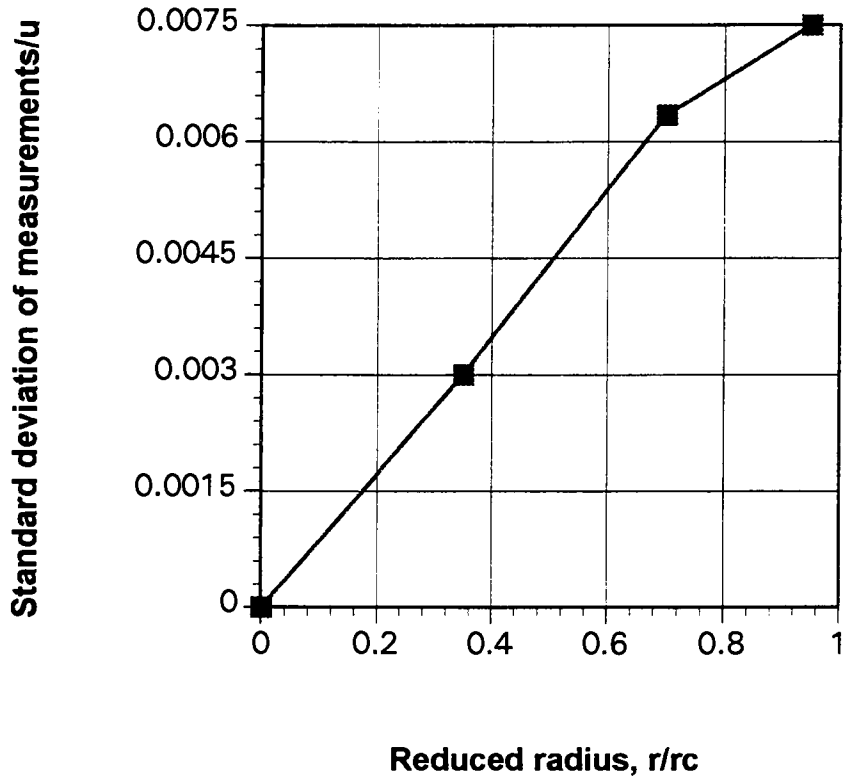

Figure 4.1.1.11 Plot of the relative standard deviation of eight measurements of the mobile phase linear velocity performed at points located on the same circle of radius r/r_c, and 45^0 apart (same column as in Figures 4.1.1.9-10).

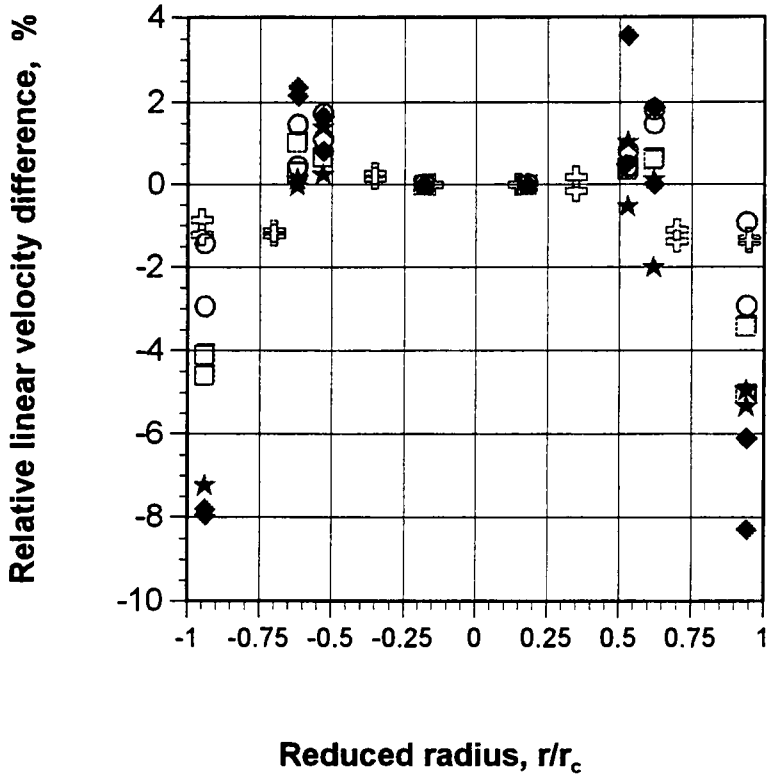

Figure 4.1.1.12 Distribution of the mobile phase velocity at the column outlet for five analytical HPLC columns. 2D plots of the linear velocity versus the radial position of detection along the two perpendicular diameters considered in Figure 3.3.2.3, overlaid. ◆ and ★ two different 4.6x240 mm columns packed with 40 μm glass beads; ❐ 4.6x200 mm column packed with 10 μm irregular porous silica; ○ 4.6x150 mm column packed with 16 μm C_{18}-modified spherical silica; ✚ 4.6x100 mm column packed with 10 μm C_{18}-modified spherical silica.

lowest values for the mobile phase linear velocity were recorded in the region of the packing situated close to the column wall, and these values were 2-8% lower than the local velocity measured at column axis, depending on the column. It is obvious that the general flow pattern in these columns has the same shape. At the same time, these plots show a series of different features. We will try to answer next the question of what makes these columns different? The immediate characteristics to consider are column length and packing material characteristics. The largest differences in local linear velocities (*i.e.*, the most uneven flow profiles) were found for the longer columns (23-24 cm) which have been packed with glass beads, while the most flat profile resulted for the shortest column (10 cm) packed with small particle size spherical silica. Furthermore, the column packed with 10 μm irregular porous silica (20 cm long) proved to exhibit a more distorted flow profile than the one not much shorter (15 cm), but packed with regular particles of 16 μm spherical C_{18}-modified silica.

The next question we tried to answer was if the column efficiency as a measure of overall column performance could be related in any way to the degree of distortion of the mobile phase flow velocity profile. In order to do this investigation, let us consider first the way the column efficiency was determined. All columns studied here were tested in a conventional HPLC chromatographic system specified in chapter 3, using nonretained analytes like benzoquinone, uracil and PM dissolved in the mobile phase described earlier. Van Deemter plots for a

4.6x100 mm column packed with Zorbax PRO-10/150 C_{18} spherical silica were presented in Figure 3.3.6.1. Similarly, Figure 3.2.5.1 showed the corresponding plot for a 4.6x150 mm column packed with Kromasil KRO100-16-C_{18} silica having a particle size of 16 μm. The determined efficiency depended strongly on the analyte of choice. The column reduced plate height was much higher for PM than that for uracil (Figure 3.3.6.1) at all commonly used flow rates (0.1-1.0 ml/min). Two parameters seem to be responsible for this phenomenon. Firstly, the diffusion coefficients for these two analytes are very different. According to the Wilke and Chang dependence of D_m on temperature, T, solute molecular weight, M, solvent viscosity, η, and solute molar volume, V:

$$D_m = 7.4\times10^{-8}\frac{TM^{1/2}}{\eta V^{0.6}} \qquad (4.1.1)$$

the calculated value for the diffusion coefficient in 40% methanol+ 60% water is 2.69×10^{-6} cm^2/s for PM, versus 6.32×10^{-6} cm^2/s for uracil. Secondly, the corrected retention time for PM on this column at a flow rate of 1 ml/min was 16% shorter. Since uracil is not retained on octadecilsylane-modified silica stationary phases (in ODS columns), the total accessible column volume experienced by PM seems to be significantly smaller than that for uracil. We compared the difference in elution volume for these two analytes with the total internal pore volume of the column [Guan *et al.*, 1996], and found that their ratio was 0.76. This result suggests that

PM in being excluded from most of the column total pore volume. It is improbable that PM be excluded based on its molecular size since its molecular weight is reasonably small (MW = 466.19 versus MW=112.09 for uracil) and the bulk of its structure is given by three condensed aromatic rings (it has a rather compact structure). More probably, PM is being excluded mostly because of repulsion that takes place between the nonpolar coating of pore walls within the packing and ionic species (PM is the disodium salt of a disulfonic acid) dissolved in an aqueous phase. Nevertheless, the ionic volume of PM may be also a factor if we consider the extra contribution of its hydration sphere. The supposition that PM is being excluded from the C_{18} surface will explain also why the dependance of the reduced HETP for PM on the mobile phase velocity is so limited. At low flow rates a small value of the diffusion coefficient should be favorable since molecular diffusion is the main contributor to the plate height. The reason this rational is not in agreement with the plots in Figure 3.3.6.1 is that an analyte with a low molecular diffusivity like PM is a better marker for the uneven mobile phase flow profile than analytes having a high D_m. Radial relaxation of the differences in the local value of the linear velocity is limited for PM and the overall axial dispersion of the analyte band is more important. Given the poor behavior of PM on ODS columns, their efficiency determined for uracil will be considered in this paper as performance criteria.

By reinvestigating the data on the radial distribution of the local relative linear velocity versus the overall efficiency of the column we could conclude that in columns having a reasonable efficiency (for uracil, as explained earlier), with the

column height equivalent to a theoretical plate, HETP < 40 μm, the flow profile showed the same general pattern as seen in Figure 4.1.1.12. Apart form this recurring picture, a completely different one was found for columns having a poor efficiency. Large changes in the mobile phase linear velocity were observed along any diameter, and the shape of the surface that represents the radial distribution of the length-averaged mobile phase velocity (calculated as the ratio of the column length and the local retention time of the breakthrough curve) was neither flat nor cylindrical. These radial profiles depend on the orientation of the diameter. A plot of the relative difference between the linear velocity at different radial positions over the column cross-section and the velocity at the center of the column is shown in Figure 4.1.1.13. This plot was obtained for a poor column with an HETP > 100 μm. The difference between the largest and the slowest velocities measured in such a column can be as high as 15%.

A plot of the linear velocity versus the radial position of the probe would be misleading for poor columns since the velocity distribution is not cylindrical. Overlaid 2-D plots (Figure 4.1.1.14) of the two profiles resulted from data recorded along the two perpendicular diameters indicated in Figure 3.3.2.3 are more appropriate. These plots show large fluctuations of the mobile phase linear velocity from one wall of the column to the opposite wall, and a poor radial symmetry of the velocity distribution. The plots also show that the trends in the change of the linear velocity along the two diameters considered are somewhat similar and correlated, although their overlap is poor. Both profiles show similar gaps on one side of the

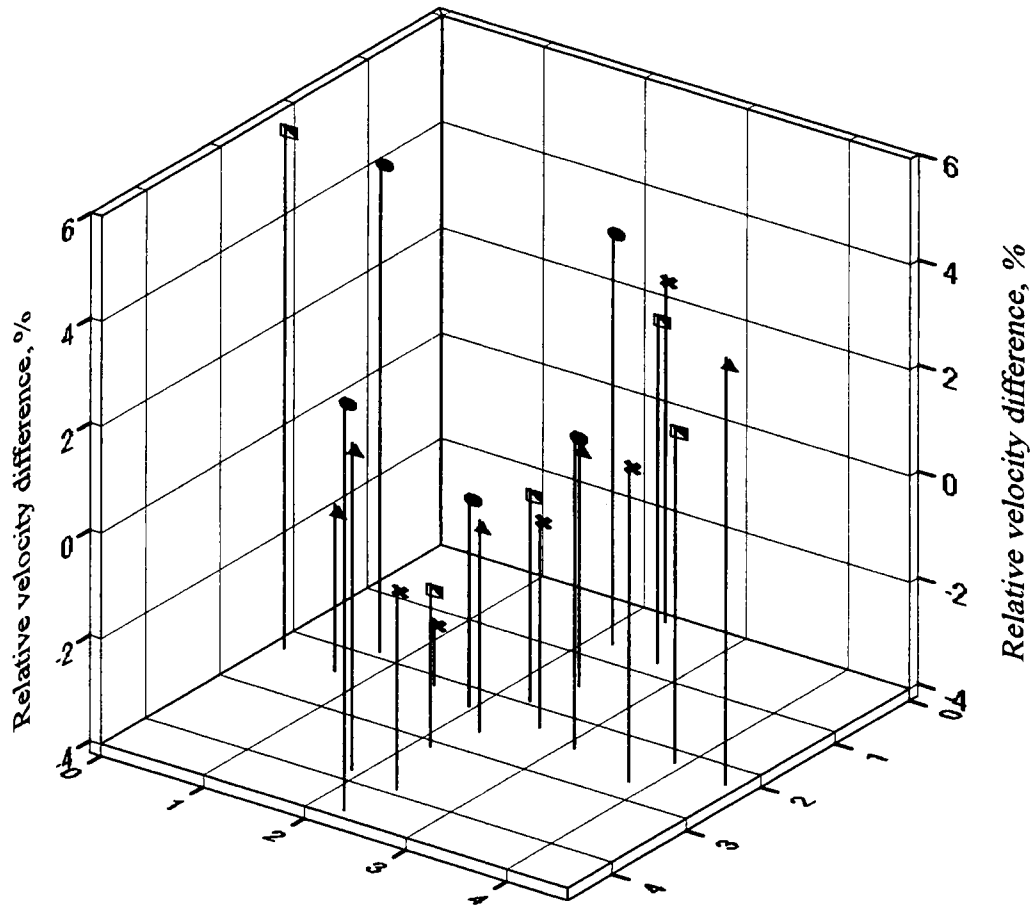

Figure 4.1.1.13 3-D view of the mobile phase velocity distribution for a Kromasil KR100-16 column packed with 16 μm particle size C_{18}-modified spherical silica, that has been used extensively and its performance decayed drastically.

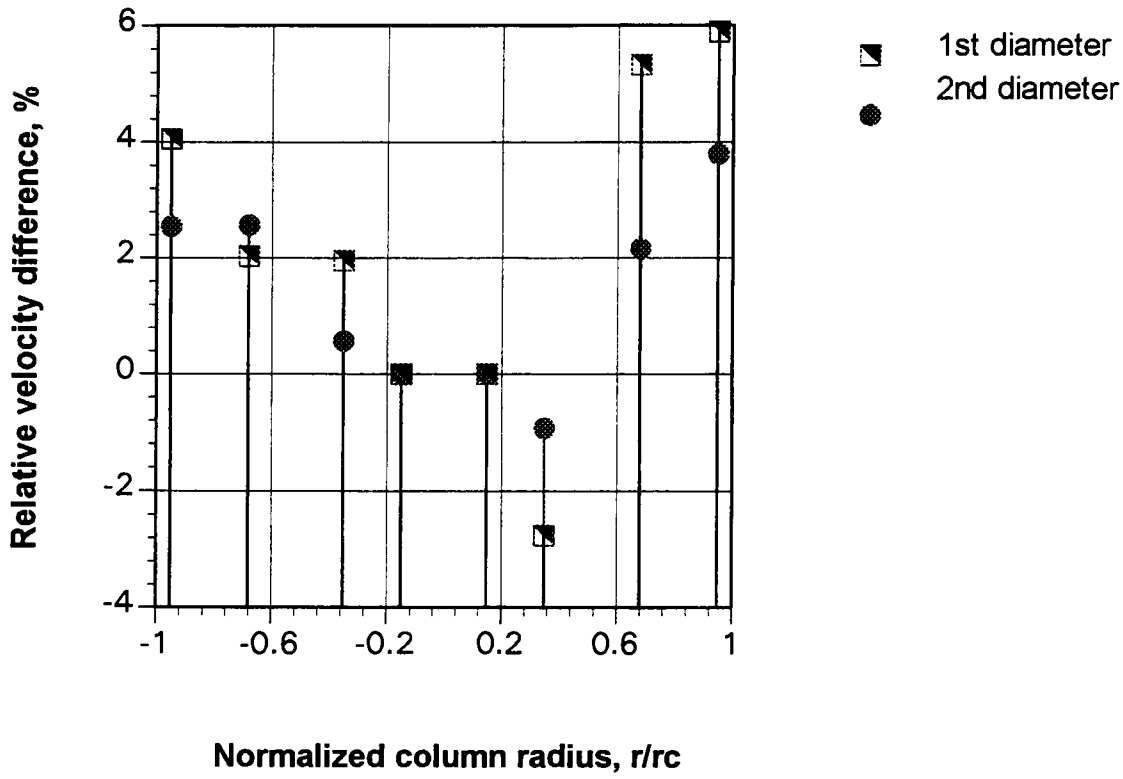

Figure 4.1.1.14 2-D view of the mobile phase flow velocity distribution along two perpendicular diameters of a Kromasil KR100-16 column packed with 16 μm particle size C_{18}-modified spherical silica (same column as in Figures 4.1.1.12-14).

column, in vicinal regions which may be a region of significant channeling. This description of the mobile phase flow profile recalls Gidding's prediction cited earlier that 'poorly packed columns, in which the range of pore sizes is large, tend to have highly variable flow rates (that is, an erratic velocity profile) within the medium' [1965].

All previous investigations on the radial dispersion of the flow velocity have been carried out at one single value of the flow rate [Knox *et al.*, 1969, 1976; Eon, 1978; Baur *et al.*, 1988, 1989]. It seems obvious that, if the packing is heterogeneous and the local permeability of the column varies across its section, the relative values of the differences between the velocity in any location and the one at column center will remain constant when changing the flow rate, since the permeability is a property of the packing itself. Figure 4.1.1.15 shows that the phenomenon is more complex than expected. As the mobile phase flow rate decreases the relative differences between the velocity at the center and the other local values of the velocity, which should remain constant within the limits of experimental errors do decrease significantly. The average values of these measurements and the corresponding standard deviations for 6-7 consecutive measurements are presented in Table 4.1.1. As the measured relative differences in local linear velocity become smaller the certainty of these measurements becomes lower. Still, the contraction of the overall elution band with decreasing the flow rate is obvious. The large values for the standard deviation of measurements is related to the complex nature of fluid flow through porous media. The history of

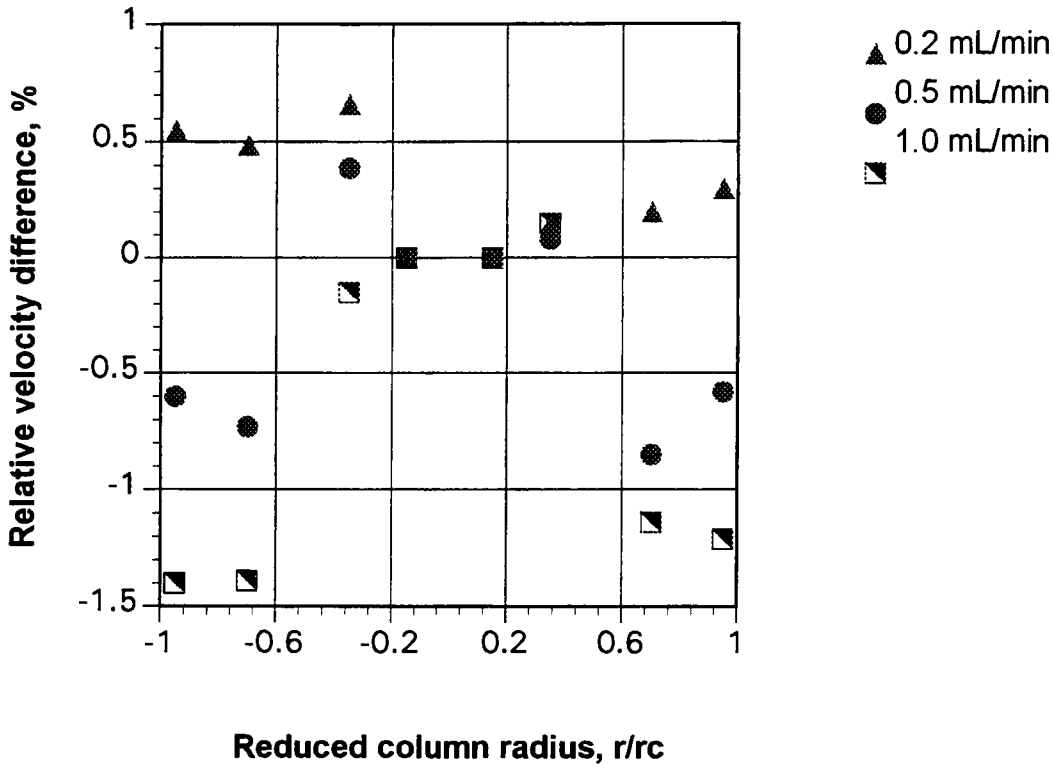

Figure 4.1.1.15 Flow profiles measured at three different mobile phase flow rates along an arbitrary diameter of a 4.6x100 mm column packed with Zorbax PRO10/150 10 μm particle size, C_{18}-modified spherical silica.

Table 4.1.1

Dependence of average mobile phase linear velocity difference on fiber tip position and mobile phase flow rate

r/r_c F ml/mi	-0.95	-0.70	-0.35	0.35	0.70	0.95
1.0	-1.40 (0.18)	-1.39 (0.15)	-0.14 (0.18)	0.15 (0.27)	-1.14 (0.25)	-1.21 (0.15)
0.5	-0.60 (0.19)	-0.73 (0.30)	0.39 (0.13)	0.08 (0.12)	-0.85 (0.27)	-0.58 (0.11)
0.2	0.55 (0.28)	0.49 (0.22)	0.66 (0.35)	0.15 (0.18)	-0.20 (0.29)	0.30 (0.31)

flow velocities along a given streamline may not be constant from one injection to the other and this may cause differences in peak characteristics.

At a flow rate of 0.5 ml/min the relative difference in linear velocity between the fastest and the slowest regions of the flow profile was of the order of 1%, about half smaller than the value observed for a flow rate of 1 ml/min. These relative

differences became even smaller and practically negligible when the column was operated at a flow rate of 0.2 ml/min, close to the optimum value for minimum HETP (0.1 ml/min in the present case). As seen in Figures 4.1.1.15 and 4.1.1.16, the profiles of the relative differences between values of the mobile phase velocity in the center of the column and at different radial positions measured along two perpendicular diameter are close. The width of these profiles (*i.e.*, the length of their projection on the ordinate axis) increases with increasing mobile phase flow rate. Since the width of the peak recorded by a bulk detector is related to this width, the apparent column HETP should increase much faster than the local HETP. However, this increase is limited by an other feature of the analyte band. We have shown earlier the concentration distribution of the analyte over the column exit cross-section area is not even, but is larger at column center than along the wall in spite of the fact that the injection profile appears to be reasonably flat itself. Consequently, the flanks of the flow profile (its ends close to the column wall) may contribute mainly to peak tailing and less to overall peak width broadening (only the latter translates necessarily into plate height increase/efficiency decrease). This supposition is in agreement with the observation that the segments of the analyte band sampled close to column wall are diffuse (broad peaks with low local analyte concentrations are recorded).

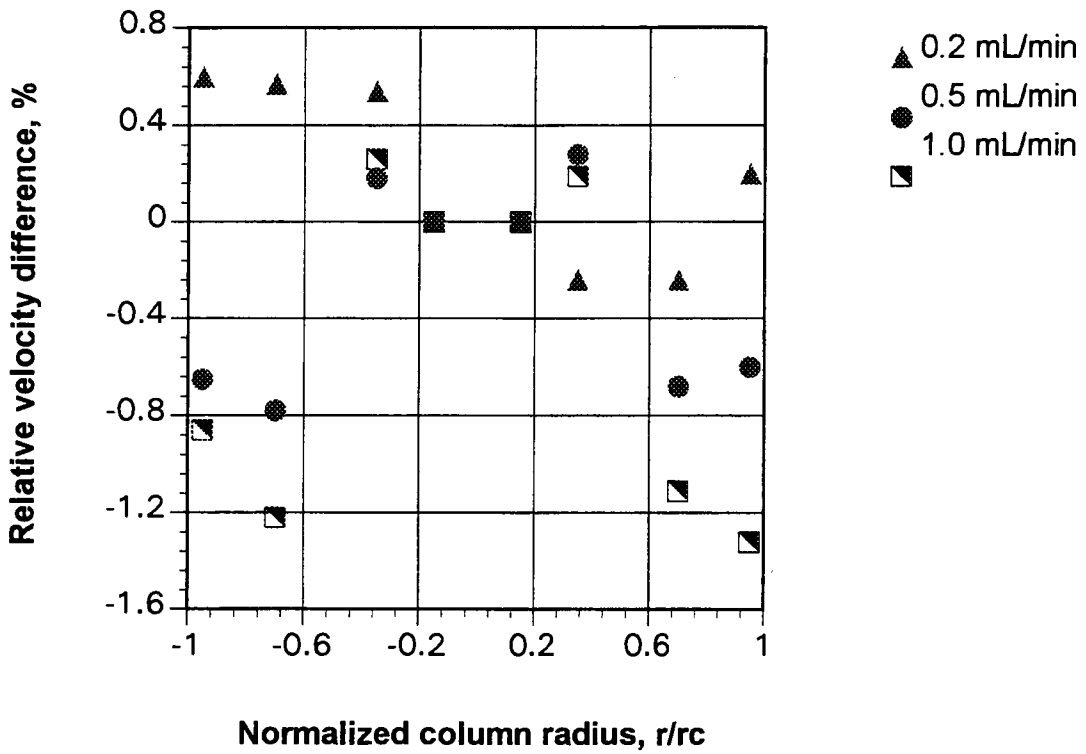

Figure 4.1.1.16 Flow profiles measured at three different mobile phase flow rates along a diameter perpendicular to the one considered in Figure 4.1.1.16 (same column), overlaid.

4.1.2 Radial Distribution of the Mobile Phase Flow Velocity in Large Diameter Columns

Considering that most of the chromatographic bed in a large diameter column undergoes sedimentation in a volume which is located far from the column wall, it would seem that a nearly homogeneous bed is to be expected. Compared to the flow velocity distribution at the outlet of an analytical size column, the corresponding distribution in a preparative column should have a much flatter profile. In opposition to this rational, the results of a few simple experiments carried out recently by Yun and Guiochon [1997] suggest that there is an important "wall effect" in preparative columns also, and that the wall region extends far from the wall, even in the case of large diameter columns. In one of these experiments, a dye was injected onto the same axial compression column as the one used here and eluted under conditions in which the dye retention factor was small. The elution was stopped when the dye had moved nearly half way through the column by switching off the pump. The column was then open, the bed of packing material was pushed out off the column and recovered as a cake, which was cut along its longitudinal axis. Examination of the resulted section showed that the dye zone was not radially flat. Its profile was more like that of a fourth or sixth degree polynomial centered on the column axis, nearly flat in the central region up to approximately two thirds of the column radius away from the column axis. In the extemal region, along the column wall, the dye zone curves slowly toward the column inlet, demonstrating that the

local mobile phase velocity decreases from the center toward the column wall. Molecules propagating in this annular region (which accounts for approximately half of the column volume) elute markedly later, the local velocity close to the wall being 13% lower than in the column center [Yun and Guiochon, 1997].

The results obtained in this study and reported here underscore this description. Figures 4.1.2.1 and 4.1.2.2 show the distribution of the relative linear velocity difference, $(u-u_c)/u_c$ (in %), between the local velocity, u, at locations along two different column diameters perpendicular to each other, and the velocity, u_c, -- at the center of the outlet column cross-section, taken as the reference, -- for a 7.8x300 mm column packed in our laboratory with 10 μm average particle size spherical, C_{18} bonded Zorbax silica. The flow profile exhibited by this column has a parabolic shape, with the value for the local linear velocity decreasing from column center to column wall with about 2.5%. Most data points acquired in the core region of the packing that has a diameter equal to the column radius show small differences in the local linear velocity relative to the velocity measured at column axis (less than 0.75%). A fast decrease is registered in the vicinity of the column wall, where the mobile phase linear velocity is 2-2.5% lower than in the center. At the same time, there seems to be a larger spread in the values for the local linear velocity acquired in the wall region of the packing. These differences become smaller as the flow rate is decreased gradually from 2 ml/min (v = 53.9) to 1 ml/min (v = 27.3) and to 0.5 ml/min (v = 13.7), as shone in Figure 4.1.2.3. This phenomenon has been observed before with standard size HPLC columns (Figures

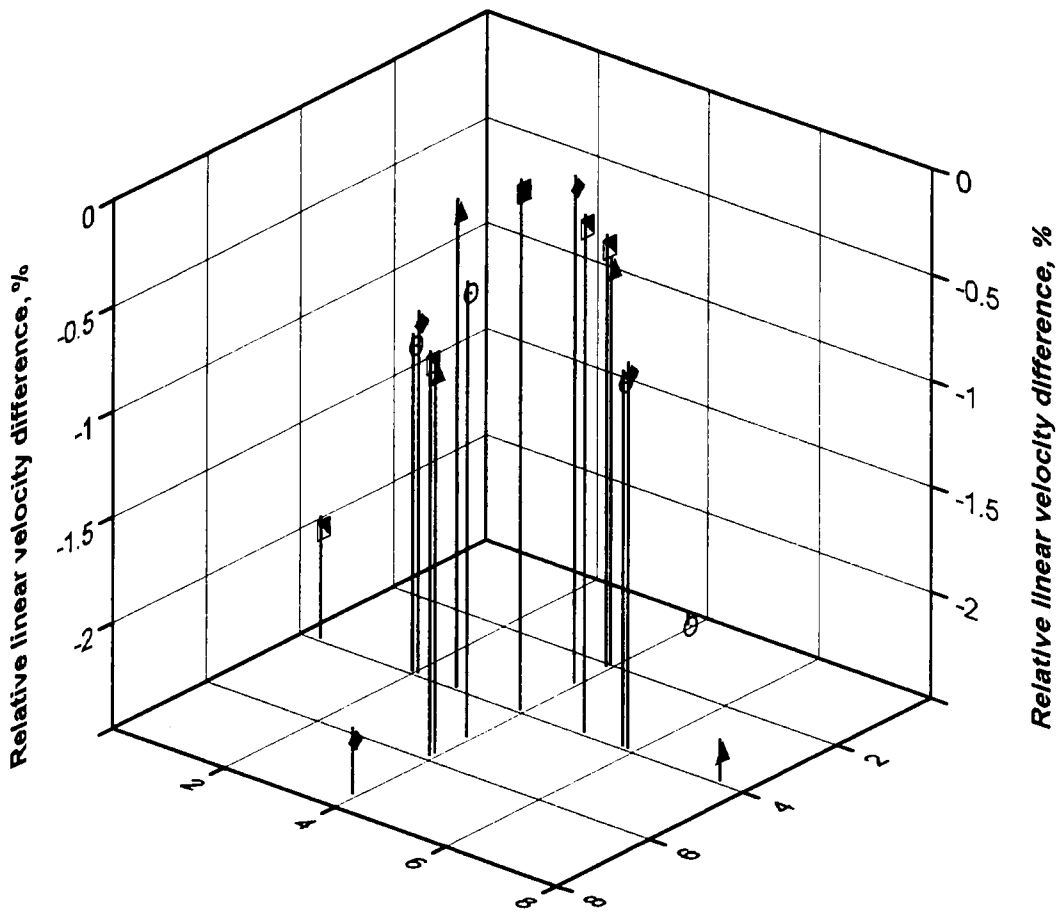

Figure 4.1.2.1 3D-view of the distribution of the mobile phase local linear velocity at the column outlet for a 7.8x300 mm column packed with Zorbax PRO-10/150 C_{18}-modified 10 μm particle size spherical silica.

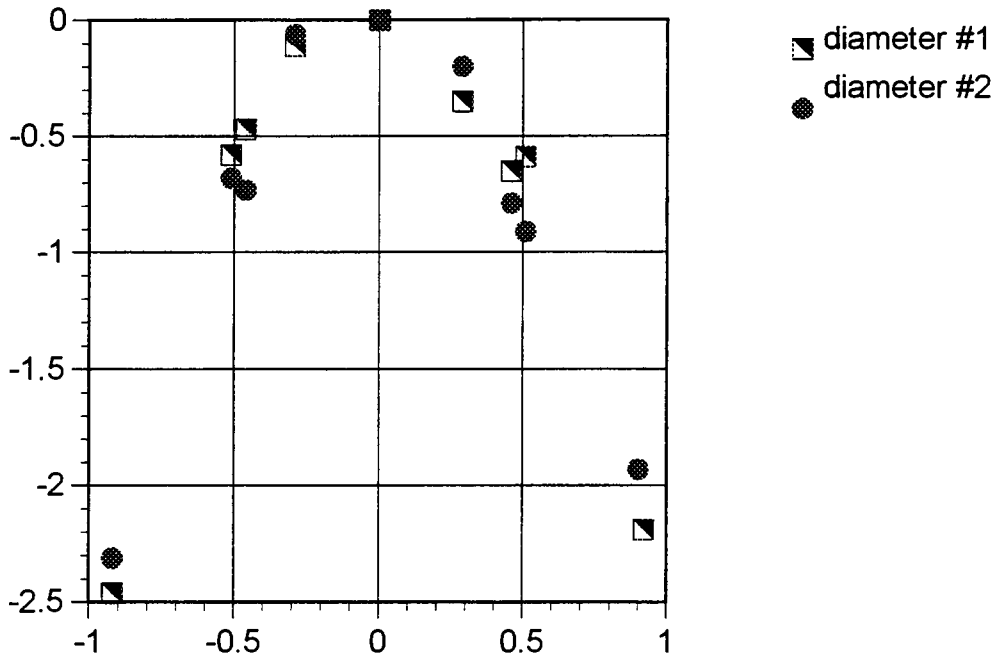

Figure 4.1.2.2 2D-view of the distribution of the mobile phase local linear velocity at the column outlet at locations along two perpendicular diameters, overlaid. Same column and data as in Figure 4.1.2.1.

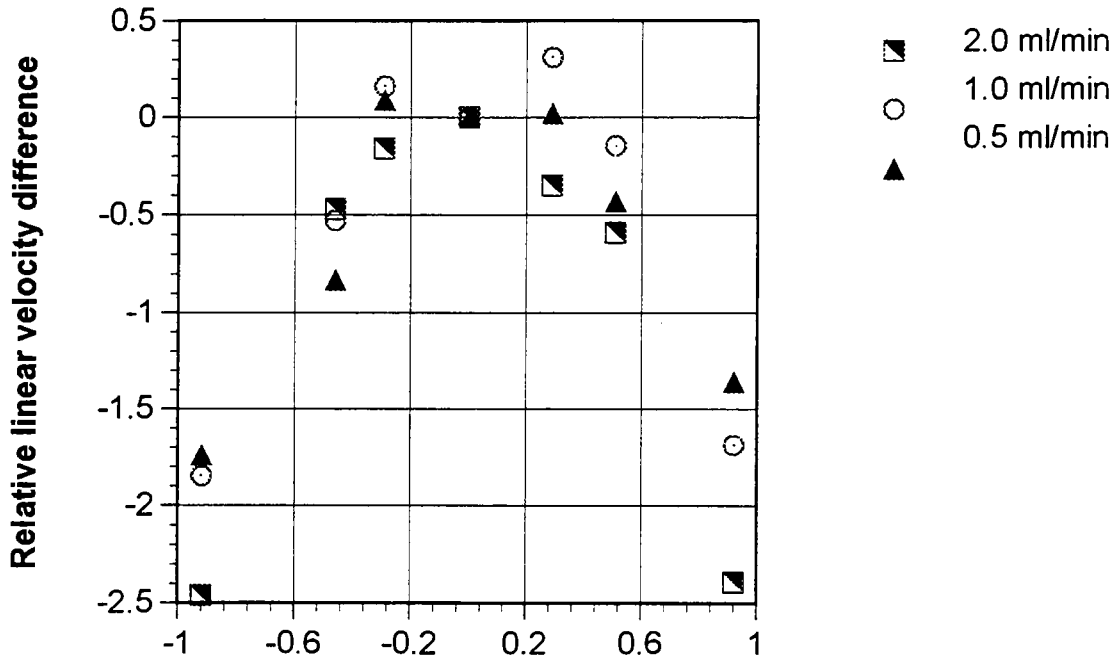

Figure 4.1.2.3 2D-view of the distribution of the mobile phase local linear velocity at the column outlet, at three different flow rates, overlaid. Same column as in Figure 4.1.2.1.

4.1.1.15 and 4.1.1.16). This contraction of the flow profile in the axial direction with the decrease of the mobile phase linear velocity may be explained by considering the theories that assume that molecular diffusion in the radial direction and anastomosis or stream splitting act toward the reduction of the dispersive effects induced by the radial heterogeneity of the flow [Gordon *et al.*, 1963; Sie and Rijders, 1966]. Because of the low diffusivities of solutes in liquids, the contraction of the flow profile with decreasing linear velocity is relatively limited, but still significant.

A 10x250 mm commercial column packed with Econosil C_{18}-modified spherical silica, having an average particle size of 10 μm, acquired from Alltech (catalog number 6235) showed a very similar flow profile (Figure 4.1.2.4 and 4.1.2.5). This profile was recorded at a flow rate of 1 ml/min, corresponding to a value of v = 18.9. The differences in the local value of the linear velocity versus the velocity measured at column axis were found to be larger for this column (up to 4%) than the ones measured for the previous column (up to 2.5%), suggesting a somewhat larger thickness of the wall region of the packing in this column. Also, the central region of the packing that experiences a relatively flat flow profile extends to a smaller fraction of the column diameter (from about $-0.4r_c$ to about $+0.4r_c$) than for the 7.8x300 mm column discussed earlier.

The most uniform flow profile measured in this study resulted for a 9.4x250 mm commercial column packed with Zorbax XDB-C8, having a particle size of 5 μm (Rockland Technologies, Newport, DE). As shone in Figure 3.3.6.3 this column exhibited an excellent efficiency for retained analytes like phenol (k'=0.72) and

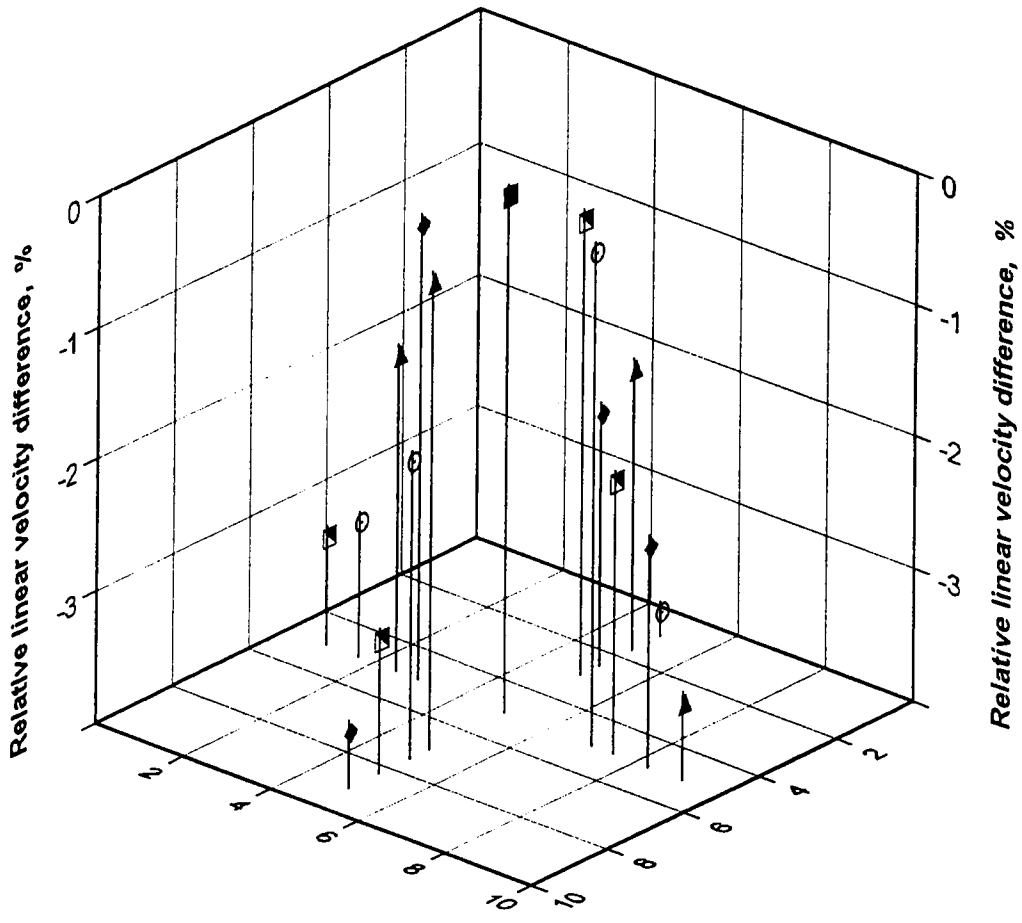

Figure 4.1.2.4 3D-view of the distribution of the mobile phase local linear velocity at the column outlet for a 10x250 mm Alltech column packed with C_{18}-modified 10 μm particle size spherical silica.

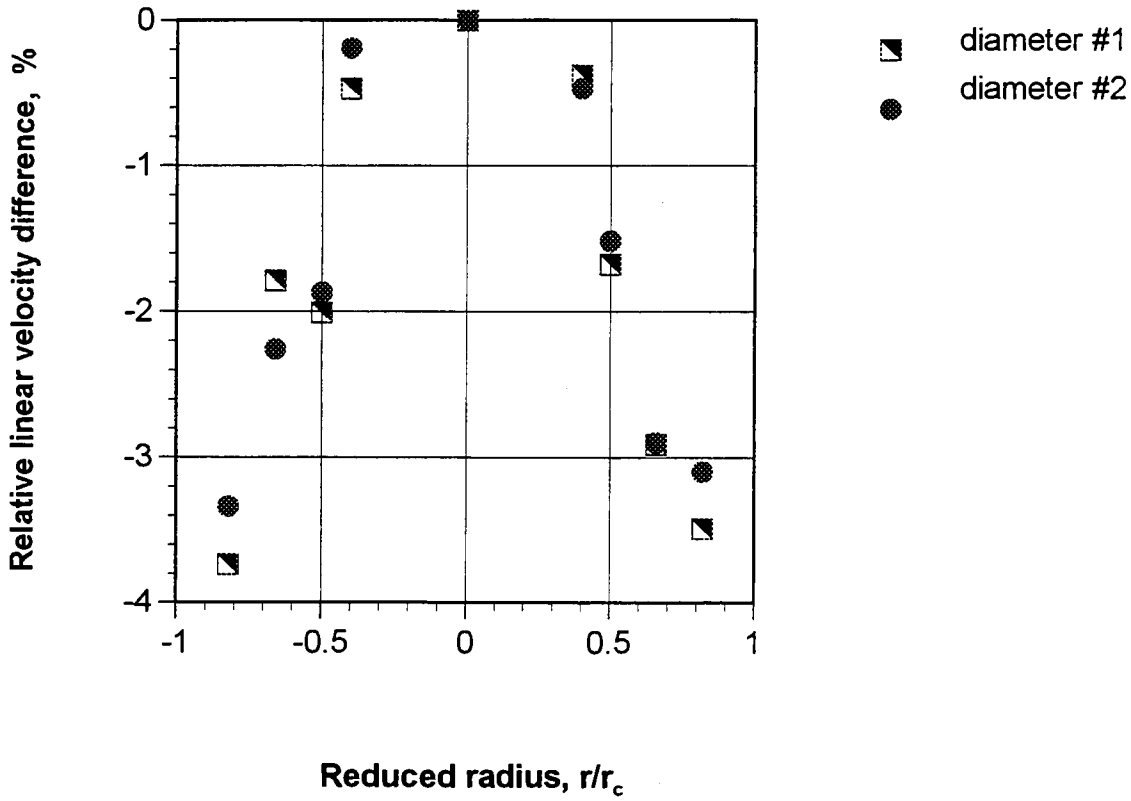

Figure 4.1.2.5 2D-view of the distribution of the mobile phase local linear velocity at the column outlet at locations along two perpendicular diameters, overlaid. Same column and data as in Figure 4.1.2.4.

toluene (k'=1.9). The reduced HETP for these analytes was as low as 2 and 2.5 at the optimum reduced mobile phase velocity, respectively. The flow profiles obtained for this highly efficient column at a flow rate of 0.9 ml/min (v = 7.1) are shone in Figure 4.1.2.6 and 4.1.2.7. The linear velocity measured close to the column wall is only on average 1.4% smaller than the one found at column axis. The more significant feature of this profile is that the central region of the packing experiencing relatively small linear velocity differences is extending from about $-0.75r_c$ to about $+0.75r_c$. This makes the wall region -- where the linear velocity is significantly smaller (but not as much as for the two columns discussed earlier in this chapter) -- relatively thin. The significance of this observation relies on the fact that in this case the region of the component zone moving at a more or less even velocity within the column packing is extending through much of the bed volume situated far from column wall. Furthermore, it is surrounded by a layer of packing where the linear velocity is not significantly lower (0.75% on average) than the average velocity experienced by the core region. This leaves less room for the wall region which affects the overall band shape because of its lower mobile phase velocity. In terms of the fraction of bed volume these three regions occupy inside the column, the core region amounts to about 0.56, the intermediate region -- corresponding to the annular region surrounding the packing core, with the approximate limits $0.75r_c$-$0.85r_c$ -- to about 0.16, while the wall region to the remaining 0.28. The latter figure is still significant, but since the difference between the linear velocity measured at column wall and center is not large compared to

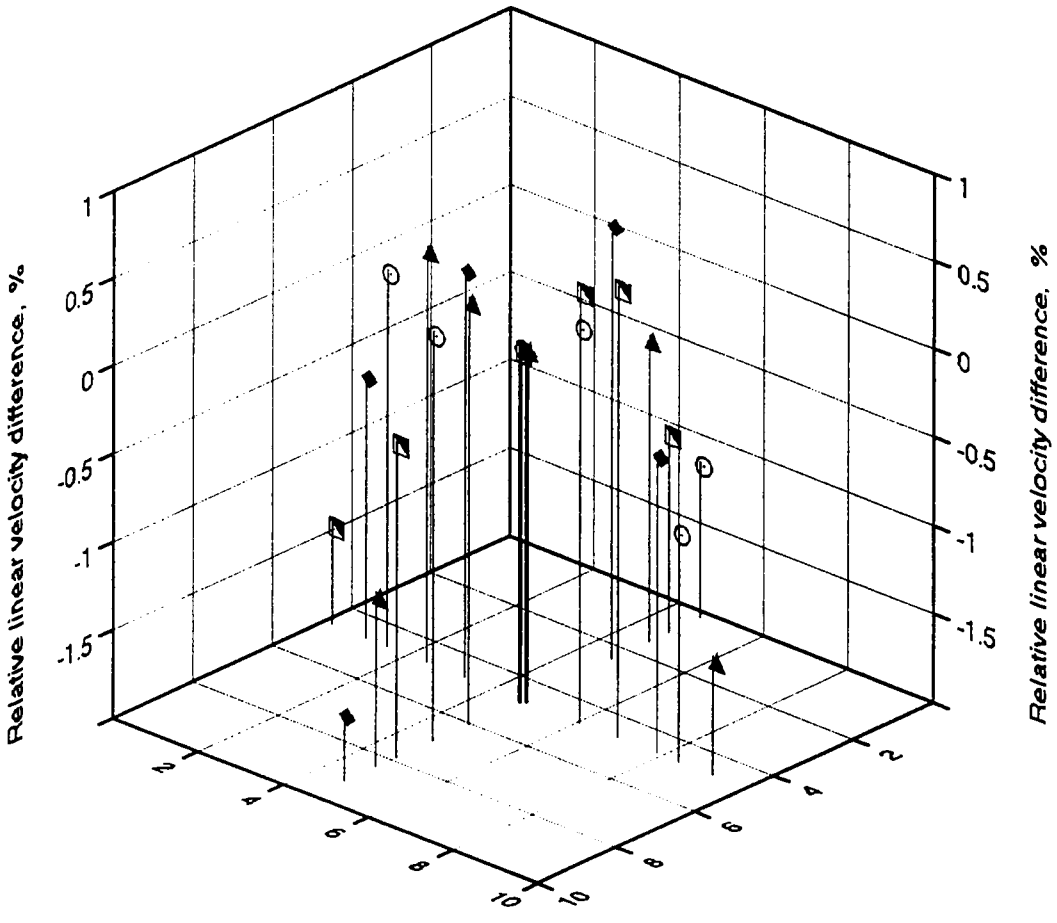

Figure 4.1.2.6 3D-view of the distribution of the mobile phase local linear velocity at the column outlet for a 9.4x250 mm Zorbax column packed with C_8-modified 5 µm particle size spherical silica.

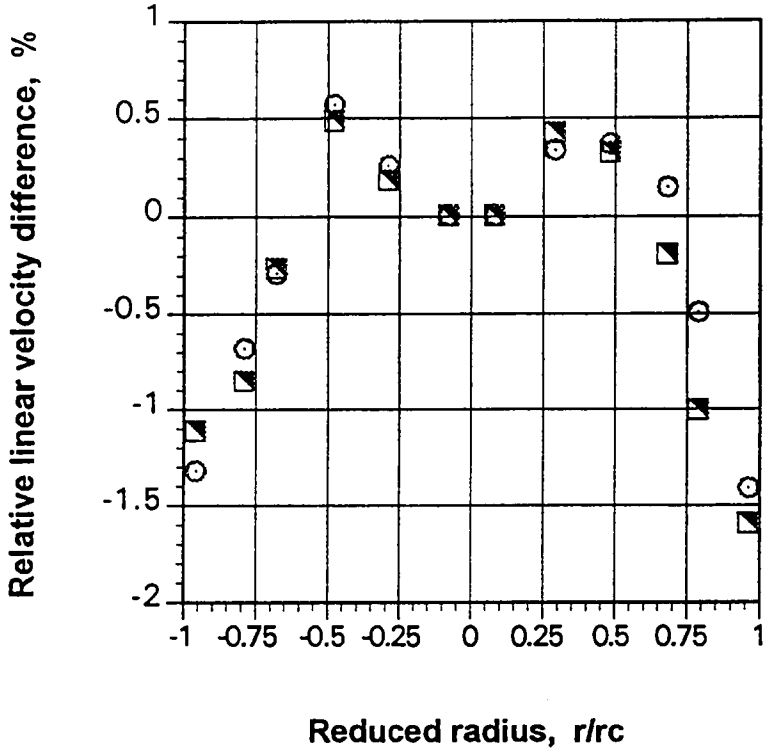

Figure 4.1.2.7 2D-view of the distribution of the mobile phase local linear velocity at the column outlet at locations along two perpendicular diameters, overlaid. Same column and data as in Figure 4.1.2.6.

what other columns investigated in this study exhibited, its effect on the shape of the integral peak is small.

The flow profiles measured for the largest columns considered in this work -two axial compression columns having the dimensions 50x150mm- are presented in Figures 4.1.2.8 and 4.1.2.9. The most obvious characteristic of these velocity profiles is their near cylindrical symmetry. It is obvious that there is a large difference between the linear velocity in the core region and the one in the wall region of a preparative scale chromatographic column. The linear velocity appears to be highest at the column axis. The profile of the velocity distribution is relatively flat around the column center and decays rapidly close to the column wall. This decay seems to be monotonous, with no points of discontinuity.

It has been a recurring observation [Farkas *et al.*, 1994, 1996] that the analyte retention time measured in efficient analytical size columns at locations situated at about one third, and up to one half of the column radius away from the column axis tends to be slightly shorter than the retention time recorded at the very center of the column. This finding suggests that there may be an annular region around the axis of efficient columns where the flow is the fastest, while the flow in the central region would somewhat lag behind (generally by no more than 1%, often by less than 0.5 %). This result is illustrated in Figure 4.1.2.10 which shows the overlaid plots of the relative velocity differences as a function of the radial position of the probe for three different columns. Many experiments made on larger columns suggested the same pattern although a definitive conclusion cannot be

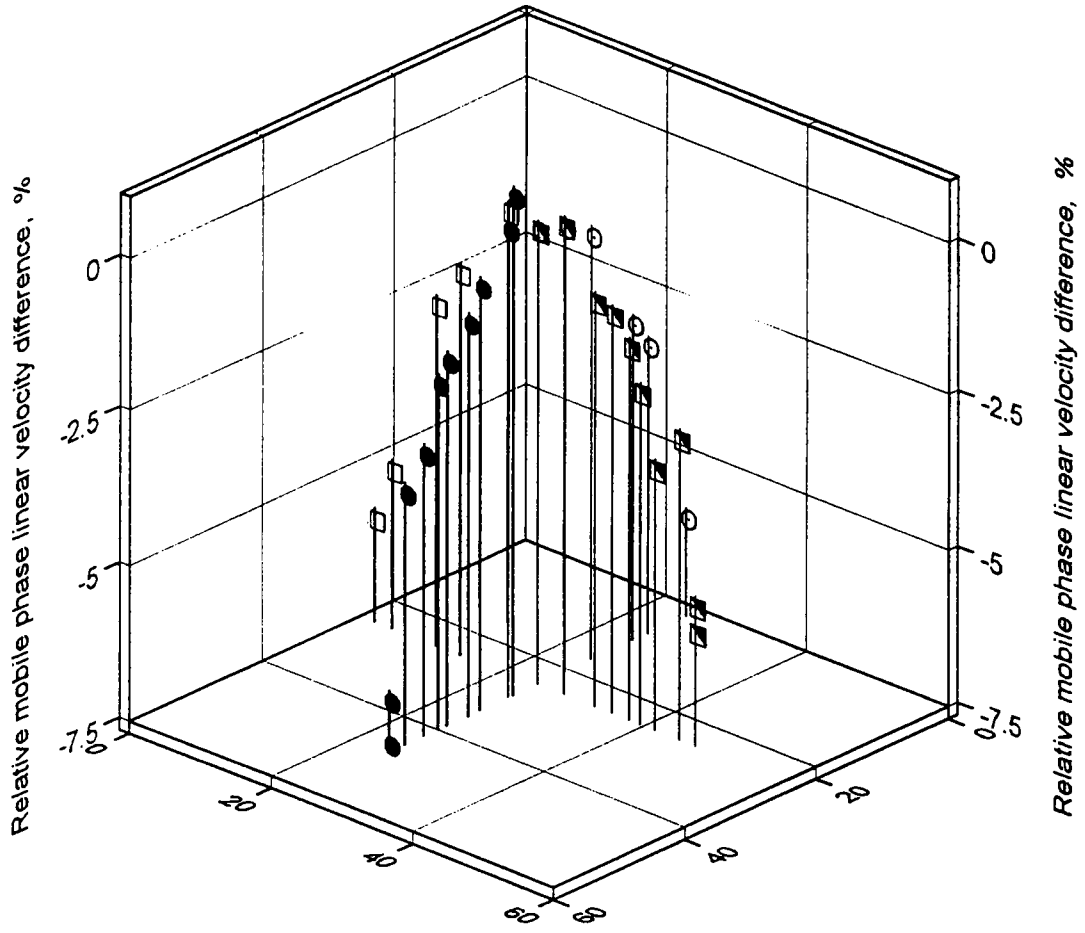

Figure 4.1.2.8 Distribution of the mobile phase velocity at the column outlet for a 50x150 mm axial compression column packed with Zorbax PRO-10/150 C_{18}-modified 10 μm particle size spherical silica (open symbols were adopted for data resulted at locations of detection situated behind the viewing angle).

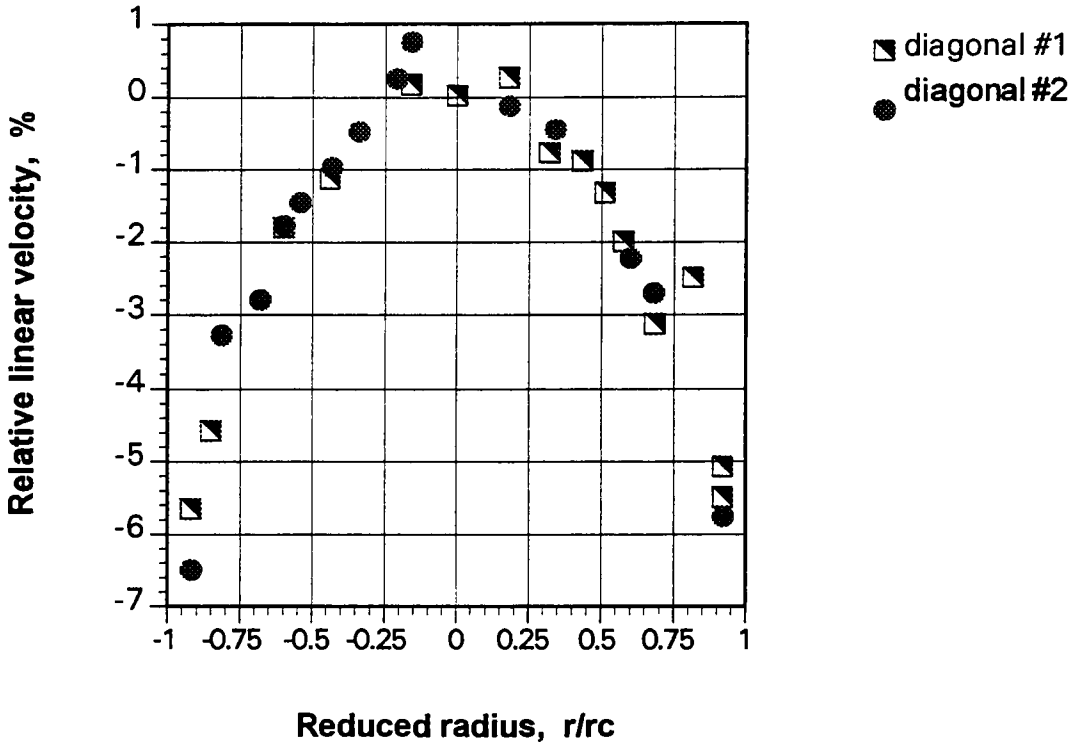

Figure 4.1.2.9 2D-view of the distribution of the mobile phase local linear velocity at the column outlet at locations along two perpendicular diameters, overlaid. Same column and data as in Figure 4.1.2.8.

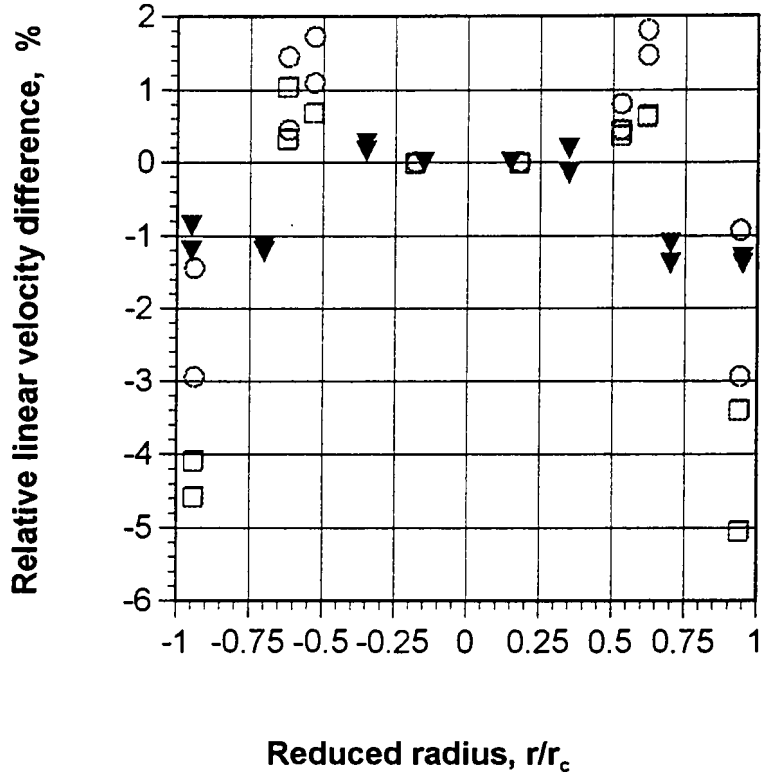

Figure 4.1.2.10 Distribution of the mobile phase velocity at the column outlet for three analytical HPLC columns, overlaid. 2D plots of the linear velocity versus the radial position where detection was performed along the two perpendicular diameters considered in Figure 3.3.2.3. □ 4.6x100 mm column packed with 10 μm irregular porous silica; ○ 4.6x150 mm column packed with 16 μm C_{18}-modified spherical silica; ▼ 4.6x100 mm column packed with 10 μm C_{18}-modified spherical

drawn for these columns. The reason for this is that too few data points were acquired in the vicinity of the column center because the column is large and we could not afford the density of data points around its center which would have been required without losing more important information close to the column wall. The precision of our measurements (the relative standard deviation is less than 3.5 % for 6 to 8 consecutive runs) precludes any doubt regarding the prevalence of locations around the column axis where the linear velocity is higher than at the column center. At the same time, however, measurements made at different locations corresponding to the same radius (i.e., along a circle centered at the column axis) resulted also in some data points contradicting this observation. Mapping out this region of the packing would have required placing all of the fiber assemblies close to the column center.

A probable explanation to these results would be that the profile of the flow velocity distribution in the core region of the bed is not flat but wavy. The reference sensor located at the column center could be only by chance (*i.e.,* rarely) located at the top of a wave; most often, the velocity in many locations around the center would be faster, but in some places it would be lower and the cylindrical symmetry would be lost for this feature. This explanation is in agreement with the results of the study of the profiles of gadolinium complexes reported recently by Tallarek *et al.* [1995] and Bayer *et al.* [1995]. Anyway, the velocity differences measured in the core region of the bed are much smaller, and consequently much less important, than the important decrease in the linear velocity in the wall region.

4.2 Radial Distribution of the Column Efficiency

On-column local, multiple channel detection has the potential of providing information not only regarding the radial distribution of the mobile phase linear velocity, but also the fluctuations in local column efficiency integrated along a certain pathway over the column cross-section. All locally detected peaks over the exit cross-section of a HPLC column are different not only in the temporal position of their maximum, but also in shape. From their width at half height we could calculate the local efficiency of the column, which is a measure of the convolution of all dispersion steps that take place along a given stream path that runs more or less parallel to column axis, and that ends at the point of detection. However surprising it can sound, the local width of the band has not much to do with the overall shape of the band, and does not necessarily influence the overall efficiency of the column! In other words, the column may show an extremely high efficiency at any position over its cross-section, and still perform extremely poorly in separating closely eluting compounds. This would be the case of a column showing a perfectly cylindrical distribution of its flow profile with large shifts in the local value of the linear velocity of the mobile phase moving in adjacent cylindrical volume elements. On the other hand, for other columns the local efficiency at given locations may be very low, while the column would still perform outstandingly. Such locations would be the finish point of stream paths that run through regions of significant channeling within the packing. In case the number of such low efficiency

points over the cross-section is small, their contribution on the overall efficiency of the column may be insignificant, the latter being determined by the composition of the majority of coeluting volume elements.

We have given in Figures 3.2.5.1, 3.3.6.1, 3.3.6.2 and 3.3.6.3 the conventional plots of the reduced column HETP versus the reduced mobile phase velocity, as measured with a UV-VIS detector for some of the columns investigated in this work. In the first case, as benzoquinone is practically not retained on most of these columns, the slope of the curve at high reduced velocities is essentially due to mass transfer resistance in the mobile phase. It is smaller for glass bead columns than for conventional silica columns, as the beads are not porous. Note, however, that because of its definition, the cross-sectional average velocity depends on the internal porosity of the particles. For a given flow rate, the hold-up time is approximately twice as large for a porous silica particle (with $\epsilon_T = 0.8$) as for non-porous glass beads, hence $\tilde{u}$ is twice smaller, while the actual values of the local solvent velocities around the particles are the same.

The width recorded for an elution band depends considerably on the location of the detection point. As seen in the Figures 4.2.1, 4.2.2, and 4.2.3, the column efficiency calculated from the width of the peak at half-height (see equation 4.2.1, where N is the number of theoretical plates, t_r the retention time of the test analyte, and $w_{1/2}$ the peak width at half height) depends much upon the radial position of the electrode. However, the results obtained with different columns show more variability in local efficiency than in local mobile phase velocity. Figure 4.2.1

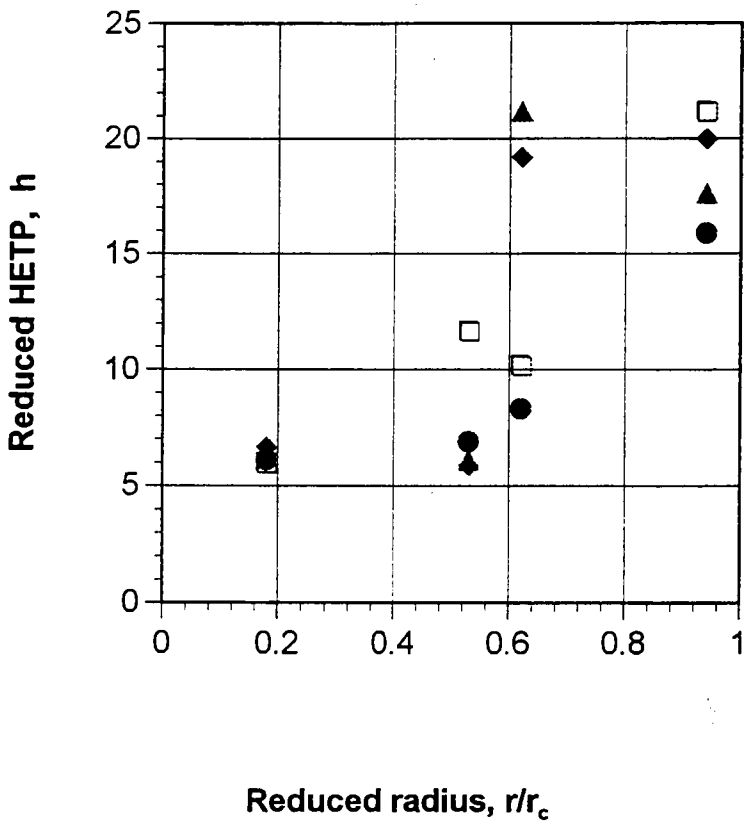

Figure 4.2.1 Plot of the column reduced HETP versus the radial position of the electrode tip for a 4.6x240 mm column packed with 40 μm glass beads. ❐ data collected when holding frit in its initial position; ●, ▲, and ◆ data collected after the holding frit has been rotated with one, two, or three steps of 90^0 each around column axis, respectively.

$$N = 5.54\times \left(\frac{t_r}{w_{1/2}}\right)^2 \qquad (4.2.1)$$

illustrates the dependence of the local efficiency on the radial position of the probe in the exit cross-section of a column packed with 40 µm glass beads. The most efficient section of this column seems to involve the core and the intermediate region corresponding to the high velocity ridge (shone in Figures 4.1.1.4-4.1.1.6). Within this central region, most of the data points are around 900 theoretical plates, corresponding to a reduced plate height of ca 5.5 (for a reduced velocity, ν, of *ca* 90). However, some values for the data points in this region can be as low as 300 plates, which is very poor, and unexpected. Such a low value for the local efficiency can be explained by the existence of stream paths running through regions of significant channeling within the packing. The local efficiency drops sharply in the region close to the column wall, where all the data points are below 350 plates (corresponding to a value of the reduced HETP, $h=L/Nxd_p$ of 15-21). Furthermore, peaks recorded at radial positions close to the wall are strongly distorted and wide and show significant tailing. Examples are shown in Figure 4.1.1.3.

Figure 4.2.2 shows a plot of the column reduced HETP over the radius for a column packed with 10 µm irregular silica particles. The result is quite similar, except for two notable differences. First, this column shows a monotonously increasing local efficiency in the core region of the packing as the detection point is moved from column center toward column wall. In the wall region -which seems

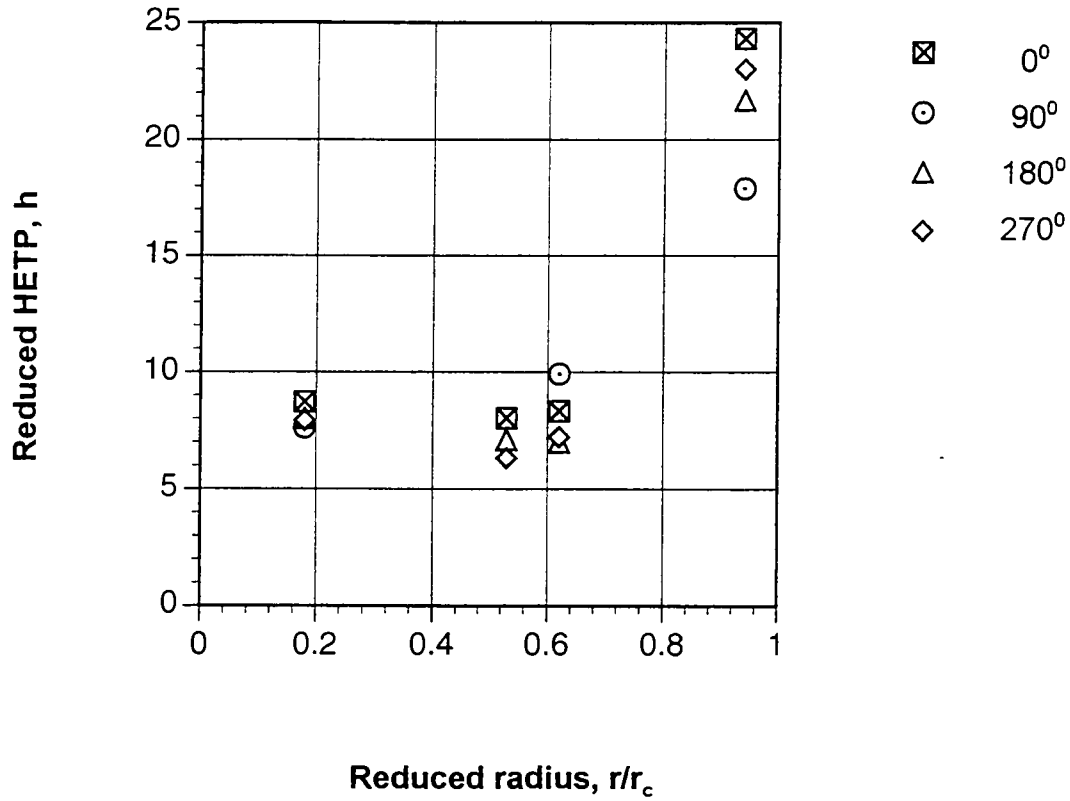

Figure 4.2.2 Plot of the column reduced HETP versus the radial position of the electrode tip for a 4.6x200 mm column packed with 10 μm particles of irregular porous silica.

to behave completely differently- this column shows the same large fluctuation in the value of local efficiency as the first column described here. Second, the distribution shows a clear maximum of the local efficiency at the maximum velocity ridge, where the efficiency is nearly three times larger than along the wall, against 2.5 times in the center. As for the previous column (Figure 4.2.1), the efficiency drop is precipitous starting around two-third of the distance between the center and the wall. As seen in both Figures 4.2.1 and 4.2.2, it seems that the column is not exactly cylindrical, since the "wall region" is thicker along some directions than along others.

As seen in Figure 4.2.3, the commercial Kromasil column, packed with 16 μm spherical particles, seems to be more homogeneous -except for one single data point- than our packed columns, although the effects are substantially the same. The shape of the plot of the column efficiency versus the radial position of detection is quite similar to those seen in Figure 4.2.2, and to that of the plot of the peak-maximum velocity versus the radius presented earlier (Figure 4.1.1.6). The column efficiency is poor at the column wall, maximum along the velocity ridge, and lower again at the center. However, the efficiency drop observed near the column wall is much less important than in the other columns. The efficiency at the wall is about 60% of the maximum, along the velocity ridge, and, quite surprisingly, more than 90% the efficiency in the core region. This column is certainly much more homogeneously packed than those made in our laboratory.

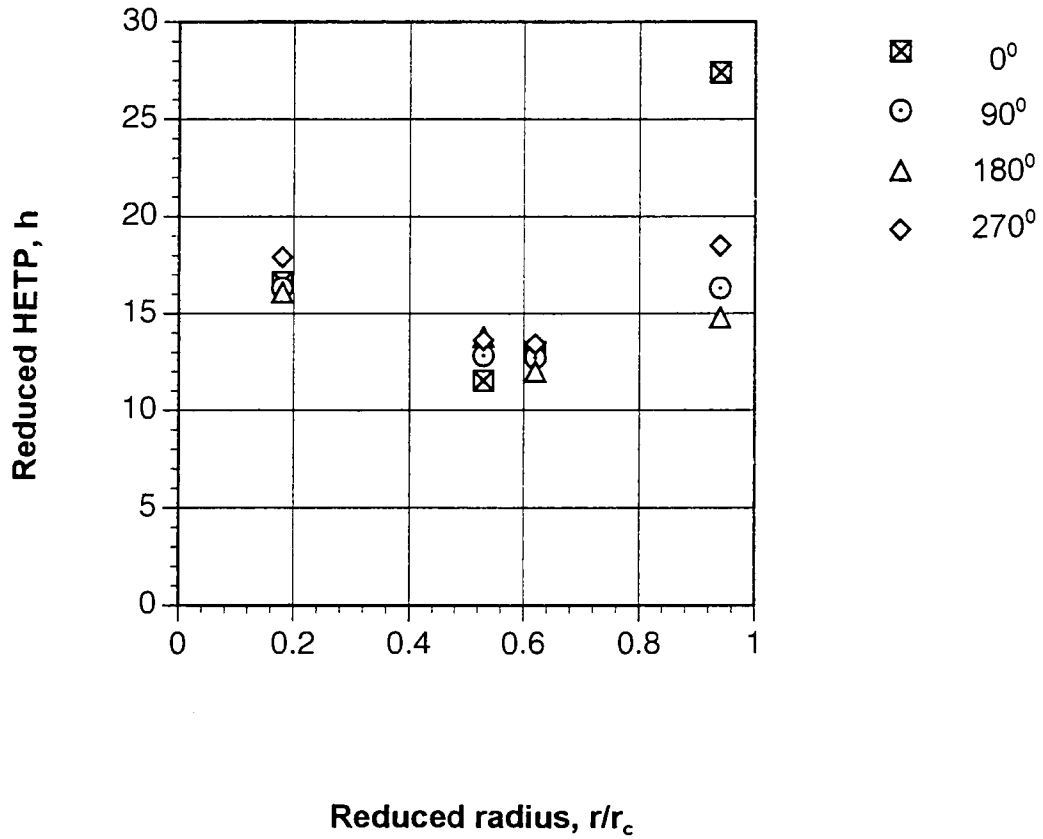

Figure 4.2.3 Plot of the column reduced HETP versus the radial position of the electrode tip for a commercial 4.6x150 mm KROMASIL KRO100-16-C_{18} column packed with 16 μm particles

We compared these findings to the local efficiency distribution resulted for analytical columns investigated with the other detection system using laser induced fluorescence. The column efficiency calculated from the peak width at half height for peaks of Pyrromethene 556 recorded at different radial locations over the exit cross-section of a 4.6x100 mm column packed with 10 μm particles of Zorbax C_{18} regular silica is plotted in Figure 4.2.4. It proves again to be much lower at and close to column wall than it is in the central region of the packing.

These results agree with those previously published, but only to a point. As reported here, Knox *et al.* [1976], Eon [1978], and Baur *et al.* [1988; 1989] found that the column efficiency is much better at the center than along the wall. The profiles of the radial distribution of the column efficiency shown by Knox *et al.* [1976], by Eon [1978], and by Baur *et al.* [1988] are similar to those shown in Figures 4.2.1-4.2.4. In all these cases and in the present work, the maximum efficiency is two to three times higher than the efficiency near the wall. However, all these authors found the column efficiency to be more or less constant in the core region of the packing (Figure 4.2.5, and see figure 5 (p. 36) in Eon [1978]; figure 5 (p. 137) in Knox et al. [1976]). This is not the case for the different columns studied here, not even for the commercial column. This shows that more work is needed to develop an improved packing technology which could reduce or eliminate the wall region and give a more homogeneous, more efficient packing bed.

We can conclude that in the case of analytical size columns, the radial distribution of the local efficiency shows a similar pattern to the distribution of the

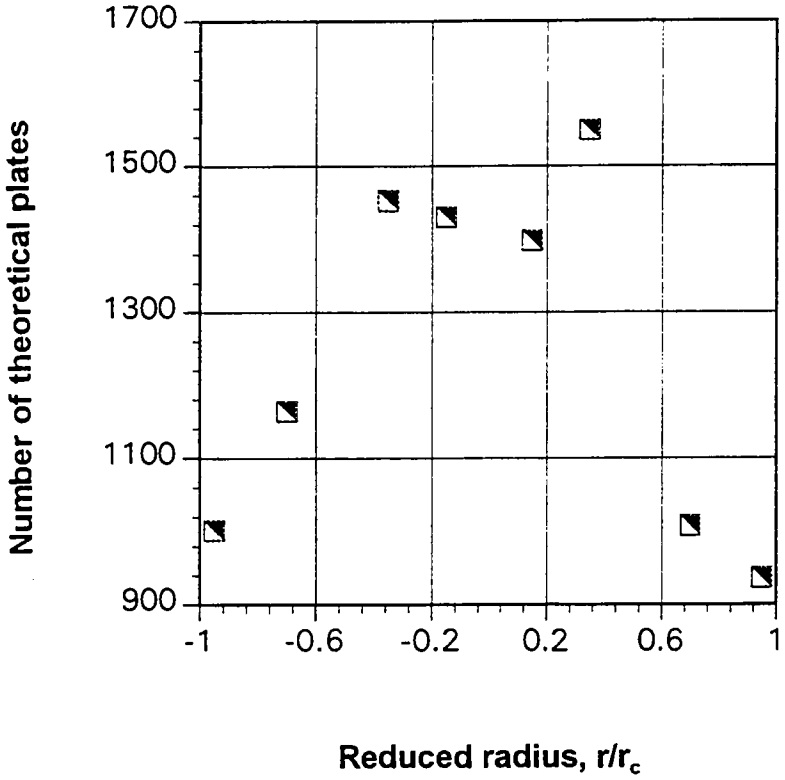

Figure 4.2.4 Plot of the column efficiency versus the radial position of the optical fiber-assembly tip for a 4.6x100 mm column packed with 10 μm Zorbax PRO-10/150 C_{18}-modified spherical silica.

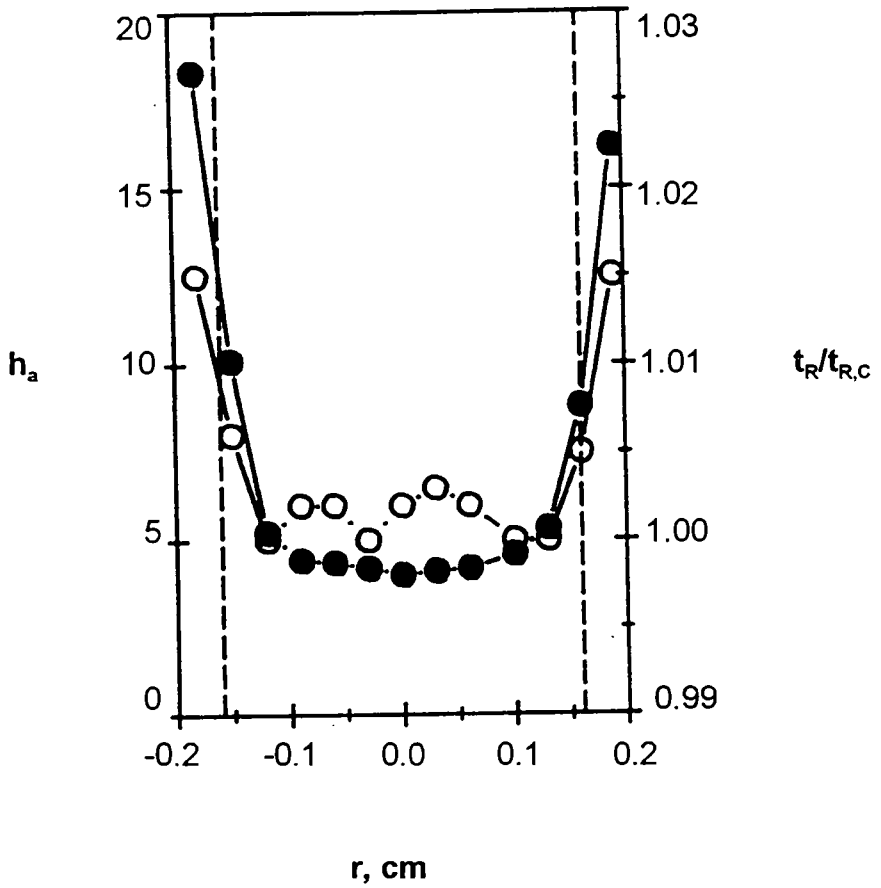

Figure 4.2.5 Normalized retention time (O) and reduced axial plate height (●) as a function of the radial position of detection for a 3.2x100 mm ODS column packed with 3 μm particles. Source: Baur *et al., Anal. Chem.*, 60 (1988), 2334.

mobile phase linear velocity. The wall region of the packing, because of its higher degree of heterogeneity, produces more disperse local analyte bands which build into a tailing of the overall band, and cause to some extent an increase in peak width (*i.e.*, a decrease in column efficiency).

The radial distribution of the local efficiency for the large diameter columns investigated in this study showed was similar to the distribution found for analytical size columns. The 7.8x300 mm Waters columns discussed in chapter 4.1.2 for its radial distribution of the local linear velocity, showed large variations in the local value of the efficiency along the column radius. Figure 4.2.6 shows data on the local efficiency measured along two perpendicular column diameters. The best efficiency was recorded close to column axis, at locations situated along a circle having the reduced radius 0.29. The local value of the reduced HETP is about 20% lower at these locations than at column axis. A sharp increase in the local value of the reduced HETP is registered as the point of detection is moved away from column axis. At locations situated at midway between column center and column wall an average value of about 9 is found, while at column wall the reduced HETP can be as high as 19.4. The peaks recorded close to column wall are much wider and asymmetrical. Overall, the distribution of the local efficiency shows a high degree of cylindrical symmetry, with noticeable angular fluctuations only in the wall region of the packing. The values for the standard deviation of the measurements performed at locations along the same circle of reduced radii 0; 0.26; 0.46; 0.51 and

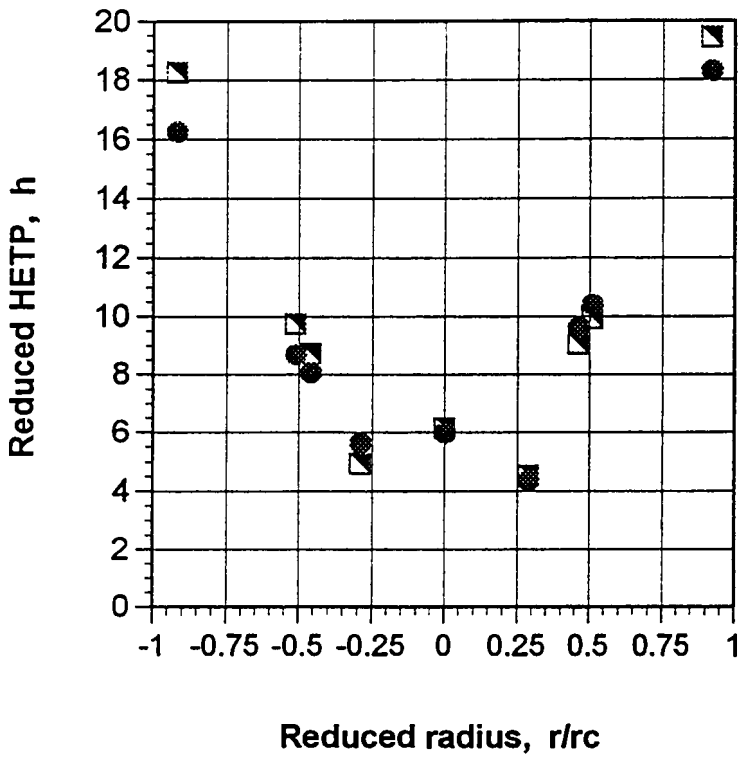

Figure 4.2.6 Plot of the column reduced HETP versus the radial position of detection for a 7.8x300 mm column packed with 10 μm particles of Zorbax C_{18} modified regular porous silica.

0.92 are 0.13; 0.56; 0.65; 0.72 and 1.31, respectively. These values show increasing fluctuations in the local efficiency as the point of detection is moved from the center of the bed close to the column wall.

A higher degree of packing heterogeneity at column walls results in a higher degree of dispersion of the analyte band and poor local efficiencies. This already diffuse cylindrical sector of the analyte band is being diluted even more by the coeluting parallel flow coming from the core region of the eluting plug where most of the analyte has left the column already. A consequence of the experimental results of previous authors, confirmed by our own results, is that markedly better separations could be performed by HPLC if only on-column detection was performed. A three-fold gain in column efficiency is a major achievement, translating into a 70% better resolution, or three times faster analyses. If this approach is used, however, the positioning of the detecting sensor should be done carefully, by locating it within the core area within half a column radius from the column axis, or even better, along the maximum efficiency ridge.

In order to exemplify the advantages of on-column detection, we investigated the separation of three laser dies on the 7.8x300 mm Waters column discussed earlier. The three chromatograms recorded with three optical fiber assemblies positioned at reduced radial locations of r/r_c equal to 0.29, 0.51 and 0.92 respectively, are presented in Figure 4.2.7. While the peaks corresponding to PM and Disodium Fluorescein are well separated in the core region of the packing, resolution is lost as the point of detection is moved away from column center. This

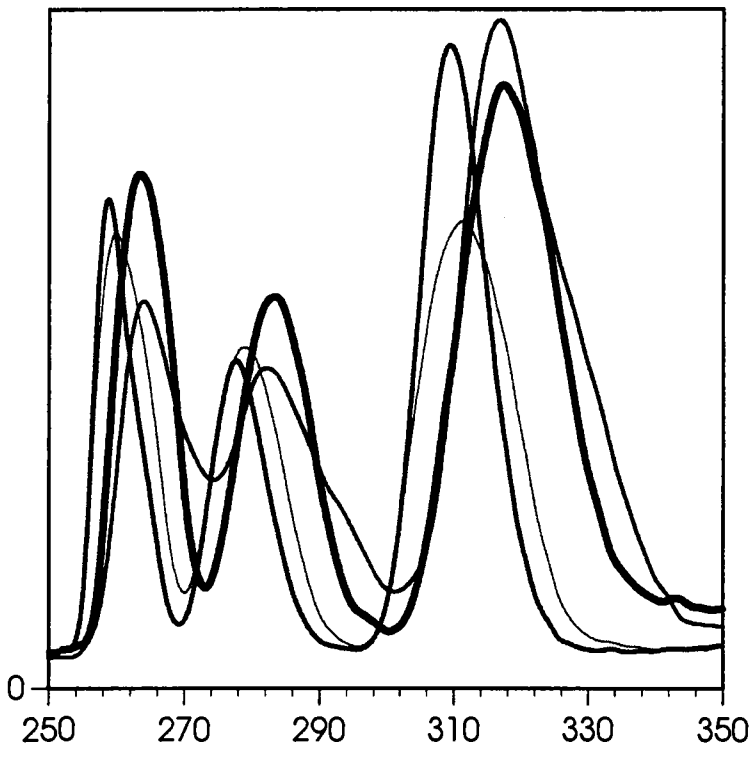

Figure 4.2.7 Chromatograms recorded at three different radial positions over the column exit cross-section and the chromatogram recorded on the bulk eluent (solid line), overlaid. The locations in the order of decreasing resolution are: r/r_c= 0.29; 0 and 0.92. Conditions: 7.8x300 mm column packed with 10 μm particles of Zorbax C_{18}-modified regular porous silica; flow rate, 1 ml/min methanol-water 60:40; sample, 20 μl solution of PM, Disodium Fluorescein and Dibromofluorescein 0.4 g/l each in methanol-water 60:40.

loss in resolution is so dramatic that in the packing region situated close to column wall the three analytes are not resolved. It is obvious that positioning the on-column detector in the region of the column outlet where the local efficiency is the highest cannot improve the column performance for a preparative application, but it can definitely improve the success of an analytical separation.

For the highly efficient Zorbax column having the dimensions 9.4x250 mm -- which showed the least deformed flow profile among all the columns investigated in this study,-- the radial distribution of the local efficiency is presented in Figure 4.2.8. The best local efficiency was registered at column center and the change in the value of the local reduced HETP was found to be less dramatic than for the other columns described earlier. An increase of about 20% for this column is much less significant than the 200-300% increase registered for all the other columns investigated in this work.

For preparative scale columns, the radial distribution of the mobile phase linear velocity was similar to the one found for analytical size and ½" i.d. columns, but in some respects also different. Keeping in mind that for analytical size columns there was a similarity in the distribution profiles for their mobile phase linear velocity and local efficiency, we investigated the two axial compression columns described earlier for their distribution in local efficiency. In Figure 4.2.9 the local reduced HETP is plotted against the column reduced radius for one of the axial compression columns. This plot proves that the local column efficiency varies systematically

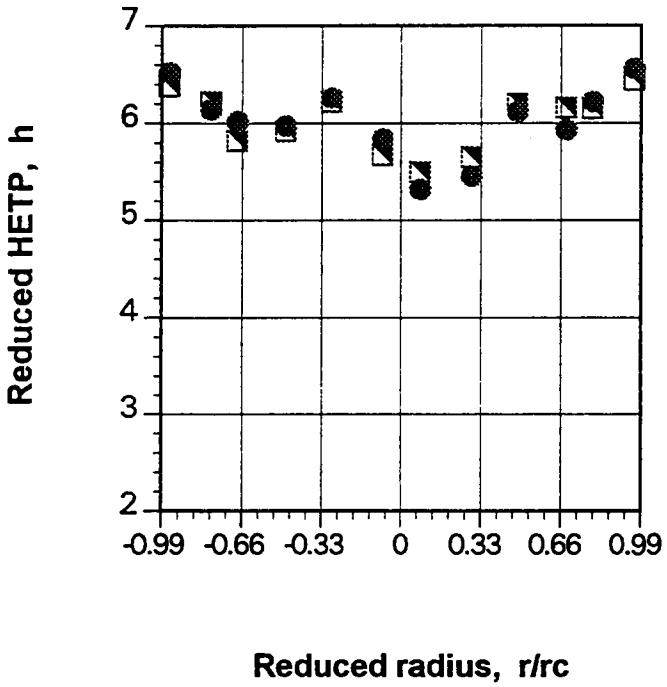

Figure 4.2.8 Plot of the column reduced HETP versus the radial position of detection for a 9.4x250 mm column packed with 5 μm particles of Zorbax C_8 modified regular porous silica.

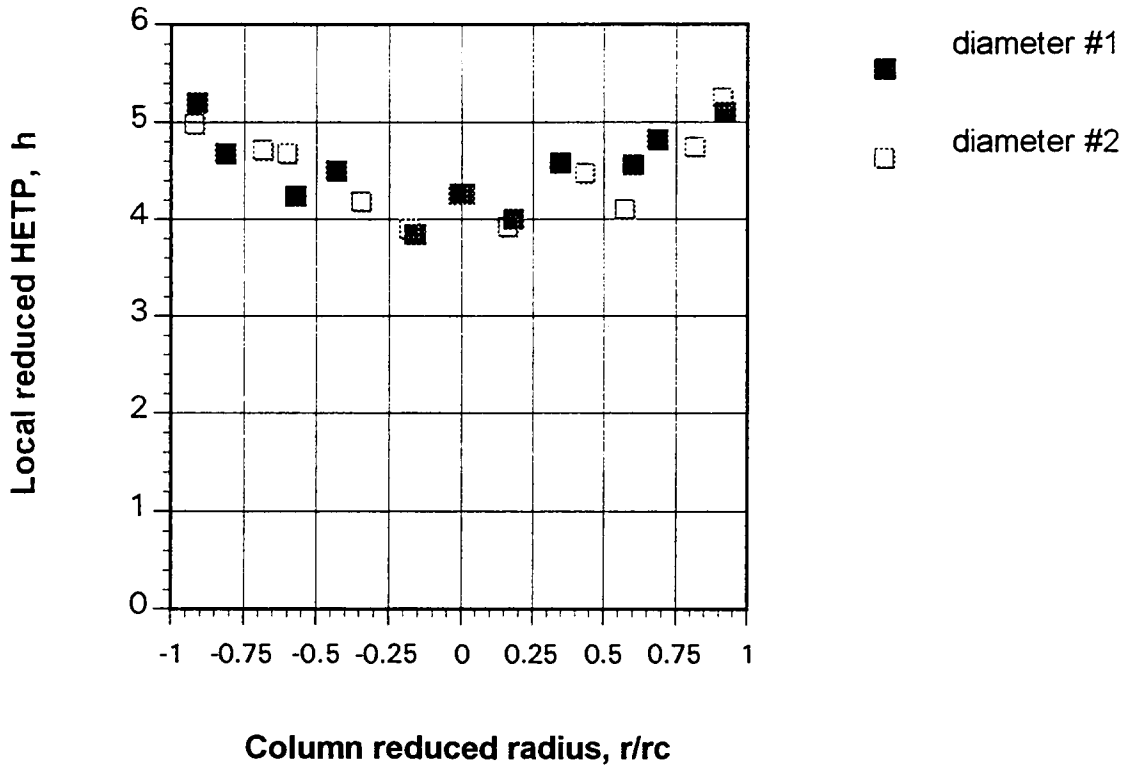

Figure 4.2.9 Plot of the local column efficiency versus the radial position of the optical fiber-assembly tip along two perpendicular diameters for a 50x150 mm axial compression column packed with 10 μm Zorbax PRO-10/150 C_{18}-modified spherical silica.

along the column diameter. The lowest values of the local reduced HETP (3.9) were recorded at locations close to the column center, while the highest values (5.1) were found close to the column wall. Thus, the reduced HETP was more than 25% larger close to the column wall than in its center. The values for the local efficiency (h = 3.9 to 5.1) are to be compared to the efficiency found for the same column in a classical instrumental set-up using an on-line detector on the bulk mobile phase. Uracil, 4,5-Dibromofluorescein and Disodium Fluorescein, all at a concentration of 0.4 g/L, were used for this purpose. Using the same mobile phase flow rate as before (50 ml/min), values of the reduced HETP of 7.2, 6.9, and 8.7 were found for uracil (k' = 0.1; ν (reduced velocity) = 11.8), Dibromofluorescein (k' = 0.88; ν = 27.7), and Disodium fluorescein (k' = 0; ν = 18.6), respectively. These average or apparent values are larger than any of the local reduced HETP values recorded.

A similar distribution of the local column efficiency was obtained for the second column studied. Figure 4.2.10 shows the overlaid distributions of the efficiency of the two columns, along an arbitrarily chosen diameter. Even though the second column was packed using the same packing material as used for the first column, after its recycling as explained above, the efficiency achieved with the second column was as good as the first ones. Actually, the values obtained for the efficiency of the second column are slightly higher, hence better, for most of the data points. The same trend was observed in the variation of the local efficiency for both columns, as shown in Figure 4.2.10.

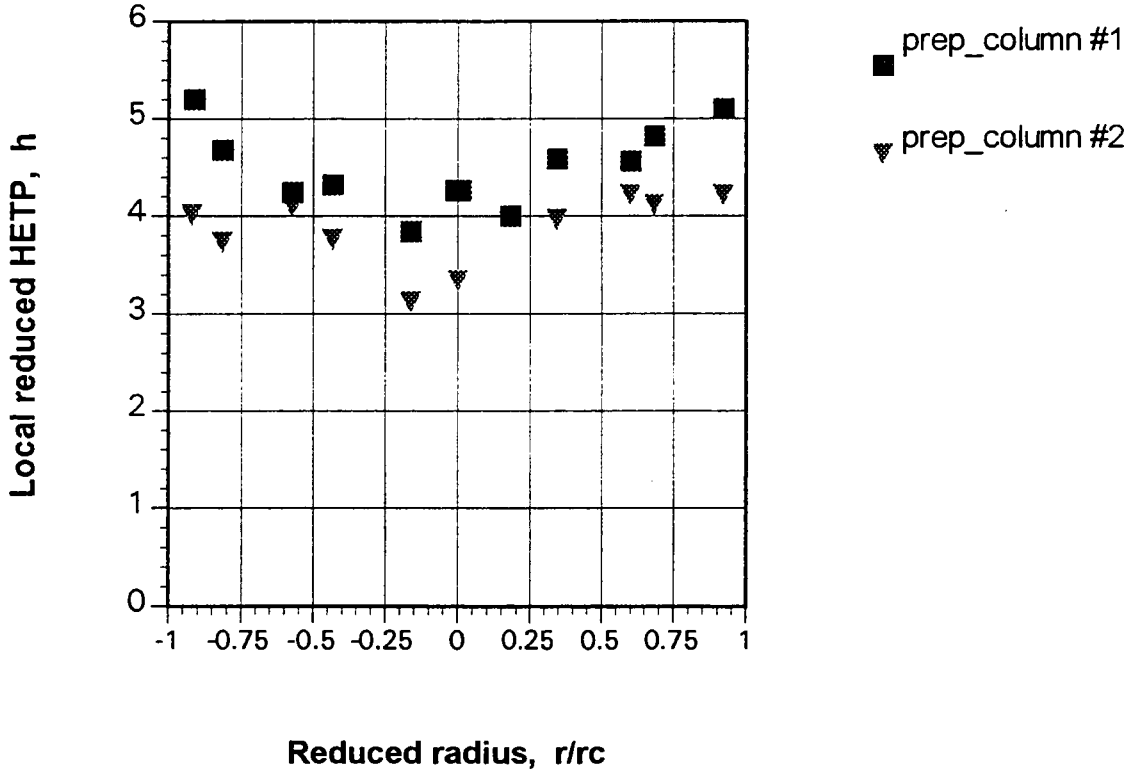

Figure 4.2.10 Plot of the local column efficiency versus the radial position of the optical fiber-assembly tip along the diameter, for two similar 50x150 mm axial compression columns packed with 10 μm Zorbax PRO-10/150 C_{18}-modified spherical silica, overlaid.

In the case of the preparative columns investigated in this work, an important part of the sample injected onto the column propagates at a lower velocity than the bulk of the zone, as we have shown in the previous section. This induces a shift in the position of the weight center of the band such that a higher elution time is recorded and at the same time the overall band width is increased significantly. As a consequence, local, on-column detection always results in narrower peaks, exhibiting less tailing and a band shape closer to a Gaussian profile, even if the local efficiency were to be constant, independent of the radial position of the detector. The local column efficiency is always higher that the apparent efficiency measured by testing the column following the conventional procedure, connecting the column exit to the cell of a bulk, on-line detector. This result is in agreement with the independent findings of Baumeister *et al.* [1995] and Tallarek *et al.* [1997] who used pulsed field gradient NMR to measure the average momentary axial dispersion coefficient in packed columns and found it to be much lower than the value given by an on-line detector.

These results illustrate the observation made long ago by Giddings [1963] that trans-column variations of the mobile phase velocity have pernicious effects on the column efficiency. The distribution of the flow velocity inside a chromatographic column has a considerable influence on the outcome of an analysis or a preparative separation. A 5% difference between the velocity in the column center and close to its wall means that when molecules of the second component of a binary mixture

with a separation factor of 1.05 leave the column center, they coelute with those molecules of the first component which migrated close to the column wall. Radial dispersion can relax the corresponding concentration gradients in a narrow bore analytical column (i.d. less than 0.5 to 1 mm), but it cannot do so in a preparative column [Knox and Parcher, 1969]. It is only if the distribution of the population density of the analyte molecules follows a narrow normal distribution along the column axis with a mean position independent of the radius that we obtain narrow and symmetrical peaks. Such peaks are required for the achievement of highly efficient separations. Any distortion of this ideal structure of the analyte zone results in dramatic loss of column efficiency. Such a loss takes place when the mobile phase propagates along the column with a radial velocity profile that is not flat.

4.3 Radial Distribution of Analyte Concentration

The ideal injection profile for any chromatographic system described earlier in chapter 3.2.3.1 defines the initial distribution of the analyte concentration and amount starting out at any point over the cross-section of the bed at column inlet. As stated before, such a profile would be ideally a rectangular band having a constant concentration throughout its entire volume. The representation of this band in concentration-time coordinates corresponds to a pulse function of constant height (which is related to the concentration of the injected sample), and a width

determined by the injection volume and the mobile phase flow rate. However, any experimental injection profile differs somewhat from this ideal model as shown before in chapters 3.2.3.1 and 3.3.7 (figures 3.2.3.1.1, 3.2.3.1.2 and 3.3.7.1.1), by the lack of a concentration plateau, at least for analytical size injection volumes, and by diffused sides which have shapes resembling more or less a Gaussian profile. We showed that in the case of the injection system used with analytical size and ½" i.d. columns for the local linear velocity and local efficiency measurements, the injection band proved to be compact and radially homogeneous. This means that all volume elements of the component zone start out on their travel through the chromatographic column packing at the same time while having the same concentration. It is obvious now that at column exit, because of the heterogeneity of the bed, the constitution of the component zone is also heterogeneous, showing significant differences between its core region and its region next to the column wall. Because of accentuated dispersion at column wall, the local concentration maximum in this region is smaller than at column center. But is it always the same amount of analyte eluting over unit of column cross-sectional area, only in a larger volume of effluent (because of larger dispersion)? We can speculate on this issue by advancing the opinion that probably this is not true. It seems to be reasonable to assume that the same spatial rearrangement of the mobile phase volume elements that resulted in the flow profiles described earlier, will bring along a radial redistribution of the flow rate itself inside the column. This means that whenever the

local flow redistributes by opting for the path of lesser resistance the amount of analyte carried along will also be redistributed.

The problems related to electrode calibration (unstable specific response caused by an increase in active area due to electrode surface electropolishing opposite to a simultaneous decrease in the same area caused by irreversible surface fouling) have been described in chapter 3.2.7. The response factors we determined for our electrodes that had their active surface changing continuously (probably even during the relatively long lasting frontal analysis experiment required for the calibration itself), may be used only with considerable skeptism. Figure 4.3.1 shows the distribution of the signal maximum over the column cross-section corrected for the differences in response compared to the electrode placed close to the column axis. Despite the relative lack of precision in the determination of the local concentrations at different values of the column radius, we see that the maximum peak height is largest at the column center and in the core region surrounding it, while it is three to four times lower along the column wall.

This result is in agreement with our previous findings regarding the distribution of the local column efficiency. Since the bands are wider and the column efficiency is poorer at the wall than in the core region, the same amount of material injected per unit surface area will give a peak shorter along the wall than in the center. The results shown in Figure 4.3.1 are in excellent agreement with those obtained by Baur *et al.* [1989] with a 3.2x40 mm column packed with 3 μm RP-18 silica. The ratio of the values of maximum concentration at the column

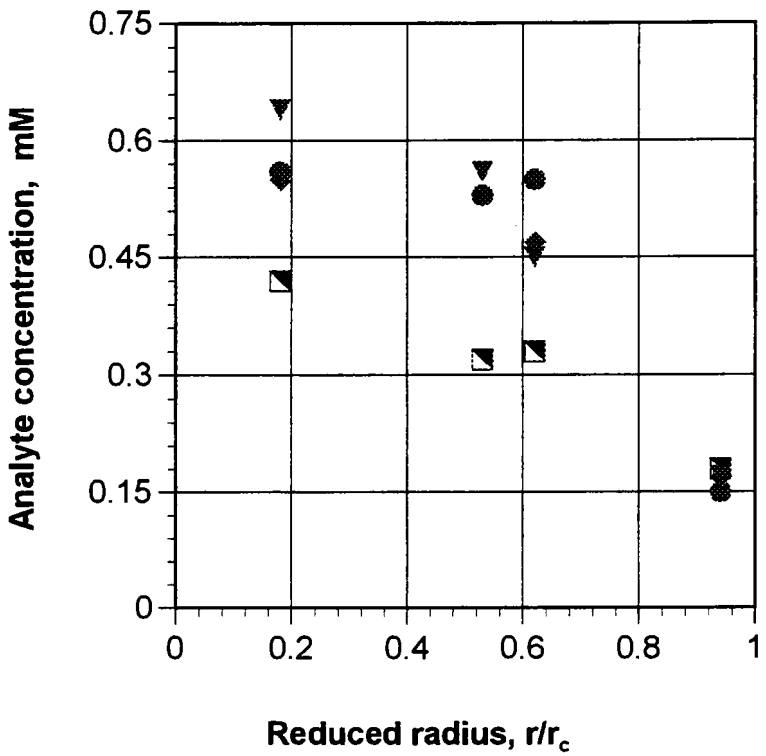

Figure 4.3.1 Radial distribution of the analyte maximum concentration in a 4.6x150 mm Kromasil KRO100-16-C_{18} column packed with C_{18}-modified 16 µm particle size spherical silica.

center and along its wall is *ca.* 5 in their results, while it is about 3 to 4 in ours (Figure 4.3.2).

The problems related to electrode response calibration in the electrochemical detection system were overcome by switching to the laser induced fluorescence detection system. Probe tip fouling is not a problem for optical fiber sensors, and their active surface stays constant and is in no way a life limiting factor. Actually, the specific response of the optical fiber assemblies we used is not related to the size of their tip surface. In this case the basis of detection is not a surface process as in amperometric detection, but the measurement of a physical property in the volume element of fluid facing and moving toward the fiber tip. Since silica particles are transparent to the excitation light, the emission fiber can see through a number of particles situated right in front of its tip and collect the emitted fluorescence coming from analyte molecules eluting with the volume element of the mobile phase heading for the fiber assembly tip. In general, it is considered that a fiber will collect the fluorescence of analyte molecules situated within two fiber diameters away from its tip [Sepaniak *et al.*, 1988]. This may be one of the reasons why this detection system proved to be much more sensitive.

The radial distribution of the local value of the analyte concentration for the 7.8x300 mm column -- discussed in chapters 4.1.2 and 4.2 for its flow profile and local efficiency distribution -- is plotted in Figure 4.3.3. The analyte concentration is highest in an annular region having a reduced radius of 0.5. The concentration measured at column axis is approximately 50% lower than the maximum local

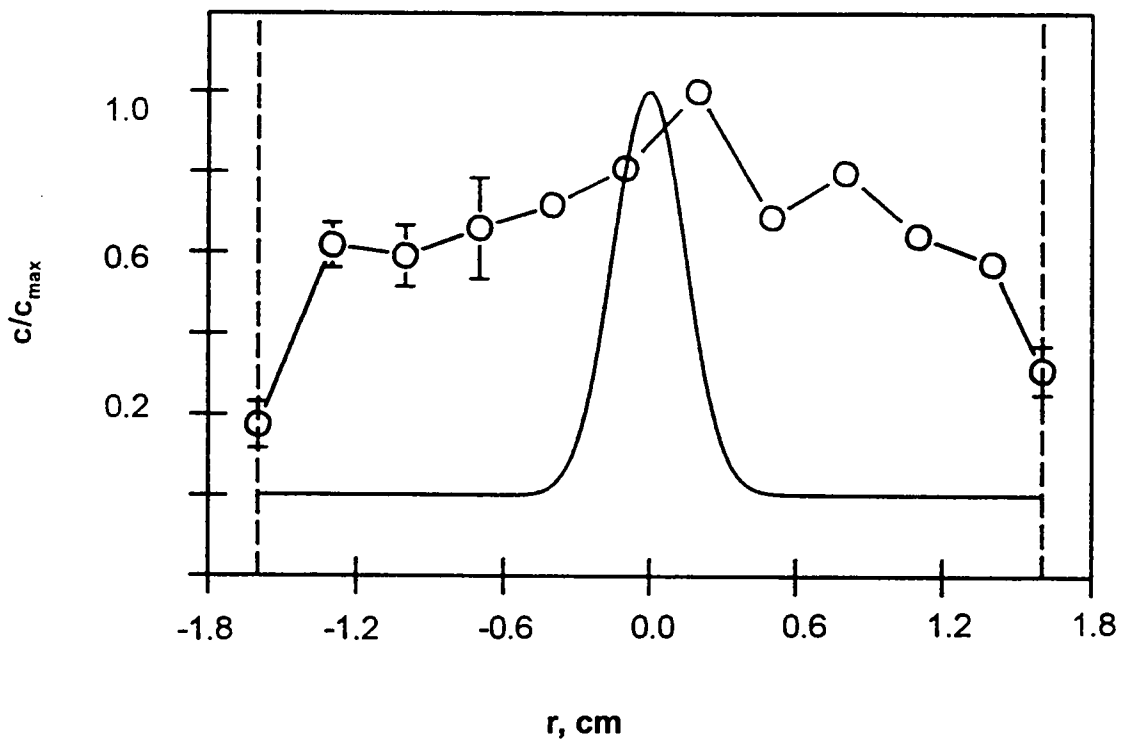

Figure 4.3.2 Radial distribution of normalized concentration maximum at column outlet for a 3.2x40 mm ODS column packed with 3 μm particles: open circles, experimentally determined distribution; solid line, calculated concentration distribution for point injection (σ_R= 0.15 mm). Source: Baur *et al.*, *J. Chromatogr.*, 482, 65 (1989).

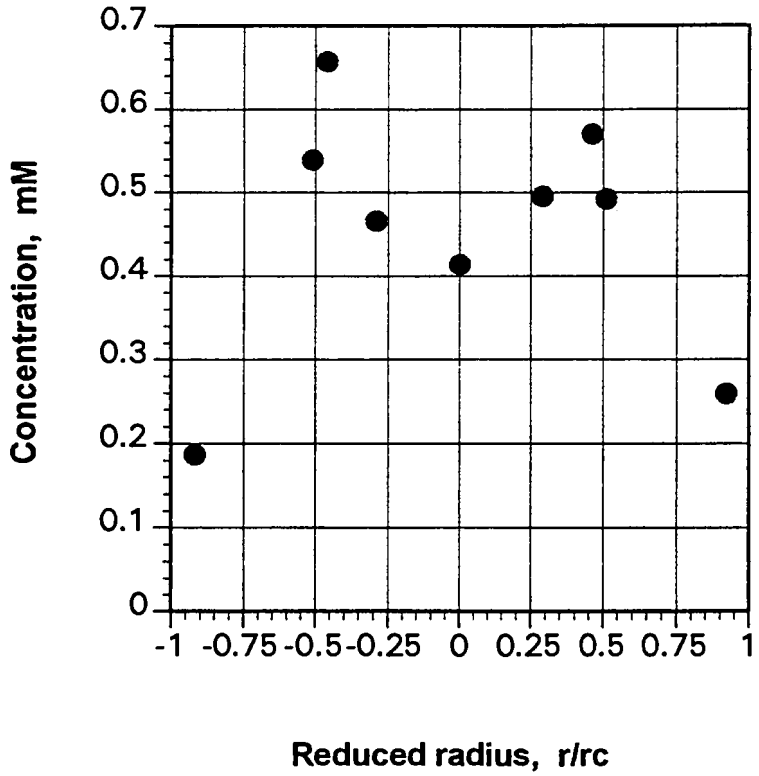

Figure 4.3.3 Radial distribution of the analyte concentration at the outlet of a 7.8x300 mm column packed with Zorbax, a C_{18}-modified 10 μm particle size spherical silica.

concentration recorded at column exit. The local value of the analyte concentration is much lower (2.5 times) in the region situated close to the column wall than the maximum concentration measured at column outlet. This distribution is resembling the one reported by Baur *et al.* [1988], for a 3.2x100 mm column packed with 3 μm ODS silica particles (Figure 4.3.4). For their column, the analyte concentration was more than 100% larger at locations of reduced radius equal to 0.62, than the value measured at column axis. At the same time, the concentration at column wall was about 70% lower than the value measured at center.

A completely different picture was obtained for the highly efficient column with the dimensions 9.4x250 mm, packed with 5 μm C_8 -modified Zorbax silica (Figure 4.3.5). The local analyte concentration showed relatively small differences between the different radial locations investigated, compared to the other columns discussed in this study. The analyte concentration was more or less the same in the core region of the packing, and only about 20% smaller in the region situated close to the column wall. This finding is in agreement with the radial distribution of the local efficiency for this column (Figure 4.2.8). The value for the reduced HETP is only 20% lower in the wall region of the packing than in the core region, which explains why the decrease in maximum concentration due to dispersion is so limited in this case.

In the case of the preparative columns, the large size of the cross-section area allows for the detection of a large number of peaks corresponding to different regions of the eluting analyte band. The peaks recorded at different locations over

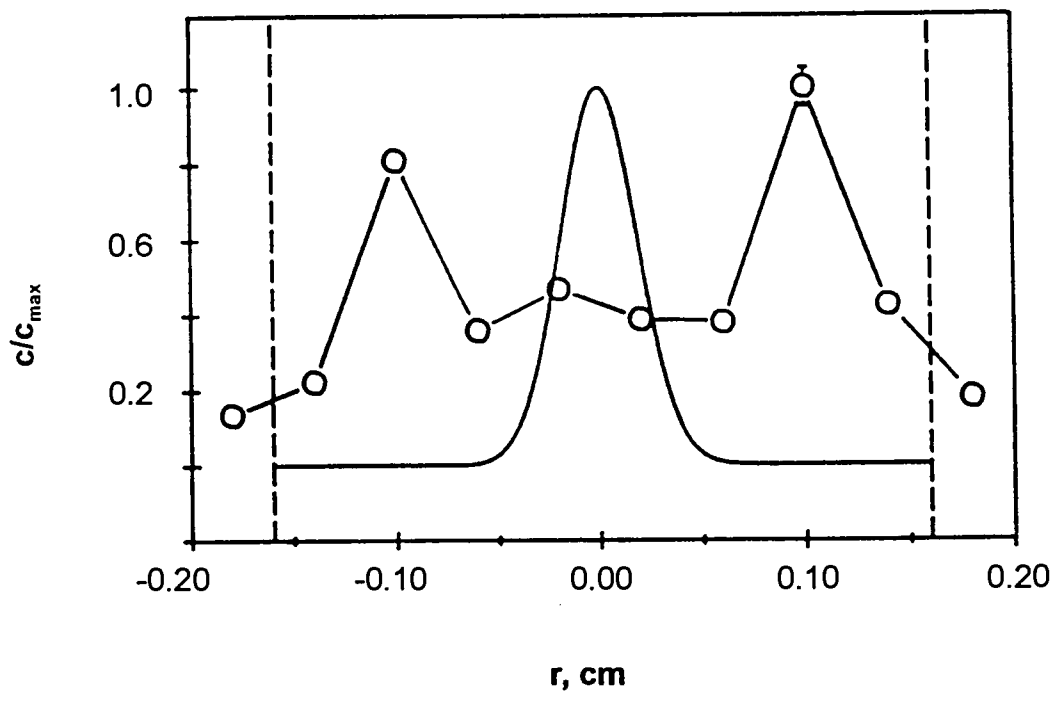

Figure 4.3.4 Radial distribution of normalized concentration maximum: solid line, theoretical for central injection with σ_R= 0.188 mm; circles, experimental. The dashed lines are the estimated position of the column walls for a 3.2x100 mm ODS column packed with 3 μm particles. Source: Baur *et al.*, *Anal. Chem.*. 60, 2334 (1988).

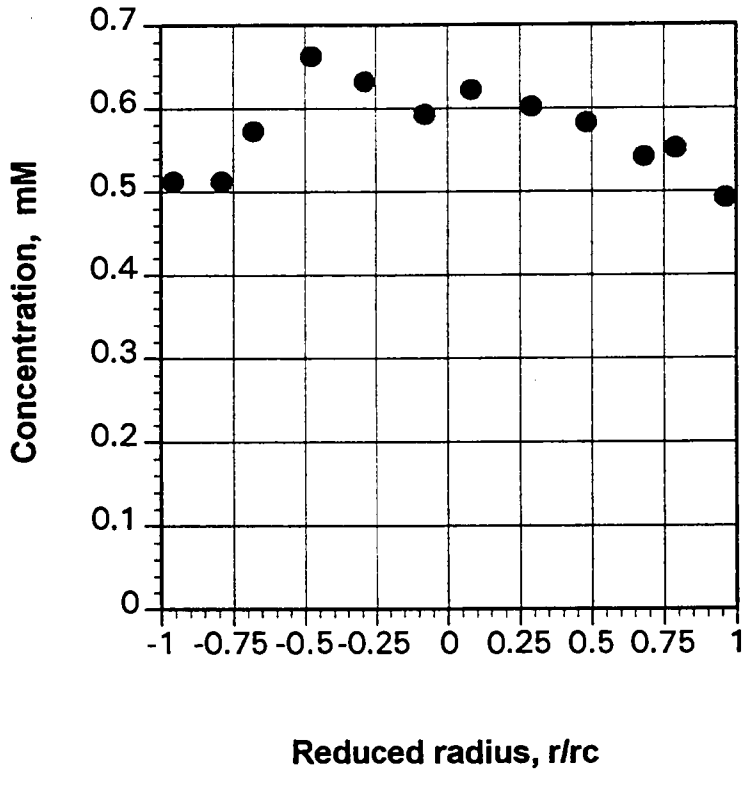

Figure 4.3.5 Radial distribution of the analyte concentration at the outlet of a 9.4x250 mm column packed with Zorbax, a C_8-modified 5 μm particle size spherical silica.

the outlet cross-section of the column, during one single run are shown in Figure 4.3.6. They differ significantly in timing (see mobile phase velocity distribution), in band width (see local efficiency distribution), and slightly in band shape. The important differences observed in the peak heights is largely due to the different response factors of the optical fiber assemblies and amplification factors of the corresponding diodes, differences which are easily corrected by proper calibration (Chapter 3.2.7). The many parameters affecting the specific response of an optical fiber assembly-diode couple were described in Chapter 3.3.2. The more important ones in the present case seem to be the fiber assembly geometry and photo diode aging. In order to compensate for these differences, signal normalization was performed by calculating correction factors as the ratios of the plateau heights obtained for each sensor during a staircase breakthrough experiment. In a breakthrough experiment, the composition of the whole effluent becomes eventually homogeneous, given enough run time, even if the packing is heterogeneous. The normalized, baseline corrected, parallel chromatograms eluted during one run are shown in Figure 4.3.7. The peaks (which are now concentration profiles) still differ in height, width and retention time, but to a much lesser extent.

From the previous results on the distribution of mobile phase velocities and local efficiencies, one would expect that the spatial distribution of the analyte molecule density (*i.e.*, of the analyte concentration profiles) within the component zone includes the following features: the elution bands recorded in different points of the central region of the column exit are more or less evenly dispersed and they

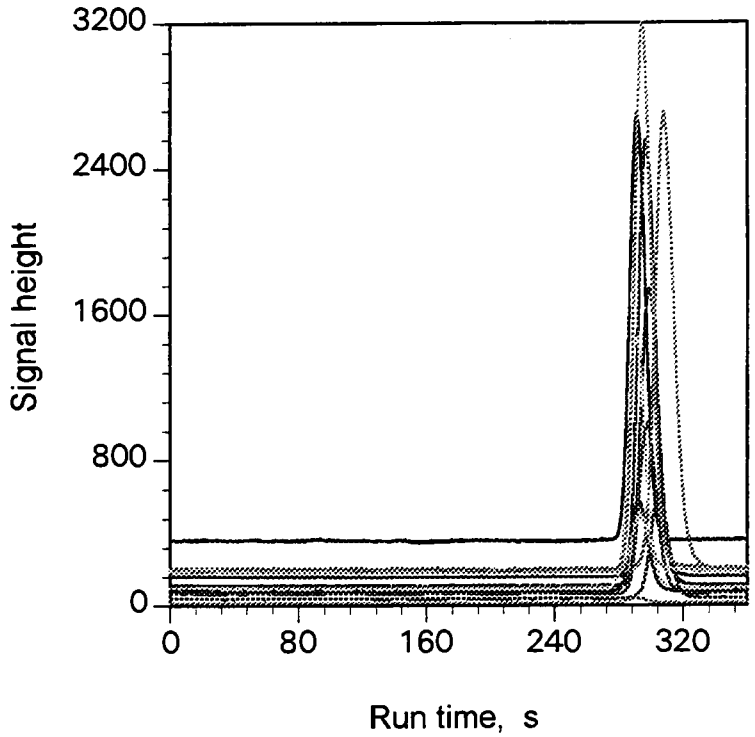

Figure 4.3.6 Peaks recorded in parallel during the same run at 11 different locations over the cross-section of a 50x150 mm axial compression column.

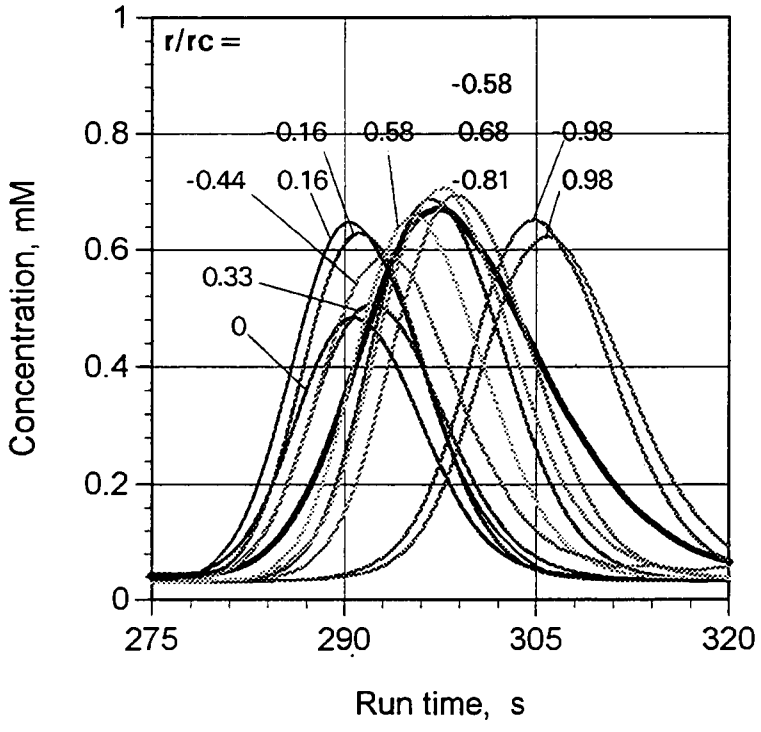

Figure 4.3.7 Normalized and baseline corrected peaks recorded during the same run at 11 different locations over the cross-section of a 50x150 mm axial compression column (same run as in Figure 4.3.6).

all move at nearly the same velocity, along parallel stream paths; bands recorded in the wall region are more diffuse, hence exhibiting lower maxima, according to the distribution of local efficiency. They migrate more slowly in the region closer to the column wall and their elution instants are shifted in time, according to the uneven flow profile induced by the bed heterogeneity. The experimental results show a somewhat different picture (Figure 4.3.7). The results agree well with the prediction as far as the distribution of average residence times is concerned. However, the distribution of the concentration maxima is not even along any portion of the column diameter, including the central core region. The maximum concentration of the bands is smaller at the column center than in the region surrounding it. As expected, it becomes smaller close to the column wall. That this observation is not an experimental artifact is suggested by the fact that the concentration maxima of the different bands vary smoothly along any column diameter. Note that peaks recorded at same or close locations with different sensors are close in heights, while peaks recorded at intermediate locations with different sensors are intermediate in heights. Analytical columns previously studied with different experimental set-ups, using either electrochemical or fluorescence detection systems, showed similar trends.

4.4 Calculation of Experimental Bands.

The set of local data acquired and discussed above allows a detailed discussion of the profile of the bands obtained with a conventional on-line detector working with the bulk eluent. All the volume elements that are part of the analyte band and elute earliest contribute to the peak front. The central part of the peak is recorded during the elution of the volume elements that are at the periphery of the central core region of the column (Figure 4.3.7). In the mean time, in the region close to the wall of the column the analyte concentration begins to build up only when the concentration in the core region of the bed has peaked and is already decreasing (Figure 4.3.7). Note in Figure 4.3.7 that the "resolution" between the peaks at the column center and at a relative radius of 0.98 is nearly unity! The rear part of the peak is recorded during the elution of the molecules moving close to the column wall, at a time when most of the other molecules have left the column. Thus, molecules eluting early build up the peak front while those lagging behind the bulk and moving in a specific region of the packing- the region close to the wall- are responsible for the apparent tailing of the peak recorded by a detector operating on the bulk eluent. Consequently, to the three conventional sources of tailing in chromatography, a tailing injection profile, too slow a detector response, and heterogeneous mass transfer kinetics, we must now add a fourth one, the effect of an uneven radial distribution of the flow velocity, causing molecules to move at different average velocities in different regions of the column cross-section.

Finally, the reconstruction of the overall peak profile obtained with a conventional detector offers a check of the consistency of all the experimental results reported here. This profile is obtained by summing up the contributions of all the slices shown in Figure 4.4.1. Each contribution is calculated as the product of the concentration profile (Figure 4.3.7) recorded by the sensor labeled in Figure 4.4.1 and the fractional area of the slice. Concentric segments of the annular regions shown in Figure 4.4.1 were chosen in such a way that each one contains at least one location where detection has been performed. When there are two sensors in a slice, the average profile was taken. For the few sectors that did not contain such a location, the value interpolated from neighboring sectors was used. The result of this calculation was the profile represented by the thick solid line shown in Figure 4.3.7. This peak is centered at the weight center of the set of locally recorded peaks which were used to generate it. Its shape reflects contributions from all these peaks. Note that its tailing is much more important than the one of any local profile. Next, this calculated peak profile is compared to the profile recorded when the column was tested in a standard instrumental set-up [Sarker and Guiochon, 1995a, 1995b], following packing and bed stabilization. Figure 4.4.2 shows that both the calculated envelope and the experimental peak profile overlay fairly well, except for a shift in their retention time. This shift is fully accounted for by the post-column dead volume of the connecting tubing required between column outlet and the detector.

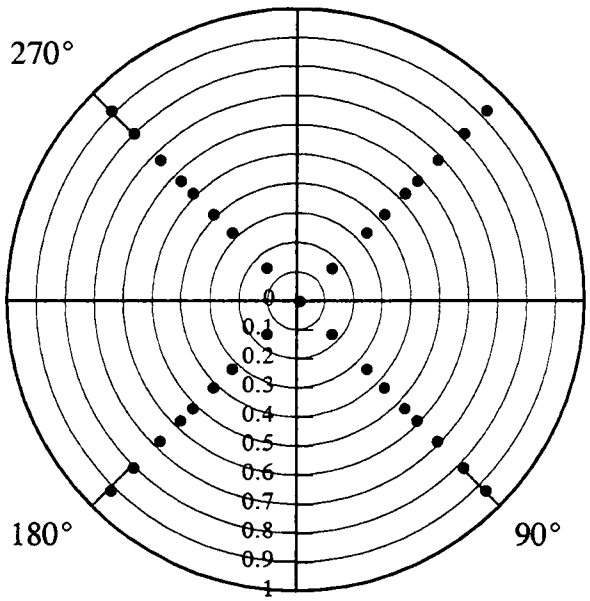

Figure 4.4.1 Partitioning of the cross-sectional area and locations where detection was performed within each sector, used in reconstructing the overall peak from individual peaks recorded in parallel.

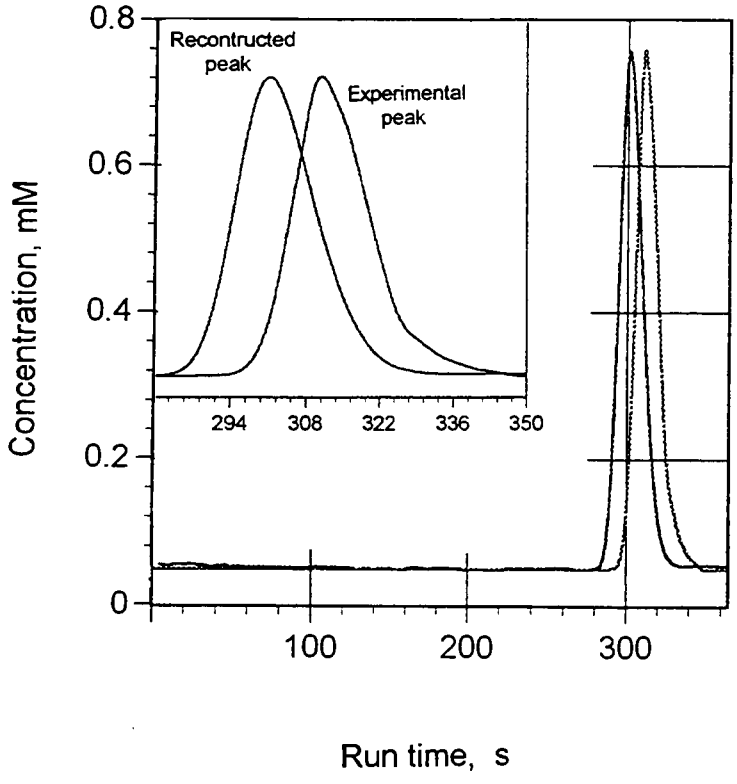

Figure 4.4.2 Comparison between the reconstructed and the experimental peak, overlaid.

CHAPTER 5

CONCLUSIONS

This work continues a long history of efforts to study the flow of fluids through packed beds-- more specifically, through beds made of uniform packing particles, and generated under high pressure, -- and to probe the sources of band broadening in liquid chromatography, referred to more commonly as axial dispersion in the chemical engineering literature. The role of radial flow heterogeneity in local and overall band broadening, as well as its consequences on the radial distribution of local analyte concentration is found to be more significant than generally expected.

Any investigation of the radial distribution of local chromatographic characteristics should consider on-column, local, multichannel detection. The results presented in this work were obtained with an experimental set-up which can accommodate at least 10 optical fiber assemblies functioning as on-column, local microdetection probes when implanted into the exit frit of an HPLC column. This number of parallel detection channels would probably be excessive to map the distribution of concentration within a chromatographic band eluting from an analytical column.

High performance liquid chromatographic columns are not radially homogeneous. A rather homogeneous core is surrounded by a thick layer of heterogeneous packing situated along the column wall. The thickness of this layer

is variable, at least 30 to 50 packing particle diameters. The flow distribution in these columns is cylindrical, nearly flat in the column center, within approximately half the column radius from the center and falls behind rather rapidly towards the wall. Most often, the wall region contributes more to band broadening than the core region of the packing depending upon the shape of the flow profile. Peaks recorded at the column wall elute later, are more diffuse and wider than those recorded in the center during the same experiment. Because the concentration profile of an analyte along the wall passes later and is wider and shorter than in the column center, the signal of a bulk detector is bound to exhibit some degree of tailing. Actually, this would result even if the peak profile at any point of the column cross-section were Gaussian and compact (which most often is not the case, as shown earlier), but the extent to which the peak tails is proportional to the degree of deformation of the mobile phase flow profile. This phenomenon could provide a likely explanation to the puzzling tailing exhibited by weakly polar or non-polar compounds on well-deactivated, end-capped, carefully bonded ODS packings. The fact that the flow distribution is not cylindrical in poor columns is expected.

The results reported here regarding the radial distribution of flow velocity at the outlet of an analytical column are mostly expected, since they confirm previous findings regarding columns with moderate and high efficiencies [Knox *et al.*, 1969, 1976; Eon, 1978; Baur *et al.*, 1988, 1989]. Although some of the details of our results are different from those obtained by these previous workers, there is a

substantial agreement regarding the nature of the phenomenon. We assume, the different packing techniques used are responsible for these differences.

The large number of parallel channels our experimental set-up permits detection to be performed on, makes this approach especially suitable for investigating the radial distribution of the properties of large diameter columns. As do analytical scale chromatographic columns, preparative columns exhibit significant cross-column variations of the local average flow velocity, the local column efficiency, and the local analyte concentration. Inside a central core region with a diameter of the order of two third the column diameter, the velocity is nearly constant. In the external region, the velocity decreases with increasing distance from the column axis. Both regions occupy comparable fractions of the packing volume. However, there is no clear boundary between these two regions. This observation is important as it does not seem to be consistent with the conventional explanation regarding the low stability of chromatographic beds in preparative columns, that these beds may be lacking "wall support" [Kamiński *et al.*, 1982].

The local column efficiency measured at different radial positions over the column outlet cross-section is at most locations higher than the overall efficiency determined with an on-line conventional detector. It varies across the column cross-section as follows: it is higher in the central core region, while in the external region it decreases with decreasing distance to the column wall. We can conclude that in chromatographic columns, the radial distribution of the local efficiency shows a

similar pattern to the distribution of the mobile phase linear velocity. A higher degree of packing heterogeneity at column walls results in an accentuated dispersion of the analyte band and poor local efficiencies. The more disperse local analyte bands formed in the wall region of the packing build into a tailing of the overall band, and cause to some extent an increase in peak width (*i.e.*, a decrease in column efficiency).

As a consequence, analytical columns are operated under experimental conditions where a significant fraction of their potential performance is wasted. A small concentration sensor placed at the column axis would see narrower, better resolved and more concentrated bands. Recent progress in the realization of microelectrode and optical fiber sensors could permit the design of improved chromatographs. The fact that the analyte is more concentrated in the areas where the efficiency is higher renders this approach more attractive. For the case of preparative chromatography, on-column, local detection should be combined with a sample collection method that would allow for discrimination between the different annular regions of the column cross-section.

The consequence of this heterogeneous behavior of the column is that the conventional elution profile is a complex convolution of the convection and dispersion phenomena taking place in a chromatographic column. This profile is not a simple consequence of the local axial dispersion and of the mass transfer phenomena taking place in the column but it is influenced, to a certain extent, by the packing heterogeneity of the column used. It has long been observed that

chromatographic peaks tail more than can be explained by most models. Our results demonstrate that this tailing is mainly caused by the uneven distribution of the local velocities. The fact that the fraction of the analyte that migrates close to the column wall does so at a lower linear velocity than the fraction that migrates in the core region is responsible for most of the observed peak tailing. Consequently, to the three conventional sources of tailing in chromatography, a tailing injection profile, too slow a detector response, and heterogeneous mass transfer kinetics, we must now add a fourth one, the effect of an uneven radial distribution of the flow velocity, causing molecules to move at different average velocities in different regions of the column cross-section. Obviously, two space coordinates, the column length and its radius and not only the former, are needed in a realistic model of chromatography [Yun and Guiochon, 1994, 1996].

The origin of the column heterogeneity described in this work has been discussed recently [Guiochon *et al.*, 1997]. It is most probably related to the interaction between the relatively high compressibility of pulverulent materials [Guiochon and Sarker, 1995; Sarker *et al.*, 1996; Taylor, 1948] and the complex distribution of stress during the compression of the packing. The latter has been abundantly illustrated by Train [1956, 1957, 1960]. The behavior of packed column beds and the dynamics of the packing methods are still poorly understood [Colin *et al.*, 1992; Sarker *et al.*, 1994; 1995]. Further progress in the performance of analytical as well as preparative columns could be expected from research done in these areas.

LIST OF REFERENCES

Baumeister, E., U. Klose, K. Albert, E. Bayer and G. Guiochon, "Determination of the apparent transverse and axial dispersion coefficients in a chromatographic column by pulsed field gradient nuclear magnetic resonance", *J. Chromatogr. A*, **694**, 321 (1995).

Baur, J.E., E.W. Kristensen and P.M. Wightman, "Radial dispersion from commercial high-performance liquid chromatography columns investigated with microvoltammetric electrodes", *Anal. Chem.,* **60,** 2334 (1988).

Baur, J.E., R.M. Wightman, "Microcylinder electrodes as sensitive detectors for high-efficiency, high-speed liquid chromatography", *J. Chromatogr. A,* **482**, 65 (1989).

Bayer, E., E. Baumeister, U. Tallarek, K. Albert, and G. Guiochon, "NMR imaging of the chromatographic process. Deposition and removal of gadolinium ions on a reversed-phase liquid chromatographic columns", *J. Chromatogr. A*, **704**, 37 (1995).

Bayer, E., W. Müller, M. Ilg and K. Albert, "Visualization of Chromatographic Separations by NMR Imaging", *Angew. Chem. Intl. Ed.,* **28** (1989) 1029.

Benenati, R.F. and C.B. Brosilow, "Void Fraction Distribution in Beds of Spheres", *A.I.Ch.E. Journal*, **8**(3), 1962, 359-361.

Bird, R.B., W.E. Steward, and E.N. Lightfoot, "Transport Phenomena", Wiley, New York, NY, 1960.

Booji, W.E., A de Jongh and F.F.M. de Mul, "Flow profile study using miniature laser-Doppler velocimetry", *Am. J. Phys.*, **63** (11), 1995, 1028-1033.

Bristow, P.A. and J.H. Knox, "Standardization of test conditions for high performance liquid chromatography columns", *Chromatographia*, **10**(6), 1977, 279-289.

Cairns, E.J. and J.M. Prausnitz, "Velocity Profiles in Packed and Fluidized Beds", *Ind. Engng Chem.*, (1959) 1441-1444.

Callaghan, P.T., A. Coy, D. Macgowan and K.J. Packer, "Diffusion of Fluids in Porous Solids Probed by Pulsed Field Gradient Spin-Echo NMR", *Journal of Molecular Liquids*, **54**(4), 1992, 239-251.

Carta, G. and W.B. Springfield, "Operating Characteristics of a Preparative-Scale Radial Compression Chromatograph in Isocratic and Gradient Elution", *J. Chromatogr. A*, **658** (1994) 407.

Coleman, J.T., J.F. Eastham and M.J. Sepaniak, "Fiber Optic Based Sensor for Bioanalytical Absorbance Measurements", *Anal. Chem.*, **56** (1984) 2246.

Colin, H., "Preparative and Production Scale Chromatography", G. Ganetsos and P.E. Barker Eds., M. Dekker, New York, NY, 1992, p. 47.

Collins, R.E., "Flow through Porous Materials", Reinhold Publishing Corporation, New York, NY (1961), 47-58.

Ebach, E.A., and R.R. White, "Mixing of Fluids through Beds of Packed Solids", *AIChE J.*, **4**, 161 (1958).

Eon, C.H., "Comparison of broadening patterns in regular and radially compressed large-diameter columns", *J. Chromatogr.*, **149**, 29 (1978).

Farkas, T., J.Q. Chambers and G.A. Guiochon, "Column efficiency and radial homogeneity in liquid chromatography", *J. Chromatogr. A*, **679**, 231(1994).

Farkas, T., M.J. Sepaniak and G.A. Guiochon, "Column radial homogeneity in HPLC", *J Chromatogr.*, **740** 169 (1996).

Fernandez, E.J., C.A. Grotegut, G.W. Braun, K.J. Kirshner, J.R. Staudaher, M.L. Dickson and V.L. Fernandez, "The Effects of Permeability Heterogeneity on Miscible Viscous Fingering: A three-dimensional magnetic resonance imaging analysis", *Phys. Fluids*, **7** (1995) 468.

Geiss, F., "Fundamentals of Thin Layer Chromatography", Hüthig Verlag, Heidelberg, Germany, 1987.

Giddings, J.C., "Principles of Column Performance in Large Scale Gas Chromatography", *J. Gas Chromatogr.*, **1**(1), 12 (1963).

Giddings, J.C., "Dynamics of Chromatography, Part I: Principles and Theory", Marcel Dekker, New York, NY (1965), p. 195-213.

Giddings, J.C., "Unified Separation Science", Wiley, New York, NY (1991), pp. 62-65.

Gladden, L.F., "NMR Studies of Porous Media", *Chem. Eng. R&D*, **71**(6), 1993, 657-674.

Guan H. and G. Guiochon, "Study of physico-chemical properties of some packing materials. I. Measurements of the external porosity of packed columns by inverse size-exclusion chromatography", *J. Chromatogr. A*, **731**, 27 (1995).

Guan, H., G. Guiochon, D. Coffey, E. Davis, K. Gulakowski and D.W. Smith., "Study of physico-chemical properties of some packing materials. II. General properties of the particles", *J. Chromatogr. A*, **736**, 21 (1996).

Guiochon, G., T. Farkas, H. Guan-Sajonz, J. Koh, M. Sarker, B. Stanley and T. Yun, "The consolidation of particles and the packing of chromatographic columns", *J. Chromatogr. A*, **762**, 83 (1997).

Guiochon, G., and M. Sarker, *J. Chromatogr. A*, "Consolidation of the packing material in chromatographic columns under dynamic axial compression. I. Fundamental study", **704**, 247 (1995).

Guiochon, G., S.G. Shirazi and A.M. Katti, "Fundamentals of Preparative and Nonlinear Chromatography," Academic Press, Boston, MA, 1994, Chapter VI.

Gunn, D.J., "Theory of Axial and Radial Dispersion in Packed Beds", *Trans. Instn. Chem. Engrs.*, **47**, T351 (1969).

Gunn, D.J., "Mixing in Packed and Fluidised Beds", *The Chemical Engineer,* **46**, CE153 (1968).

Hiby, J.W., in Rottenburg, P.A. (Ed.), "Interaction between Fluids and Particles", p. 312, Institution of Chemical Engineers, London (UK) (1962).

Karger, B., L. Snyder and Cs. Horváth, "An Introduction to Separation Science", Wiley, New York, NY (1973), p. 90-92.

Kirkland, J.J., W.W. Yau, H.J. Stoklosa and C.H. Dilks, Jr., "Sampling and Extra-Column Effects in High-Performance Liquid Chromatography; Influence of Peak Skew on Plate Count Calculations", *J. Chromatogr. Sci.*, **15** (1977) 303.

Klawiter, J., M. Kamiński and J.S. Kowalczyk, "Investigation of the relationship between packing methods and efficiency of preparative columns. I Characteristics of the tamping method for packing preparative columns.", *J. Chromatogr.*, **243** (1982), 207-224.

Kamiński, M., J. Klawiter and J.S. Kowalczyk, "Investigation of the relationship between packing methods and efficiency of preparative columns. II Characteristics of the slurry method of packing chromatographic columns". *J. Chromatogr.*, **243** (1982), 225-244.

Knecht, L.A., E.J. Guthrie and J.W. Jorgenson, "On-Column Electrochemical Detector with a Single Graphite Fiber Electrode for Open-Tubular Liquid Chromatography", *Anal. Chem.*, **56** (1984) 479.

Knox, J.H., G.R. Laird and P.A. Raven, "Interaction of radial and axial dispersion in liquid chromatography in relation to the "infinite diameter effect"", *J. Chromatogr.*, **122**, 129 (1976).

Knox, J.H., and J.F. Parcher, "Effect of column to particle diameter ratio on dispersion of unsorbed solutes in chromatography", *Anal. Chem.*, **41**, 1599 (1969).

Körösi, G., A.M. Siouffi and G. Guiochon, "Study of the Performances of Thin Layer Chromatography. V. Flow Rate in Reversed Phase Plates", *J. Chromatogr. Sci.*, **18** (1980) 324.

Krejči, M., D. Kouřilová and R. Vespalec, "Electrokinetic Detection at Different Points in a Narrow-Bore Glass Column in Liquid Chromatography", *J. Chromatogr.*, **219** (1981) 61.

Lerou, J.J., Froment, G.F., "Velocity, Temperature and Conversion Profiles in Fixed Bed Catalytic Reactors", *Chem. Eng. Sci.*, **32** (1977), 853-861.

Morales, M., C.W. Spinn, and J.M. Smith, "Velocities and Effective Thermal Conductivities in Packed Beds", *Ind. Eng. Chem.*, **43** (1951), 225-232.

Northrup, M.A., J.T. Kulp and S.M. Angel, "Application of Fluorescent Particle Imaging to Measuring Flow in Complex Media", *Anal. Chim. Acta*, **255**(2), 1991, 275-282.

Patzay, G. And K. Takács, "Modeling of Flow Distribution and Mass-Transfer in Packed Columns", *Hungarian Journal of Industrial Chemistry*, **22**(1), 1994, 47-50

Prusiewicz, K., M. Kamiński and J. Klawiter, "Devices for packing preparative chromatographic columns by 'dry packing' techniques", *J. Chromatogr. A*, **238** (1982), 232-236.

Peters, D.G., J.M. Hayes and G.M. Hieftje, "Chemical Separations and Measurements", Saunders Golden Sunburst Series, Philadelphia, PA, (1974), 531-533.

Poole, C.F., and S.K. Poole, "Chromatography Today", 2nd ed., Elsevier, Amsterdam, The Netherlands (1993).

Rigby, S., K.Y. Cheah and L.F. Gladden, "NMR Imaging Studies of Transport Heterogeneity and Anisotropic Diffusion in Porous Alumina Pellets", *Applied Catalysis A-General*, **144**(1-20), 1996, 377-388.

Sarker, M., and G. Guiochon, "The packing stability of dynamically compressed preparative chromatography columns", *LC-GC*, **12** (1994) 300.

Sarker, M., and G. Guiochon, "Study of the packing behavior of axial compression columns for preparative chromatography", *J. Chromatogr. A*, **702**, 27 (1995a).

Sarker, M., and G. Guiochon, "Study of the operating conditions of axial compression columns for preparative chromatography", *J. Chromatogr. A*, **709**, 227 (1995b).

Sarker, M., A.M. Katti and G. Guiochon., "Consolidation of the packing material in chromatographic columns under dynamic axial compression II. Consolidation and breakage of several packing materials", *J. Chromatogr. A*, **719**, 275 (1996).

Scheidegger, A.E., "The Physics of Flow in Porous Media", University of Toronto Press, Toronto, Canada (1974), p126-135.

Schwartz, C.E. and J.M. Smith, "Flow Distribution in Packed Beds", *Ind. Eng. Chem*, **45** (1953), 1209-1218.

Sepaniak, M.J., B.J. Tromberg and T. Vo-Dinh, "Fiber Optic Affinity Sensors in Chemical Analysis", *Progr. Analyt. Spectrosc.*, **11** (1988) 481.

Sepaniak, M.J., "The Clinical Use of Laser-Excited Fluorometry", *Clinical Chemistry*, **31** (1985) 671.

St. Claire. R.L., and J.W. Jorgenson, "Characterization of an On-Column Electrochemical Detector for Open-Tubular Liquid Chromatography", *J. Chromatogr. Sci.*, **23** (1985) 186.

Sie, S.T. and N. van den Hoed, "Preparation and Performance of High-Efficiency Columns for Liquid Chromarography", *J. Chromatogr. Sci.*, **7** (1969), 257-266.

Staller, T.D., "Novel Detection Alternatives for Capillary Electrokinetic Separations", PhD Dissertation, The University of Tennessee, Knoxville, TN, 1994.

Stanley, B.J., M Sarker and G. Guiochon, "Consolidation of the packing material in chromatographic columns under dynamic axial compression. IV. Mechanical properties of some packing materials", *J Chromatogr. A*, **741**, 175 (1996).

Stanley, B.J., C.R. Foster and G. Guiochon, "On the reproducibility of column performance in liquid chromatography and the role of the packing density", *J Chromatogr. A*, in press (B 1078).

Sternberg, J.C., "Extracolumn Contributions to Chromatographic Band Broadening", in Advances in Chromatography, **2** (1966) 205.

Tallarek, U., K. Albert, E. Bayer and G. Guiochon, "Measurement of transverse and axial apparent dispersion coefficients in packed beds", *A.I.Ch.E. J.* **42**(11), 3041-3054 (1997).

Tallarek, U., E. Baumeister, K. Albert, E. Bayer, and G. Guiochon, "NMR imaging of the chromatographic process. Migration and separation of bands of gadolinium chelates", *J. Chromatogr. A*, **696**, 1 (1995).

Taylor, D.W., "Fundamentals of Soil Mechanics", Wiley, New York, NY, 1948.

Train, D., "An investigation into the compaction of powders", *J. Pharm. Pharmac.*, **8**, 745 (1956).

Train, D., "Transmission of forces through a powder mass during the process of pelleting", *Trans. Instn. Chem. Engrs.*, **35**, 258 (1957).

Train, D., and J.A. Hearsey, "The use of laminar lubricants in compaction processes", *J. Pharm. Pharmac.*, **12**, 97T (1960).

Tilly-Melin, A., Y. Askemark, K.-G. Wahlund and G. Schill, "Retention Behavior of Carboxylic Acids and Their Quaternary Ammonium Ion Pairs in Reversed Phase Chromatography with Acetonitrile as Organic Modifier in the Mobile Phase", *Anal. Chem.*, **51** (1979) 976.

van Dyke, M., "An Album of Fluid Motion", The Parabolic Press, Stanford, CA (1982).

Venneti, M., H. Govindarao and G.F. Froment, "Voidage Profiles in Packed Beds of Spheres", *Chem. Eng. Sci.*, **41** (1986), 533-539.

Vortmeyer D. and K. Michael, "The effect of non-uniform flow distribution on concentration profile and breakthrough curves of fixed bed adsorbers", *Chemical Engineering Science,* **40**(11), 1985, 2135-2138.

Vortmeyer, D. and J. Schuster, "Evaluation of Steady Flow Profiles in Rectangular and Circular Packed Beds by a Variational Method", *Chem. Eng. Sci.*, **38** (1983), 1691-1699.

Yun, T. and G. Guiochon, "Visualization of column packing heterogeneity", *J. Chromatogr.* A, **760** (1997), 17-24.

Yun, T. and G. Guiochon, "Modeling of Radial Heterogeneity in Chromatographic Columns. Columns with Cylindrical Symmetry and Ideal Model", *J. Chromatogr. A,* **672**, 1 (1994).

Yun, T. and G. Guiochon, "Modeling of Radial Heterogeneity in Chromatographic Columns. II - Separation of a Two-Component Mixture on a Column with Cylindrical Symmetry", *J. Chromatogr. A*, **734**, 97 (1996).

VITA

Tivadar Farcas was born on December 4, 1958 in Cluj, Romania. He attended high school in his home town, and graduated in June 1977. He studied Organic Chemical Technology at Babes-Bolyai University, Cluj, and graduated in 1983. He worked for three years as a Chemist in a Quality Control laboratory at Maratex Textile Company, Baia Mare, Romania.

In 1988 Tivadar Farcas joined the gas-chromatography method development group at the Atom Physics Institute in Cluj. During 1990-1992 he acted as an assistant-lecturer at the Chair of Analytical Chemistry of the Department of Chemistry at Babes-Bolyai University, Cluj. In this position he taught Separation Methods of Analysis at undergraduate level.